

**SYNTHESIS AND CHARACTERIZATION OF NICKEL
COMPLEXES DERIVED FROM DIBENZO TETRAAZA[14]
ANNULENE FOR LIQUID CRYSTAL APPLICATION**

NOORAZIAH BINTI MOHD LAIR

**FACULTY OF SCIENCE
UNIVERSITY OF MALAYA
KUALA LUMPUR**

2018

**SYNTHESIS AND CHARACTERIZATION OF NICKEL
COMPLEXES DERIVED FROM DIBENZO
TETRAAZA[14] ANNULENE FOR LIQUID
CRYSTAL APPLICATION**

NOORAZIAH BINTI MOHD LAIR

**THESIS SUBMITTED IN FULFILMENT OF THE
REQUIREMENTS FOR THE DEGREE OF
DOCTOR OF PHILOSOPHY**

**DEPARTMENT OF CHEMISTRY
FACULTY OF SCIENCE
UNIVERSITY OF MALAYA
KUALA LUMPUR**

2018

UNIVERSITY OF MALAYA
ORIGINAL LITERARY WORK DECLARATION

Name of Candidate: **NOORAZIAH BINTI MOHD LAIR**

I.C/Passport No:

Matric No: **SHC100021**

Name of Degree: **Ph.D.**

Title of Project Paper/Research Report/Dissertation/Thesis ("this Work"):

**SYNTHESIS AND CHARACTERIZATION OF NICKEL COMPLEXES
DERIVED FROM DIBENZO TETRAAZA[14] ANNULENE FOR
LIQUID CRYSTAL APPLICATION**

Field of Study: **Inorganic Chemistry**

I do solemnly and sincerely declare that:

- (1) I am the sole author/writer of this Work;
- (2) This Work is original;
- (3) Any use of any work in which copyright exists was done by way of fair dealing and for permitted purposes and any excerpt or extract from, or reference to or reproduction of any copyright work has been disclosed expressly and sufficiently and the title of the Work and its authorship have been acknowledged in this Work;
- (4) I do not have any actual knowledge nor do I ought reasonably to know that the making of this work constitutes an infringement of any copyright work;
- (5) I hereby assign all and every rights in the copyright to this Work to the University of Malaya ("UM"), who henceforth shall be owner of the copyright in this Work and that any reproduction or use in any form or by any means whatsoever is prohibited without the written consent of UM having been first had and obtained;
- (6) I am fully aware that if in the course of making this Work I have infringed any copyright whether intentionally or otherwise, I may be subject to legal action or any other action as may be determined by UM.

Candidate's Signature



Date: 25-1-18

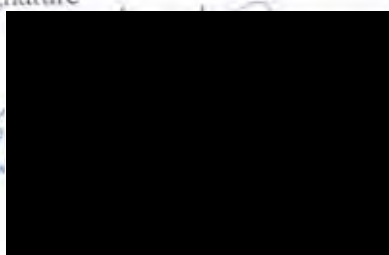
Subscribed and solemnly declared before,

Witness's Signature

Date:

Name:

Designation:



SYNTHESIS AND CHARACTERIZATION OF NICKEL COMPLEXES DERIVED FROM DIBENZO TETRAAZA[14] ANNULENE FOR LIQUID CRYSTAL APPLICATION

ABSTRACT

A new series of macrocyclic dibenzotetraaza[14]annulenes (DBTAA) bearing 5-alkoxy-3,3-dimethylindole on meso positions and four aliphatic ether side chains on dibenzo structure, that consist of 6, 10, 12, 14 carbon length, respectively, were synthesized. The new compounds of macrocyclic DBTAA were synthesized through 2:2 condensation of 4,5-bis(alkoxy)benzene-1,2-diaminium chloride and 2-(diformylmethylidene)-5-(alkyloxy)-3,3-dimethylindole with glacial acetic acid as catalyst. The intermediate of 4,5-bis(alkoxy)benzene-1,2-diaminium chloride has been synthesized from alkylation on catechol using bromoalkyl ($\text{BrC}_n\text{H}_{n+1}$, $n = 6, 10, 12, 14$) followed by nitration with concentrated nitric and sulphuric acid and finally reduction by Tin(II) chloride. As for 2-(diformylmethylidene)-5-(alkyloxy)-3,3-dimethylindole, the compound was synthesized from 4-methoxy phenylhydrazine via fischer synthesis followed by demethylation using boron tribromide, alkylation by alkylbromide, and lastly, Vilsmeier-Haack reaction was applied to afford the required compounds of diformyl. Reaction of nickel(II) acetate in glacial acetic acid on the synthesized macrocyclic DBTAA compounds has resulted in the target 1:1 type (ligand/metal ratio) of new DBTAA complexes. The new macrocyclic compounds and their nickel complex structures were characterized by ATR-FTIR, CHN, ^1H and ^{13}C NMR, UV-Vis, TGA and X-Ray crystallographic studies. In this study, as predicted the nickel complex possess a planar structure and four nitrogen atoms were coordinated to nickel atom in a square planar geometry which appeared as a weak d-d transition 500 to 505nm range in UV-Vis spectra. Liquid crystal properties of this new macrocyclic ligand and its complexes were

studied under OPM and confirmed by DSC measurement. Macrocyclic ligands consisting of ether aliphatic chains of 12 and 14 carbon length were found to show liquid crystal properties. Nickel complexes with alkyl chains of 10 and 12 carbons also exhibited clearly the fan-shaped texture of discotic columnar liquid crystal properties under OPM. However, the rest of the macrocyclic ligands and complexes changed directly to crystal lattice upon cooling or heating. This observation was confirmed by DSC measurement, and the exact transition temperature with the enthalpy change (ΔH) can be identified on the observed peak at nearly the same temperature as when the texture appeared in OPM. The synthesized macrocyclic ligands and their nickel complexes which are having columnar liquid crystal properties could be suitable materials for organic semiconducting and optical storage.

Keywords: Macrocyclic, liquid crystal, nickel complex, discotic columnar, OPM, DSC.

**SINTESIS DAN PENCIRIAN KOMPLEKS NIKEL YANG
DITERBITKAN DARI DIBENZO TETRAAZA[14] ANULENA UNTUK
APLIKASI HABLUR CECAIR**

ABSTRAK

Satu siri baru makrosiklik dibenzotetraaza[14]anulena (DBTAA) yang mengandungi 5-alkoksi-3,3-dimetilindola pada kedudukan meso dan empat rantaian sisi eter alifatik pada struktur dibenzo, yang mempunyai 6, 10, 12 dan 14 karbon panjangnya telah disintesis. Sebatian makrosiklik DBTAA yang baru ini telah disintesis melalui kondensasi 2:2 4,5-bis(alkoksi)benzena-1,2-diaminium klorida dan 2-(diformilmetilidena)-5-(alkoksi)-3, 3-dimetilindola dengan asid asetik glasial sebagai mangkinnya. Sebatian perantaraan 4,5-bis(alkoksi)benzena-1,2-diaminium klorida telah disintesis daripada pengalkilan katekol menggunakan bromoalkil ($\text{BrC}_n\text{H}_{n+1}$, $n=6,10,12,14$) diikuti penitratan menggunakan asid nitric dan asid sulfuric pekat, diakhiri dengan penurunan menggunakan stanum(II) klorida. Manakala sebatian perantaraan 2-(diformilmetilidena)-5-(alkoksi)-3, 3-dimetilindola yang mana juga telah disintesis daripada 4-metoksifenilhidrazina melalui sintesis Fischer diikuti dengan pendemetilan menggunakan boron tribromida sebagai reagenya, kemudian pengalkilan dengan alkilbromida dan akhir sekali tindakbalas Vilsmeier-Hack diaplikasikan untuk menghasilkan sebatian diformil yang dikehendaki. Tindakbalas nikel(II) asetat terhadap sebatian makrosiklik DBTAA yang telah disintesis, di dalam asid asetik glasial dapat menghasilkan sasaran jenis 1:1 (nisbah ligan/logam) bagi kompleks DBTAA yang baru. Struktur sebatian-sebatian makrosiklik yang baru dan kompleks nikelnya telah dicirikan dengan ATR-FTIR, CHN, ^1H and ^{13}C NMR, UV-Vis, TGA dan kajian X-Ray kristalografi. Dalam kajian ini, sebatian kompleks nikel seperti yang memang dijangka

memiliki struktur menyatah dan empat atom nitrogen telah terkoordinasi kepada ion nikel dalam geometri satah segi empat dimana tertara sebagai transisi d-d lemah pada julat 500 ke 505 nm dalam spectrum UV-Vis. Sifat hablur cecair ke atas ligan makrosiklik yang baru dan kompleksnya telah dikaji dibawah OPM dan disahkan melalui pengukuran DSC. Ligan makrosiklik yang mengandungi rantaian alifatik eter bagi 12 dan 14 panjang karbonnya didapati menunjukkan sifat hablur cecair. Kompleks nikel dengan rantai alkil 10 dan 12 karbonnya juga memperlihatkan tekstur berbentuk kipas yakni sifat hablur cecair turus diskotik dibawah OPM. Manakala, ligan makrosiklik dan kompleks yang lain terus merubah ke kekisi hablur apabila disejukan atau dipanaskan. Pemerhatian ini disahkan melalui pengukuran DSC dan suhu transisi yang tepat dengan perubahan entalpi (ΔH) dapat dikenalpasti pada puncak yang tercerap pada suhu yang hampir sama semasa pembentukan tekstur kelihatan di bawah OPM. Macrosiklik ligan dan nikel kompleks yang mempunyai sifat-sifat turus hablur cecair berkemungkinan adalah bahan yang sesuai sebagai semikonduktor organic dan storan optikal.

Kata kunci: Makrosiklik, hablur cecair, kompleks nikel, turus diskotik, OPM, DSC.

ACKNOWLEDGEMENTS

Firstly, I would like to express my sincere gratitude to my supervisor Professor Dr. Hapipah Mohd Ali for the continuous support of my Ph.D. study and related research, for her patience, motivation, and immense knowledge. Her guidance helped me in all the time of research and writing of this thesis. I could not have imagined having a better supervisor and mentor for my Ph.D. study.

Besides my supervisor, I would like to thank my second supervisor, Professor Noel Francis Thomas for his insightful comments and encouragement, but also for the hard question which incanted me to widen my research from various perspectives.

I thank my fellow lab mates in for the stimulating discussions, for the sleepless nights we were working together before deadlines, and for all the fun we have had in the last few years. In particular, I am grateful to Dr. Hamid Khaledi for enlightening me the first glance of this research.

I would like to acknowledge the financial and technical support of the University of Malaya, especially for the research grant IPPP-PG064/2014B, all staff, technicians, and lecturer for their support, a great assistance to handle the instruments.

Last but not the least, I would like to thank my family: my parents, my siblings and to my Husband, Nor Azmi Mohd Nor and my children, Saiful Afiq and Saiful Azam, for supporting me throughout my studies, writing this thesis and my life in general.

TABLE OF CONTENTS

ABSTRACT	iii
ABSTRAK	v
ACKNOWLEDGEMENTS	vii
TABLE OF CONTENTS	viii
List of Figures	xi
List of Table	xvi
List of Symbols and Abbreviation	xvii
CHAPTER 1 : INTRODUCTION	1
1.1 Introduction	1
1.2 List of Research Objectives	6
CHAPTER 2 : LITERATURE REVIEW	8
2.1 Review On Dibenzotetraaza[14]Annulenes (DBTAA)	8
2.2 Review Of Indole Compounds	13
2.3 Review Of Diformylindolenine	17
2.4 Review on Columnar Liquid Crystal	19
2.5 Review On Metallomesogens Columnar Liquid Crystal Of N₄-Macrocycles	21
CHAPTER 3 : RESEARCH METHODOLOGY	24
3.1 Experimental	24
3.2 Synthesis	25
3.2.1 Overall Synthesis Route	25
3.2.2 Synthesis of 4,5-bis(alkoxy)benzene-1,2-diaminium chloride compounds	26
3.2.2 Synthesis of alkylated Catechol intermediate enroute to 1,2-Dialkyloxybenzene	27

3.2.3	Nitration of bis(alkyloxy)benzenes to produce intermediate compounds of 1,2-Dinitro-4,5-bis (alkyloxy)benzene	29
3.2.4	Reduction of 1,2-Dinitro-4,5-bis(alkyloxy)benzene to produce 4,5-bis(alkyloxy)benzene-1,2-diaminium chloride compounds.	32
3.3	Synthesis of intermediate compounds of 2-(diformylmethylidene)-5-alkoxy-3,3-dimethylindole	34
3.3.1	Fisher synthesis of 5-methoxy-2, 3, 3-trimethylindoline 13	34
3.3.2	Demethylation using BBr ₃ to produce intermediate compound of 5-hydroxy-2,3,3-trimethylindolenine 14	35
3.3.3	Phase transfer reaction to get series of 5-Alkoxy-2,3,3-trimethylindolenine	36
3.3.4	Synthesis of new series compounds of 2-(diformylmethylidene) -5-(alkyloxy)-3,3-dimethylindole.....	37
3.5	Synthesis series of Macrocyclic compounds of DBTAA with six aliphatic chains.....	41
3.6	Synthesis of Nickel complex of Macrocyclic dibenzotetraaza[14] annulene 6-alkyloxy.....	46
3.7	Synthesis of macrocyclic ligand from <i>o</i> -phenylenediamine and 2-(diformylmethylidene)-5-(hexyloxy)-3,3-dimethylindole 19.....	49
CHAPTER 4 : RESULT AND DISCUSSION.....		51
4.1	Suggested Reaction Mechanisms.....	51
4.1.1	Reaction Mechanism for Fischer indole synthesis.....	51
4.1.2	Reaction Mechanism for Vilsmeier-Haack reaction on 5 Alkoxy-2,3,3-trimethylindolenine	51
4.2	Physical properties of macrocyclic ligands and complexes.....	53
4.3	Elemental Analysis Studies (CHN) and Mass Spectra (LCMS data)	55

4.4	Infrared Spectroscopy Study	56
4.5	NMR Spectra of intermediate compounds.....	60
4.5.1	¹ H NMR and ¹³ C NMR for intermediate compounds of 4,5-bis(alkoxy) benzene-1,2-diaminium chloride.....	60
4.5.2	¹ H and ¹³ C NMR for intermediate compounds of 2-(diformyl methylidene)-5-(alkoxy)-3,3-dimethyl-indole.....	64
4.6	¹ H and ¹³ C NMR for Macrocyclic compounds of dibenzotetraaza[14] annulene 6-alkyloxy.	67
4.7	¹ H and ¹³ C NMR for Nickel Complexes of Macrocyclic compounds of dibenzotetraaza [14]annulene 6-alkyloxy.....	72
4.8	Thermogravimetric Analysis (TGA).....	75
4.9	UV-Visible Spectra Studies.....	76
4.10	X-Ray Crystallography Studies.....	77
CHAPTER 5 : LIQUID CRYSTAL STUDIES.....		82
5.1	Optical Polarized Microscopy Studies (OPM).....	82
5.2	Differential Scanning Calorimetry (DSC) studies	87
CHAPTER 6 : CONCLUSION.....		90
LIST OF REFERENCES		92
APPENDIX.....		104
Appendix A: Mass Spectroscopy (LCMS QTOF)		104
Appendix B: IR spectrum.....		106
Appendix C: ¹ H NMR spectrum.....		115
Appendix D: ¹³ C NMR spectrum.....		129
Appendix F: UV-Vis spectrum		149
Appendix G: DSC Spectrum		150

LIST OF FIGURES

Figure 1.1: Dibenzotetraaza[14]annulenes (DBTAA)	1
Figure 1.2: 16-membered ring of porphyrin.....	2
Figure 1.3: New substituted dibenzotetraaza[14] annulenes.....	4
Figure 1.4: Crystal structure of meso-bis(5-hexyloxy-3,3-dimethylindoleninyl) dibenzotetraaza[14] annulene of nickel complex.....	4
Figure 1.5: New series macrocyclic ligands of DBTAA and its nickel complex.	6
Figure 2.1: 14-membered conjugated unsaturated macrocyclic ligands by Jager (1969)	8
Figure 2.2: Dibenzotetraaza[14]annulenes by Sigg et al. (1982).....	9
Figure 2.3: Discotic columnar liquid crystal structure for optical storage by Forget and Kitzerow (1997)	10
Figure 2.4: Liquid crystalline derivative of dibenzotetraaza[14]annulene by Grolik et al. (2006).....	11
Figure 2.5: Indolenine meso-Substituted Dibenzotetraaza[14]annulene by Khaledi et al. (2013).....	12
Figure 2.6: Nickel(II) Complex from Indolenine meso-Substituted Dibenzotetraaza[14] annulene by Khaledi et al. (2013)	13
Figure 2.7: Indole and indole derivatives.....	13
Figure 2.8: Fischer synthesis of indole	14
Figure 2.9: New series of D- π -A type organic dyes using indeno[1,2-b]indole.....	15
Figure 2.10: 2-aryl-6-(aryleneethynylene)-1H-indoles	15
Figure 2.11: Spiroindolinonaphthooxazine(SO) derivatives.....	16
Figure 2.12: Activated DMF by POCl ₃	17
Figure 2.13: Vilsmeier-Haack reaction on indolenine by Baradarani et al. (2006)	17
Figure 2.14: Two possible alternative explanations on formylation process.....	18
Figure 2.15: Benzene derivatives with six long n-alkyloxy tails	19

Figure 2.16: Image of the fan-like texture of discotic columnar under OPM. (Zheng et al., 2010). <i>The Image is reproduced with permission of the author.</i>	21
Figure 2.17: Columnar liquid crystal of N4-Macrocycles (Gregg et al., 1989).....	22
Figure 2.18: Substituted dibenzotetraza[14]annulenes containing divalent Ni, Pd, Pt, Co, or Cu.....	22
Figure 3.1: Overall Synthesis Route	25
Figure 3.2: Synthesis of 4,5-bis(alkoxy)benzene-1,2-diaminium chloride compounds.	26
Figure 3.3: Chemical structure of Compound 1	27
Figure 3.4: Chemical structure of Compound 2	28
Figure 3.5: Chemical structure of Compound 3	28
Figure 3.6: Chemical structure of Compound 4	29
Figure 3.7: Chemical structure of Compound 5	30
Figure 3.8: Chemical structure of Compound 6	30
Figure 3.9: Chemical structure of Compound 7	31
Figure 3.10: Chemical structure of Compound 8	31
Figure 3.11: Chemical structure of Compound 9	32
Figure 3.12: Chemical structure of Compound 10	33
Figure 3.13: Chemical structure of Compound 11	33
Figure 3.14: Chemical structure of Compound 12	33
Figure 3.15: Summary of synthesis of new compounds of 5-Alkoxy-2,3,3-trimethylindolenine compounds.....	34
Figure 3.16: Chemical structure of Compound 13	35
Figure 3.17: Chemical structure of Compound 14	35
Figure 3.18: Alkylation process by mean of phase transfer reaction using tetrabutylammonium bromide.....	36

Figure 3.19: Vilsmeier-Haack reaction to get series of 2-(diformylmethylidene)-5-(alkoxy)-3,3-dimethylindole	37
Figure 3.20: Chemical structure of Compound 19	38
Figure 3.21: Chemical structure of Compound 20	39
Figure 3.22: Chemical structure of Compound 21	39
Figure 3.23: Chemical structure of Compound 22	40
Figure 3.24: Condensation reaction of new series macrocyclic ligands of DBTAA.	41
Figure 3.25: Chemical structure of Macrocyclic ligand 23	42
Figure 3.26: Chemical structure of Macrocyclic ligand 24	43
Figure 3.27: Chemical structure of Macrocyclic ligand 25	44
Figure 3.28: Chemical structure of Macrocyclic ligand 26	45
Figure 3.29: Synthesis of nickel complex from Macrocyclic DBTAA 6-alkoxy.	46
Figure 3.30: Chemical structure of Complex 27	47
Figure 3.31: Chemical structure of Complex 28	48
Figure 3.32: Chemical structure of Complex 29	48
Figure 3.33: Synthesis of macrocyclic ligand and its nickel complex from <i>o</i> -phenylenediamine and 2-(diformylmethylidene)-5-(hexyloxy)-3,3-dimethylindole 19	50
Figure 4.1: Reaction Mechanism for Fischer indole synthesis. (Clayden et al., 2012)..	51
Figure 4.2: Activation of DMF molecule by POCl ₃	51
Figure 4.3: Rearrangement of 5-Alkoxy-2,3,3-trimethylindolenine	52
Figure 4.4: Reaction mechanism of the first attack from activated molecule of DMF on 5-alkoxy-2,3,3-trimethylindolenine	52
Figure 4.5: Reaction mechanism of the Second attack from activated molecule of DMF on 5-alkoxy-2,3,3-trimethylindolenine	53

Figure 4.6: Comparison between IR spectrum intermediate compound of diformyl, macrocyclic ligand and its nickel complex	59
Figure 4.7: Chemical structure for 1,2-Dialkyloxybenzene	60
Figure 4.8: ¹ H NMR spectra of compound 1	61
Figure 4.9: Chemical structure of 1,2-Dinitro-4,5-bis(alkyloxy)benzene.....	62
Figure 4.10: ¹ H NMR spectra of compound 8	62
Figure 4.11: ¹³ C NMR spectra of compound 8	63
Figure 4.12: Chemical structure of 4,5-bis(alkyloxy)benzene-1,2-diaminium chloride	63
Figure 4.13: Chemical structure for 2-(diformylmethylidene)-5-(alkoxy)-3,3-dimethyl-indole	64
Figure 4.14: ¹ H NMR spectra of compound 19	65
Figure 4.15: ¹ H NMR spectra 6.7-7.3ppm for compound 19	65
Figure 4.16: ¹ H NMR spectra 0.8-1.9ppm of compound 19	66
Figure 4.17: ¹³ C NMR spectra of compound 19	67
Figure 4.18: Chemical structure for Macrocyclic compounds of dibenzotetraaza[14]annulene 6-alkyloxy	67
Figure 4.19: ¹ H NMR spectra of compound 23	68
Figure 4.20: ¹ H NMR spectra 0.7-2.7ppm for compound 23	69
Figure 4.21: ¹³ C NMR spectrum of macrocyclic ligand 25	71
Figure 4.22: Chemical structure for Nickel Complexes of Macrocyclic compounds of dibenzotetraaza[14]annulene 6-alkyloxy	72
Figure 4.23: ¹ H NMR spectrum of complex 27	73
Figure 4.24: ¹³ C NMR spectrum (400 MHz, CDCl ₃) of Complex 27	74
Figure 4.25: UV-Vis spectra of macrocyclic ligand 25 and its complex 29	76
Figure 4.26: View of basic nickel complex 32 looking down a axis.	78
Figure 4.27: Default view on c* axis.	79

Figure 4.28: Packing diagram of nickel complex 32	80
Figure 5.1: Image from OPM for Macrocyclic ligand 23 at 182.2°C	83
Figure 5.2: Image from OPM for Macrocyclic ligand 24 at 179.1°C	83
Figure 5.3: Image from OPM for Complex 27 at 209.7°C	84
Figure 5.4: Image from OPM for Complex 25 at 177.5°C	85
Figure 5.5: Image from OPM for Macrocyclic ligand 26 at 159.8°C	85
Figure 5.6: Image from OPM for Complex 28 at 202.2 °C	86
Figure 5.7: Image from OPM for Complex 29 at 195.7°C	86
Figure 5.8: DSC measurement of macrocyclic ligand 24 on scanning rate 10°C/min. .	89

University of Malaya

LIST OF TABLE

Table 4.1: Physical properties of macrocyclic ligands and complexes.....	54
Table 4.2: Summary CHN data on new synthesized compounds.	55
Table 4.3: Summary of LCMS of new synthesized compounds.....	56
Table 4.4: Summary of IR spectra (refer to Appendix B).....	57
Table 4.5: Summary of TGA analysis on synthesized compounds.....	75
Table 4.6: Selected bond lengths (Å) and bond angles (°) for this nickel complex.	81
Table 5.1: DSC measurement of the macrocyclic ligands and complexes.....	88

LIST OF SYMBOLS AND ABBREVIATION

°C	degree Celsius
^{13}C NMR	^{13}C -Carbon Nuclear Magnetic Resonance
^1H NMR	^1H -Proton Nuclear Magnetic Resonance
Å	Angstrom
BBr_3	Boron tribromide
br	broad
$\text{CD}_2\text{Cl}_2-d_2$	deuterated dichloromethane
CDCl_3-d_1	deuterated chloroform
CHN	Carbon, Hydrogen, Nitrogen
d	doublet
DBTAA	Dibenzo tetraaza[14]annulene
DCM	Dichloromethane
dd	doublet-doublet
DMF	Dimethylformamide
DSC	Differential scanning calorimetry
FT-IR	Fourier-Transform infrared
g	gram
Hz	Hertz
J	Coupling constant
kJ/mol	kilo joule per mole
MHz	megahertz
mW	milli watts
nm	nanometre
OPM	Optical Polarized Microscopy

POCl_3	Phosphorus Oxychloride
ppm	parts per million
s	singlet
ss	singlet-singlet
t	triplet
TMS	Tetramethylsilane
UV-Vis	Ultraviolet-visible spectroscopy
w	weak
δ	NMR chemical shift
ΔH_f	enthalpy change of fusion

University of Malaya

CHAPTER 1 : INTRODUCTION

1.1 Introduction

Dibenzotetraaza[14]annulenes (DBTAA), as shown in Figure 1.1, belong to the class of tetraaza macrocycles that are of bioinorganic relevance (Miljanić et al., 2012; Reddy et al., 2012). They are known and appreciated for their synthetic accessibility and rich chemistry (de Sousa Sousa et al., 2015; Kaźmierska et al., 2013; Wang et al., 2013). DBTAA compounds are among the most extensively studied synthetic of macrocycles, mainly due to their resemblance to the naturally occurring porphyrins (Gawinkowski et al., 2010). Tetraazaannulene rings, especially when coordinated to metal centres, are good models of biological systems as well as the application of materials science (Mames et al., 2015; Zhao et al., 2008). Their complexes are also importance in enhancing various industrial applications and in a number of biological processes such as photosynthesis and dioxygen transport catalytic properties (Muena et al., 2008), potential applications as metal extractants (Basiuk et al., 2013), radiotherapeutic and medical imaging agents (Bhattacharjee et al., 2012) and potency towards DNA binders (Vinay Kumar et al., 2012) with a high potential in anti-tumor therapy (Stojković et al., 2010), has increased interest for investigation of the metal ion chemistry of these macrocyclic systems, as well as its cyclic ligand.

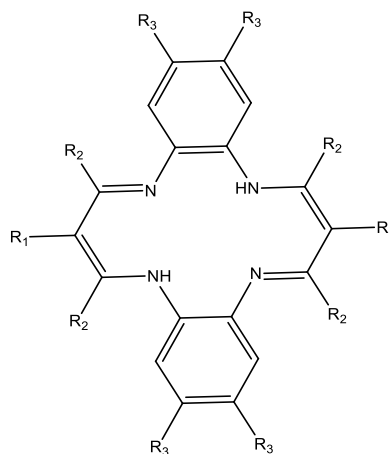


Figure 1.1: Dibenzotetraaza[14]annulenes (DBTAA)

Like porphyrins (Figure 1.2), DBTAA possesses an N₄ core that can accommodate various metal ions. However, compared with the 16-membered ring of porphyrin, their ring is composed of 14 atoms, which results in a relatively smaller N₄ core size (Yusoff et al., 2014; Zwolińska & Eilmes, 2016). It was shown that upon reaction with nickel (2+), the N₄ core was doubly deprotonated to accommodate the metal atom inside the cavity (Whyte et al., 2012).

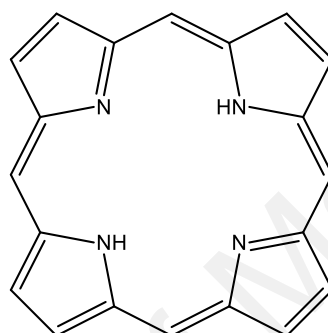


Figure 1.2: 16-membered ring of porphyrin

Khaledi et al. (2013) introduced a dibenzotetraaza[14]annulene bearing two 3,3-dimethylindoleninyl fragments at the meso positions (R_1), $R_2 = H$ (Figure 1.1). Similar to porphyrin, a number of first-row transition metals (II/III) can be inserted in the central cavity of dibenzotetraaza[14]annulenes. It also appeared that the introduction of four 3,7-dimethyloctyloxy substituents to the phenylene part of the macrocyclic core allowed for the generation of a liquid-crystalline behaviour (Senthilkumar et al., 2013; Zheng et al., 2010). In particular, mesogens based on chiral disc-like molecules have recently attracted considerable attention as systems exhibiting a helical supramolecular organisation of the mesophase. Therefore, they are responsible for a number of interesting properties (Lagerwall & Scalia, 2012; Wöhrle et al., 2016). Thus, ferroelectric switching, high charge-carrier mobility, exceptional second-order nonlinear optical susceptibilities and biomedical application were found to be associated in discotic columnar mesophases with a helical architecture (Mewis & Archibald, 2010; Pisula et al.,

2010; Reddy et al., 2014; Tanaka et al., 2012; Zalevsky & Abdulhalim, 2014; Zheng et al., 2010).

A number of known discotic liquid crystals are based on macrocyclic compounds, containing extended aromatic cores and large polyaromatic hydrocarbons (PAH), and show an intrinsic high tendency to aggregate into infinite one-dimensional columnar stacks (Feng et al., 2009; Śliwiński et al., 2004). The DBTAA core is nearly flat, and rich in π delocalised areas (Gawinkowski et al., 2010). Therefore, it seems to be well-suited to play the role of a disc-shaped tecton. In addition, peripheral reactivity and the capability of accommodating various substituents in the phenylene rings and imine carbons make this system very attractive for the designing and synthesizing materials-directed building blocks (Pathak et al., 2016; Rabaa et al., 2015).

Among the transition metal complexes of substituted dibenzotetraaza[14] annulenes, nickel complexes of it have been found to exhibit liquid crystalline properties. Hunziker (1985) and Forget and Veber (1997b) have studied their mesomorphic behaviour as a function of the structure, length and number of peripheral groups. An optical storage effect was later demonstrated in one of these mesomorphic nickel complexes (Forget & Kitzerow, 1997; Setia et al., 2016). Here, we report our results in preparing the new DBTAA-based discotic columnar liquid crystals mesophase. To promote molecular self-assembly as columnar in liquid crystal phases, we have designed and synthesized new conventional mesogenic molecules that have a rigid core, are flat and aromatic and are equipped with six flexible aliphatic side chains that surround the core. Herein, we describe a new liquid crystal based on a metal-free dibenzotetraaza[14] annulene macrocycle, bearing two meso 5-alkyloxy-3,3-dimethylindoleninyl substituents and four alkyloxy groups (6, 10, 12, 14 carbon chains) attached to *o*-phenylene moieties (Figure 1.3).

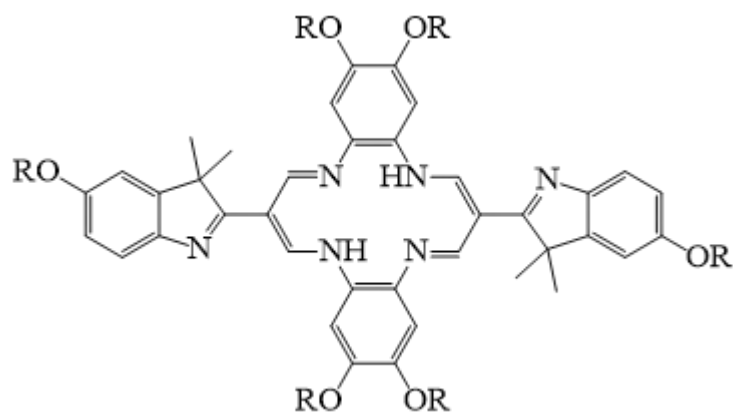


Figure 1.3: New substituted dibenzotetraaza[14] annulenes

The crystal structure of meso-bis(5-hexyloxy-3,3-dimethylindoleninyl) dibenzotetraaza[14] annulene of nickel complex as shown in Figure 1.4 is appeared flat and rich in π delocalised areas, and therefore seemed to be suitable to play the role of a disc-shaped building block. In addition, aromatic π - π stacking interactions, involving planar central moieties and meso-phenyl rings of neighbouring molecules, are clearly evidenced in the crystal structure published by Khaledi et al. (2013)

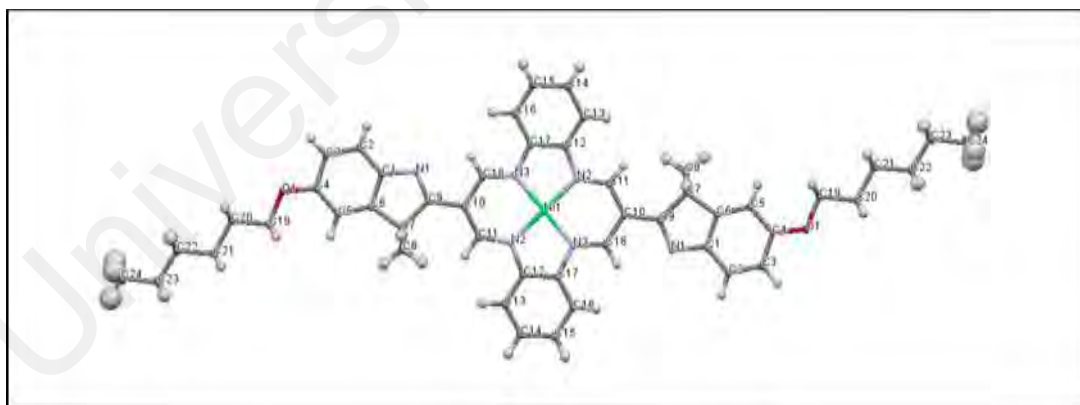


Figure 1.4: Crystal structure of meso-bis(5-hexyloxy-3,3-dimethylindoleninyl) dibenzotetraaza[14] annulene of nickel complex

Studies on mesomorphic materials have established that in the most often encountered columnar mesophases, the disc-like molecules self-assemble into columns by stacking one upon another and self-organise into various arrangements that differ in

the degree of order and in the two-dimensional symmetry of the column packing (Collings, 1990; Hirose et al., 2014; Rosen et al., 2009). In designing mesogens, self-assembly and self-organisation are of importance for inducing mesomorphic behaviour in discotic materials and are mostly influenced by the core structure, number and the length of flexible pendant chains that surround the discotic units (Donnio, 2014; Tschierske, 2013). We have selected nickel ions in designing these new metalomesogenic compounds as it will confirm the planarity of the central core of compounds, thus promoting the self-stacking arrangement of discotic columnar liquid crystal mesophase (Bin et al., 2010; Lee et al., 2012).

In this study, we have managed to synthesize a new liquid crystalline compound derived from dibenzotetraaza[14]annulene bearing two 3,3-dimethylindolenine compounds at the meso positions. Six aliphatic side chains consisting of 6, 10, 12, 14 carbon length have been attached surrounding the macrocyclic compounds. In order to produce such macrocyclic compounds, new substituted 2-(diformylmethylidene)-5-(alkoxy)-3,3-dimethylindole needs to be synthesized and then reacted with respective intermediate compounds of 4,5-bis(alkyloxy)benzene-1,2-diaminium chloride. Treatment of these new macrocyclic ligands with nickel(II) acetate will produce new metallomesogens compounds (Paquette et al., 2015; Shen et al., 2011).

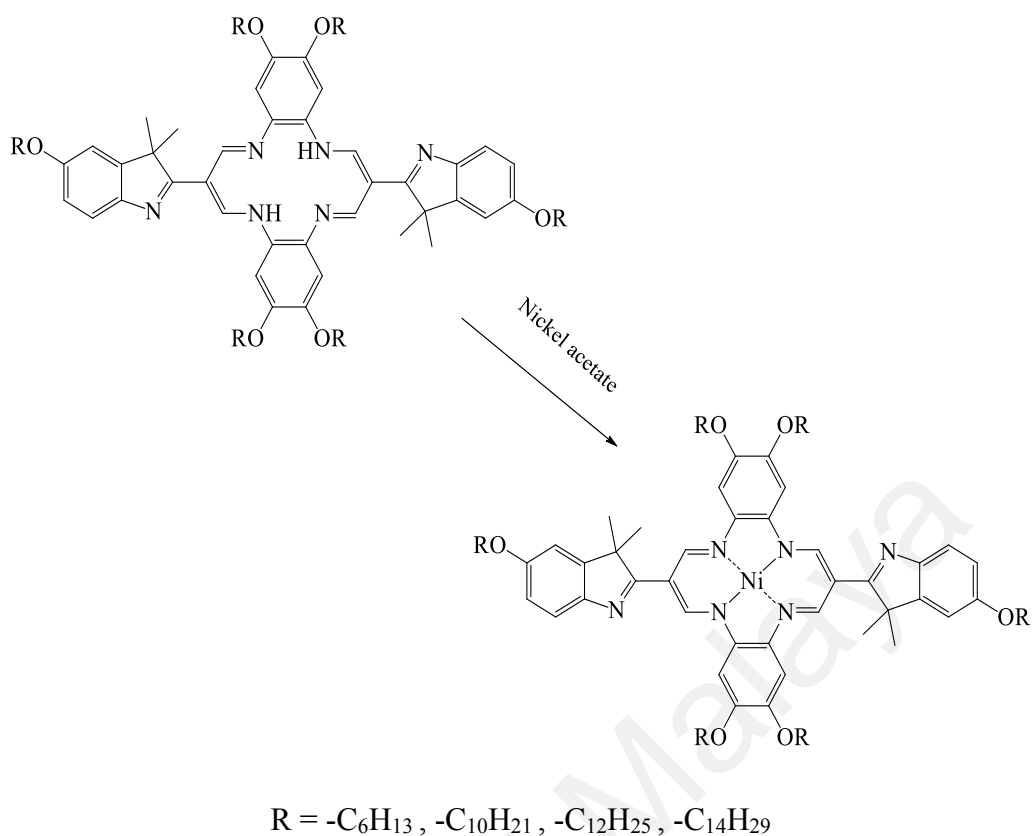


Figure 1.5: New series macrocyclic ligands of DBTAA and its nickel complex.

1.2 List of Research Objectives

This research was planned and carried out according to the listed objectives below:

1. To synthesize *o*-phenylenediamine derivatives with two alkoxy chains on positions 4 and 5 as intermediate compounds.
2. To synthesize new 2-(diformylmethylidene)-3,3-dimethylindole derivatives with one alkoxy chain on 5th position.
3. To synthesize a series of new macrocyclic ligands derived from indolenine meso-substituted dibenzotetraaza[14]annulene with six aliphatic alkyl chains (6,10,12 and 14 carbons) attached around the macrocyclic compounds.
4. To synthesize nickel complexes using the newly synthesized macrocyclic ligands.
5. To characterize the chemical structures of the new synthesized compounds by various physico-chemical techniques such as elemental analysis (CHNS), Fourier

transforms infrared spectroscopy (ATR-FTIR), nuclear magnetic resonance spectroscopy (^1H and ^{13}C NMR), ultraviolet-visible spectroscopy (UV-Vis), thermal gravimetric analysis (TGA), and single crystal X-ray crystallography.

6. To determine the liquid crystal properties of the synthesized compounds using optical polarized microscopy (OPM) and confirm by differential scanning calorimetry (DSC).

University of Malaya

CHAPTER 2 : LITERATURE REVIEW

2.1 Review On Dibenzotetraaza[14]Annulenes (DBTAA)

Research in synthetic macrocyclic compounds of dibenzotetraaza[14]annulenes (DBTAA), shown in Figure 2.1, was started way back in 1969 by German Chemist, Jager, E.G. The interest in this molecular structure results from the fact they are formally anti-aromatic, but at the same time structurally resemble the aromatic porphyrins (Honeybourne, 1973). The DBTAA have four special nitrogen donor atoms that are coplanar to each other, with a few double bonds which contribute π delocalized electrons from benzenoid rings and 1,3-diiminato fragments. Unlike porphyrins, macrocyclic DBTAA are Hückel anti-aromatic ($4n$) and have a 14-membered inner ring as compared to the larger 16-atom inner porphyrin ring (Ricciardi et al., 1995).

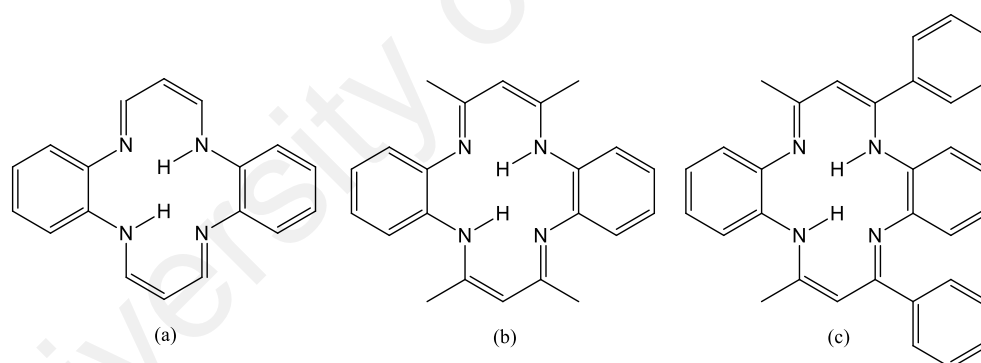


Figure 2.1: 14-membered conjugated unsaturated macrocyclic ligands by Jager (1969)

Macrocyclic DBTAA compounds are known to have potential applications, as they are relatively easy to synthesize, highly reactive at the meso positions, and capable of accommodating various substituents on the phenylene rings and as well as the diimine carbons. X-ray crystallographic studies have found that they adopt various conformations ranging from planar to saddle-shaped, depending on the ring substitution (Cotton & Czuchajowska, 1990). DBTAA are also suitable as ligands for transition metals and main group elements, which can offer a wide variety of coordination modes and geometries.

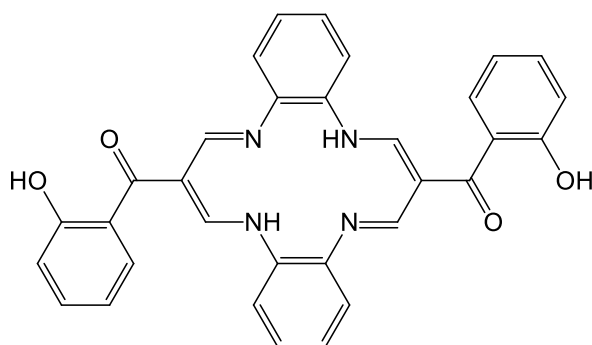


Figure 2.2: Dibenzotetraaza[14]annulenes by Sigg et al. (1982)

In 1982, a study on preparation on meso-substituted dibenzotetraaza[14]annulenes (Figure 2.2) was carried out (Sigg et al., 1982). The outcome on characterization is significant from the data collected by Hiller (1968), who was the first to report on non-template methods using *o*-phenylene diamines and either propynal or substituted acroleins for achieving DBTAA compounds. The six protons of the 14-membered ring form two identical A_2X systems, as two olefinic protons of the same chemical shift form trans-coupling with the same coupling constant (6Hz) with one amino proton to form a triplet peak in 1H NMR spectra (Hiller et al., 1968). This is an important characteristic for this type of ring system, whereas there are only two different chemical shifts for the two phenylenediamine aromatic rings and four for the salicyloyl aromatic rings (Honeybourne, 1974). These macrocyclic of DBTAA were highly symmetrical (D_{2h}) in the 1H NMR time scale. The macrocycle is eminently suitable for the formation of chelates with the transition metals, especially nickel and cobalt, as the ring system reacts well with the metal ion (Hiller et al., 1968).

Several studies on liquid crystalline materials have been carried out based on macrocyclic systems such as porphyrins, phthalocyanines, and azacrowns, including macrocyclic Schiff bases. Normally, this type of liquid crystalline macrocyclic has a rigid core, is mostly flat and contains aromatic groups, well surrounded by numbers of long

aliphatic side chains ranging from 4 to 8 chains. A few transition metal complexes of substituted dibenzotetraaza[14]annulenes (Mountford, 1998) have been found to demonstrate liquid crystalline properties on their mesomorphic phase, which were influenced by the core structure, length and number of peripheral groups. An optical storage effect was later demonstrated in one of the mesomorphic nickel complexes as shown in Figure 2.3 (Forget & Veber, 1997a).

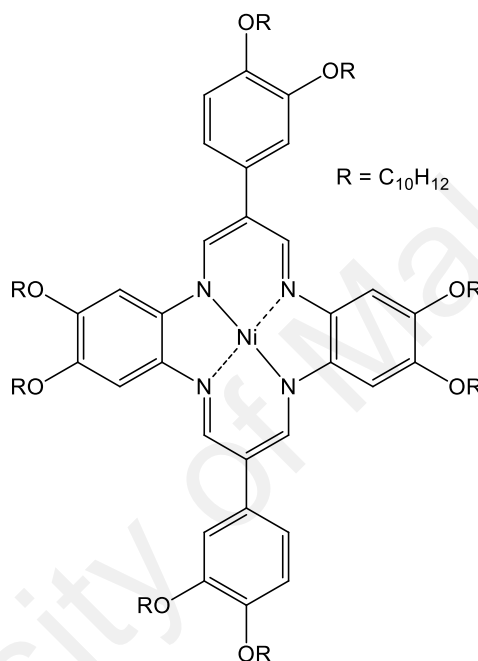


Figure 2.3: Discotic columnar liquid crystal structure for optical storage by Forget and Kitzerow (1997)

In 2010, a new invention of DBTAA compounds was patented, on a preparation method and its application in respect of an optical recording media. The dibenzotetraaza[14]annulene materials which are provided by the invention have the advantages of high luminous sensitivity, good thermal stability (TG decomposition temperature is more than 250°C), high solubility, easy dissolution and good crystallization resistance. The used of the compounds improved the recording performance of the discs, at the same time meeting the requirement of current BD-R and HD DVD-R optical disks on the recording media (Bin et al., 2010).

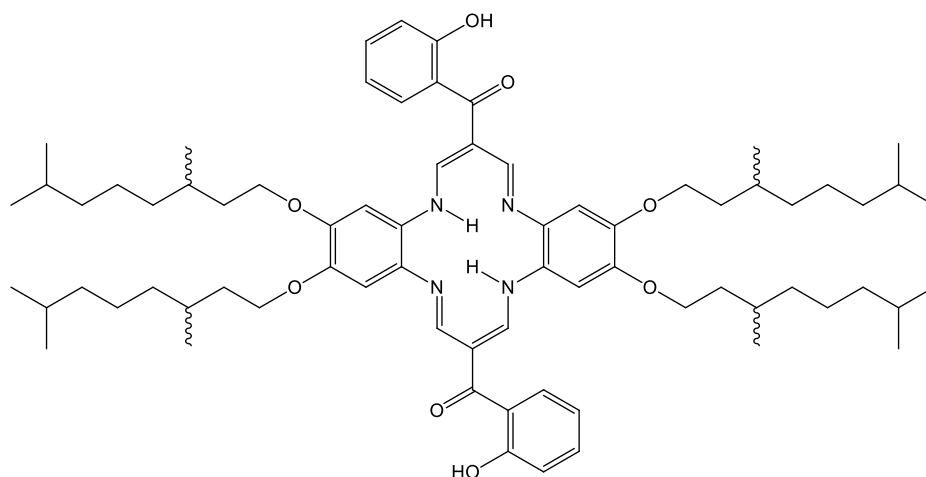


Figure 2.4: Liquid crystalline derivative of dibenzotetraaza[14]annulene by Grolik et al. (2006)

In designing mesogenic compounds that could undergo self-assembly and self-organisation, the most important factors to create discotic columnar substance are the influences of the structure and number of flexible pendant chains attached to the discotic units as in Figure 2.4. Therefore, in order to produce such supramolecular compounds, the final products were created with four additional peripheral substituents which were attached surrounding the macrocyclic core. Grolik et al. (2006) had also suggested that this work can be easily broadened to other derivatives of the meso substituted macrocycle, which would contribute to new liquid crystal compounds. Metallomesogens compounds derive from macrocyclic ligands of DBTAA are known to be suitable for dye-sensitized solar cell, organic or inorganic light-emitting diode, biosensor and optical storage.

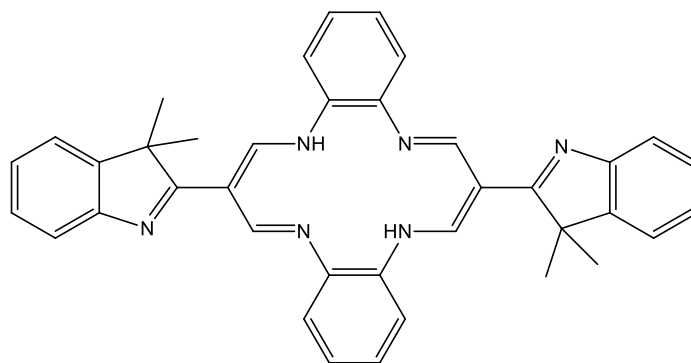


Figure 2.5: Indolenine meso-Substituted Dibenzotetraaza[14]annulene by Khaledi et al. (2013)

According to the Cambridge Structural Database, it is revealed that 248 dibenzotetraaza[14]annulene (DBTAA) metal complexes have been crystallographically characterized, but only 21 of those are for β -unsubstituted TAAs. (Allen, 2002). In 2013, Khaledi et al. had been successful in synthesizing a new β -unsubstituted dibenzotetraaza[14]annulene, bearing two 3,3-dimethylindolenine fragments at the meso positions (Figure 2.5). The Indolenine meso-Substituted Dibenzotetraaza[14]annulene (DBTAA) compounds were so rich in π -delocalized electron areas, that they were further introduced as a ligand to transition metals.

The presence of the electron withdrawing imine groups at the meso positions was found to enhance the reactivity of the axial coordination sites to form metal complexes as in Figure 2.6 (Khaledi et al., 2013).

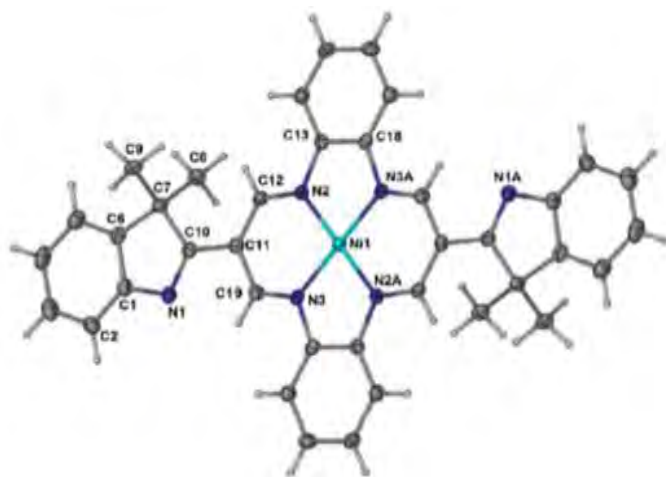


Figure 2.6: Nickel(II) Complex from Indolenine meso-Substituted Dibenzotetraaza[14]annulene by Khaledi et al. (2013)

2.2 Review Of Indole Compounds

Indole derivatives as a kind of important heteroaromatic compounds have been extensively investigated as electron donors in organic photoelectric materials due to their electron-rich structure, strong charge transfer, and flexible synthetic characteristics. Various efficient organic dyes employing indole-based fused heterocycle compounds including indolocarbazole, indoloquinoline, and triindole moieties have been researched and reported by Simoneau and Ganem (2005).

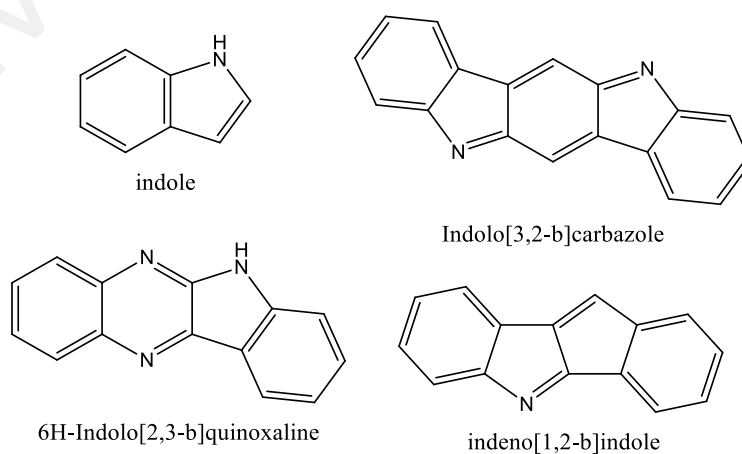


Figure 2.7: Indole and indole derivatives

Over a century ago Emil Fischer discovered that hydrazones **1**, prepared from arylhydrazines and enolizable ketones, rearranged upon heating in acid with loss of ammonia to afford indoles **4** (Figure 2.8). The process involved initial tautomerization to an ene-hydrazine **2** that underwent a [3,3]-sigmatropic rearrangement to **3** followed by ring closure and aromatization. We reasoned that identifying other reactant combinations leading to intermediates in Figure 2.8 might increase the dimensionality of the Fischer indole synthesis, thus widening its scope (Simoneau & Ganem, 2005).

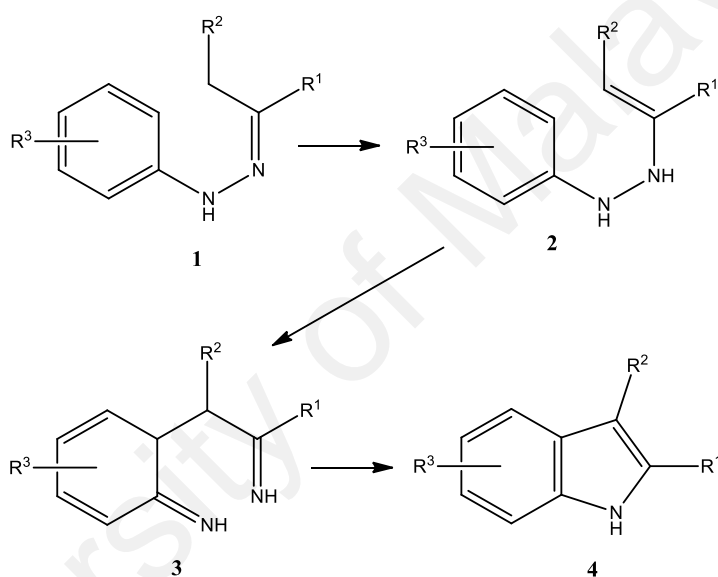


Figure 2.8: Fischer synthesis of indole

Besides Figure 2.9, this indole unit has been proven to be an excellent candidate for donor segment because of their strong light-capturing and electron-donating abilities. Some sensitizers containing indole unit as a donor have been synthesized and shown very promising performance (Qian et al., 2017).

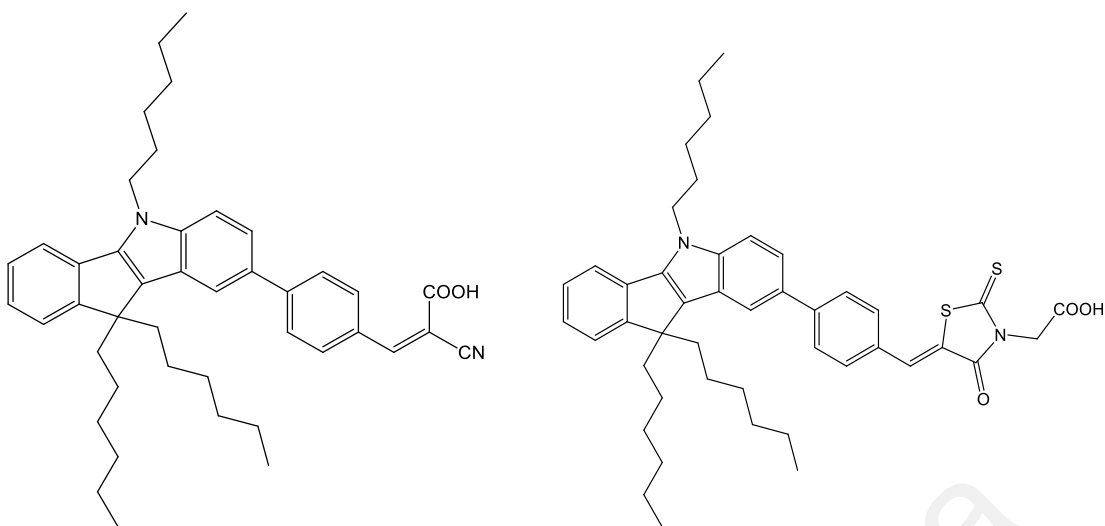


Figure 2.9: New series of D- π -A type organic dyes using indeno[1,2-b]indole

Qian et al. (2017) have designed and synthesized a new series of D- π -A type organic dyes using indeno[1,2-b]indole as the donor moiety (Figure 2.9). Indeno[1,2-b]indole can be considered as an indole unit fused with an indene unit, and the expanded conjugated system is beneficial for electron delocalization. The alkyl groups introduced on the indene moiety present a certain angle with the indenoindole plane which is in favour of suppressing the intermolecular aggregation of dye molecules and improving photovoltaic performances.

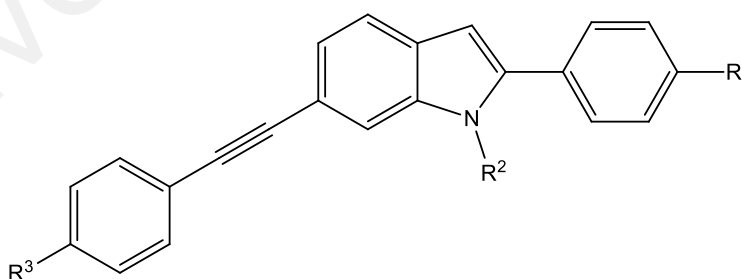


Figure 2.10: 2-aryl-6-(aryleneethynylene)-1H-indoles

Fluorescent indole derivatives Figure 2.10 are common structures used for the design of fluorescent probes for a myriad of analytical applications. Some of the compounds display nonlinear optics and have served to prepare two photon fluorescent

probes for cellular imaging and have used for photothermal ablation of cancer cells. Indole-derived compounds have also display photochromism and electroluminescence and thus have the potential for application in optoelectronic materials and solar cells.

Based on the high fluorescence of 2-arylindoles, more derivatives with an additional structural group that could expand the conjugated system and modifies its properties. The arylalkyne moiety was chosen for its well-documented participation in aryleneethynylene (AE) chromophores of high quantum yield. This led to the preparation of 2-aryl-6-(aryleneethynylene)-1H-indoles of Figure 2.10 for photophysical and electronic properties of highly fluorescent compounds (Flores-Jarillo et al., 2016).

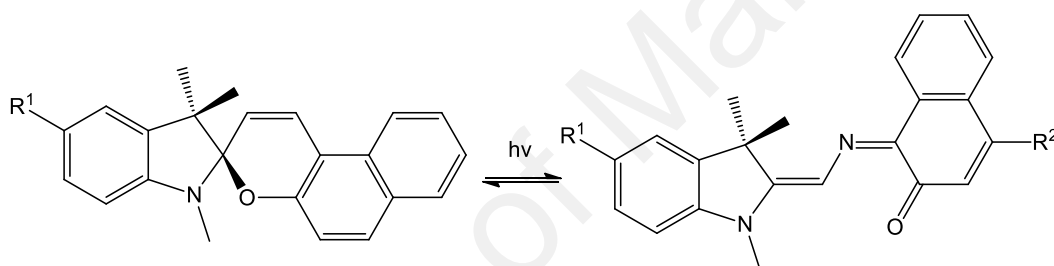


Figure 2.11: Spiroindolinonaphthooxazine(SO) derivatives

Organic photochromic materials have been widely investigated because of their potential applications in molecular photonic devices such as optical memories and switching devices. Among all kinds of photochromic compounds, because of the ability to give intense photo colouration, fast thermal relaxation and excellent fatigue resistance, spiroindolinonaphthooxazine (SO) derivatives (Figure 2.11) were a most promising candidate for applications as multifunctional optoelectronic materials. The photochromism of SO derivatives is due to the photochemical cleavage of the spiro C-O bond upon UV light irradiation, which leads to the extension of π -conjugation in the colored photomerocyanine (PMC) and thus shifts the absorption to the visible region (Li et al., 2015).

2.3 Review Of Diformylindolenine

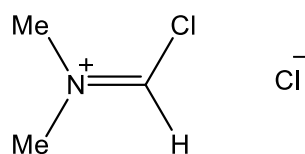


Figure 2.12: Activated DMF by POCl_3

The recognition of the power of the species produced by the combination of phosphoryl chloride with the amide of a secondary amine as shown in Figure 2.12. N-methylformanilide and dimethylformamide have been most often utilised its origins in a paper in 1896 (Meth-Cohn & Tarnowski, 1982). The process has been clarified by Vilsmeier and Haack (1927) and made it into a widely used regimen for the acylation, especially formylation of reactive aromatic and hetero-aromatic compounds, and indeed, non-aromatic compounds. The reaction of the amide with phosphorus oxychloride produces an electrophilic iminium cation. The subsequent electrophilic aromatic substitution produces an iminium ion intermediate, which aqueous alkali is used to hydrolyse the initial product of the desired aryl ketone or aryl aldehyde.

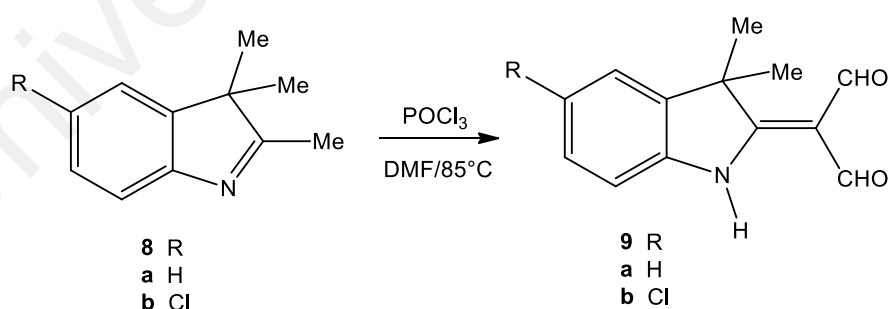


Figure 2.13: Vilsmeier-Haack reaction on indolenine by Baradarani et al. (2006)

Baradarani et al. (2006) have used the standard interpretation of the Vilsmeier reaction sequence in their studies, there seem to be two possible alternative explanations for the formation of products **9** (Figure 2.13). One possibility is that formylation does not take place on nitrogen, but that a small equilibrium concentration of the enamine tautomer **10** is successively C-substituted twice and thus, that before hydrolysis, species **11** is present. Alternatively, if the electrophilic attack at nitrogen is the first step, an intermediate of form **12** would have to be present before hydrolysis. They favour the former explanation though they do not have direct evidence for the tautomeric equilibrium, $8 \rightleftharpoons 10$ (Figure 2.14).

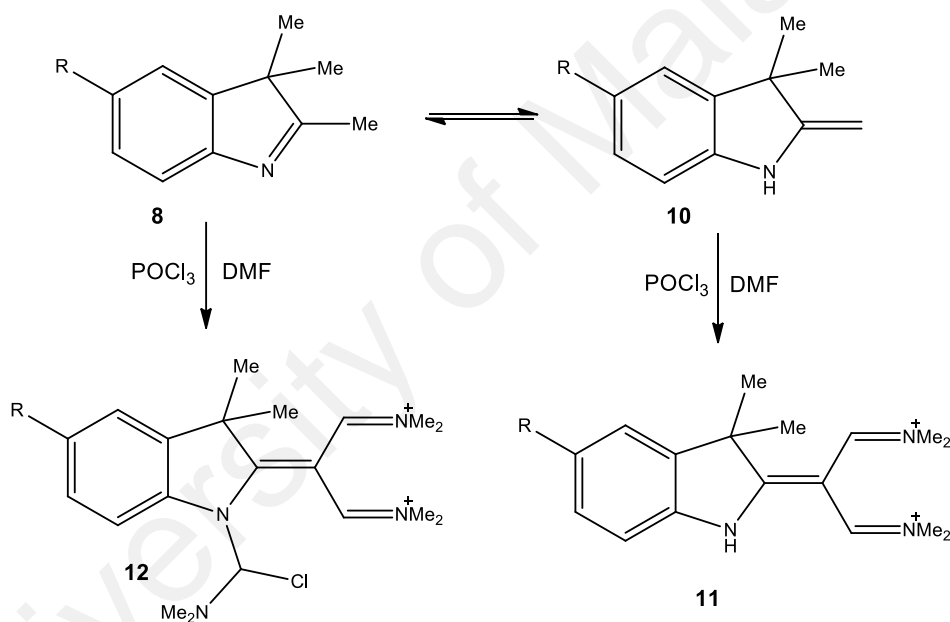


Figure 2.14: Two possible alternative explanations on formylation process

2.4 Review on Columnar Liquid Crystal

Liquid crystals form a state of matter intermediate between the solid and the liquid. The terms mesomorph (Greek, mesos morphe, between two states, forms) and mesophase are also used; a mesogen is a molecule which gives rise to a mesophase (Giroud-Godquin & Maitlis, 1991). Organic liquid crystals have been known for over a century. They can be divided into two broad families, the thermotropic and the lyotropic.

Thermotropic liquid crystals change phase on heating or cooling; the crystal phase melts to the mesophase, which then clears to the isotropic liquid at a higher temperature. Some exhibit polymorphism: they show several mesophases. Lyotropic phases are formed by molecules in a solvent (generally water) and the appearance of the mesophase is controlled by the concentration.

In a thermotropic mesophase, the positional order is largely absent, giving a fluidity, while some orientational order is retained, giving the anisotropy. The transition from the crystal to the mesophase is often termed the melting point, and that from the highest mesophase to the isotropic, the clearing point, reflecting the fact that mesophases often appear turbid while the isotropic liquid is clear.

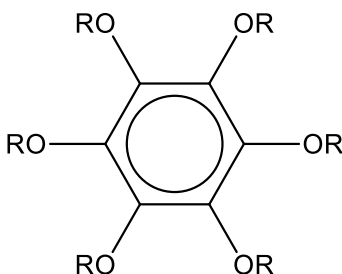


Figure 2.15: Benzene derivatives with six long n-alkyloxy tails

Discotic liquid crystalline phases are obtained with disk-like molecules where the director is perpendicular to the molecular plane; columnar and nematic as well as other

types are known. Typical organic discotics are benzene derivatives (Figure 2.15) with six long n-alkyloxy tails; many metallomesogens (such as those based on phthalocyanine, porphyrin, or even P-diketonate ligands) also form discotic phases (Gaspard et al., 1985). The two-dimensional network of such a columnar mesophase can be hexagonal, rectangular, or oblique, and the molecules can be either ordered or disordered along the long axes of the columns.

To exhibit liquid crystalline properties organic compounds require strongly polarizable groups, such as aromatic rings esters, or other oxy- or nitrile-functions. Rod-like thermotropic mesogens also require a long rigid group (often phenyl rings which form a core), while a rigid conjugated platelike grouping is usually associated with the core of a discotic mesogen. Both types need several long flexible n-alkyl- (or n-alkyloxy-) tails (R) as in Figure 2.15 (Markovitsi et al., 1984). The rod- or disk-like shapes, together with the polarizable groups, increase the molecular anisotropy and facilitate the formation of liquid crystal phases.

The characterization of thermotropic mesophases relies first, on optical microscopy, where the different phases show characteristic textures when viewed between crossed polarizers, as the temperature is changed. Mixing with a known mesophase is widely used to confirm the observations since two identical mesophases are frequently miscible. These optical methods are complemented by Differential Scanning Calorimetry (DSC), and by low angle X-ray scattering in the mesophase. Figure 2.16 shows the fan-like texture by Zheng et al. (2010)

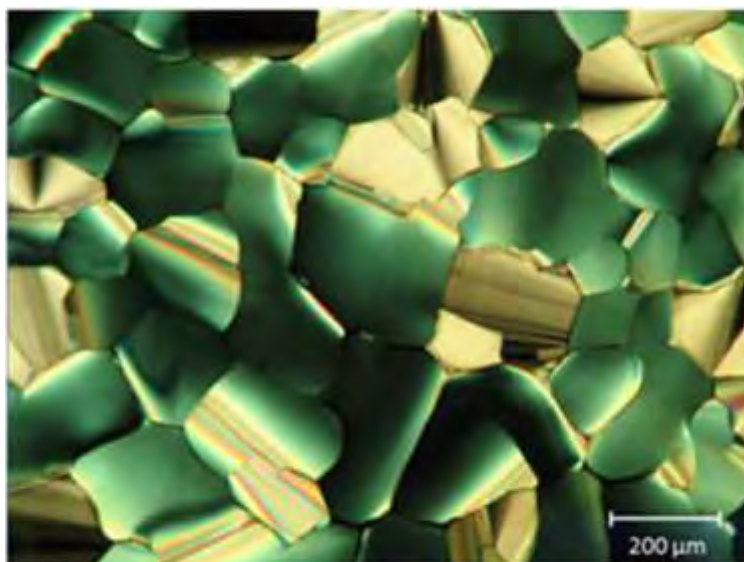


Figure 2.16: Image of the fan-like texture of discotic columnar under OPM. (Zheng et al., 2010). *The Image is reproduced with permission of the author.*

2.5 Review On Metallomesogens Columnar Liquid Crystal Of N₄-Macrocycles

Mesogenic metal-containing porphyrin complexes (R = CH, OH, M = Cu, Cd, Zn, and Pd) have been reported, as well as some which are not mesogenic but which, on mixing with long-chain alkanes or n-alkyl halides, form monotropic mesophases. The disk-like octadodecyltetrapyrzainoporphyrazine (Figure 2.17) (R = C₁₂H₂₅) and its copper complex show discotic mesophases (Gregg et al., 1989). Although the structure of this ligand differs little from that of its copper complex, there is still a change of mesomorphic character. The former shows a hexagonal disordered columnar mesophase (D_{hd}) between 118 and 238°C, the decomposition temperature, while the copper complex has a rectangular disordered columnar mesophase (D_{rd}) between 114°C and the decomposition temperature 288°C (Gaspard et al., 1985).

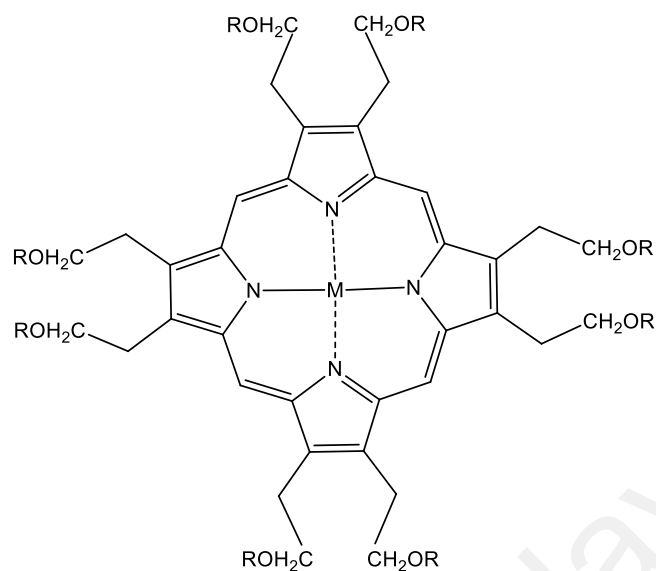


Figure 2.17: Columnar liquid crystal of N4-Macrocycles (Gregg et al., 1989)

Discotic phases have been reported in a patent for a series of substituted dibenzotetraza[14]annulenes (Figure 2.18) containing divalent Ni, Pd, Pt, Co, or Cu. The complexes have been considered for use in electro- or thermo-optical displays (Hunziker, 1985).

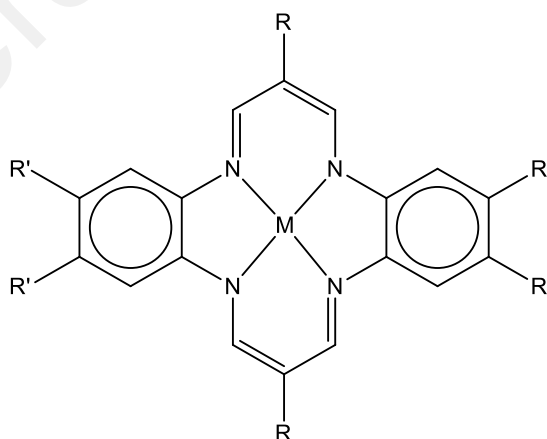


Figure 2.18: Substituted dibenzotetraza[14]annulenes containing divalent Ni, Pd, Pt, Co, or Cu

The use of liquid crystalline host materials containing coloured compounds, which absorb laser light and cause local heating, has been considered for laser addressed devices. The brightly coloured phthalocyanines, their benzo-homologues (the naphthalocynines), and eight complexes with Cu, and one each with Ni and Zn have been investigated for this purpose. Major changes in spectra are achieved by introduction of nuclear alkyloxy substituents; changing the metals offers the opportunity for further spectral fine tuning (Giroud-Godquin & Maitlis, 1991).

University of Malaya

CHAPTER 3 : RESEARCH METHODOLOGY

3.1 Experimental

Catechol, 4-methoxy phenylhydrazine hydrochloride, tin(II) chloride dihydrate and tetrabutylammonium bromide were purchased from Fisher Scientific, whereas boron tribromide from Merck chemicals company was available courtesy of other research groups, as this reagent can no longer be purchased because its import is banned in Malaysia. Ethanol was distilled prior to use. Melting points of the new synthesized compounds were determined by open capillary melting point apparatus without further corrections. Mass spectroscopy analysis was done using LCMS Agilent Technologies 6550 iFunnel Q-TOF LC/MS on positive ions and acetonitrile (100%) as the mobile phase. Microanalyses were carried out on a Perkin Elmer 2400 elemental analyzer. The IR spectra were taken on a Perkin Elmer Spectrum 400 ATR-FT-IR spectrometer. NMR spectra were recorded on a JEOL ECX 400 MHz FT-NMR spectrometer. Chemical shifts were given in δ values (ppm) using TMS as the internal standard. The electronic spectra were measured using Shimadzu UV-3600 UV-Vis-NIR spectrophotometer in the region 200-1200 nm. X-ray diffraction data were collected on a Bruker APEX II CCD diffractometer using Mo $K\alpha$ radiation. The structures were solved by direct methods and refined by a full-matrix least-squares procedure based on F^2 .

3.2 Synthesis

3.2.1 Overall Synthesis Route

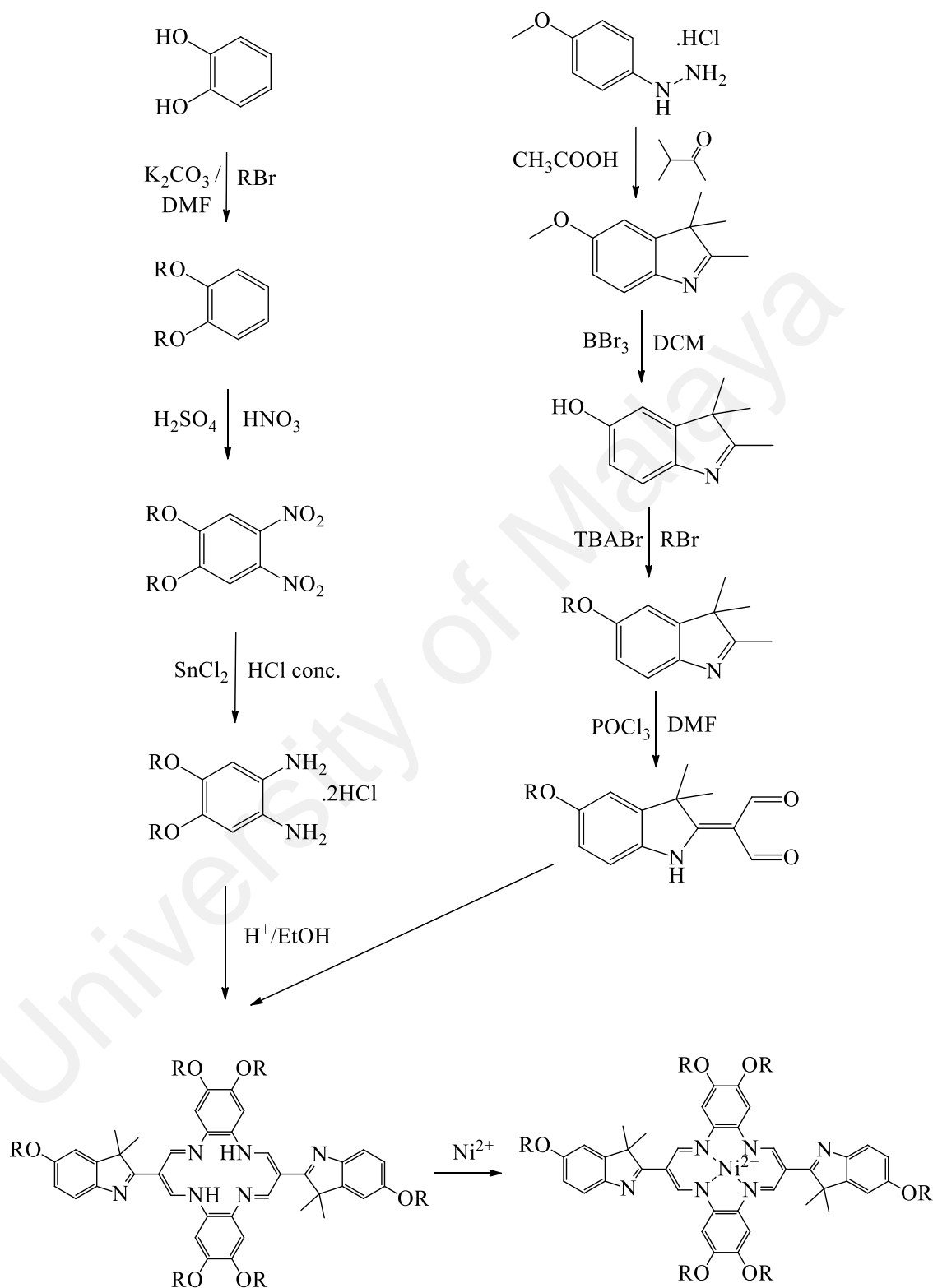


Figure 3.1: Overall Synthesis Route

3.2.2 Synthesis of alkylated Catechol intermediate enroute to 1,2-Dialkyloxybenzene

General procedure: In a three-neck round-bottomed flask (1 L) fitted with a condenser and a dropping funnel, catechol (227.0 mmol, 1 equiv.) and K_2CO_3 (62.75 g, 454.0 mmol, 2 equiv.) were stirred at room temperature in DMF (600 ml) for 50 min under a nitrogen atmosphere. 1-Alkylbromide (454.0 mmol, 2 equiv.) was added dropwise to the turquoise suspension. After stirring for 30 min at room temperature, the mixture was heated to $80^\circ C$ and refluxed overnight. Upon cooling, the mixture was added with dichloromethane (DCM) and the organic layer was collected, then washed with water (2 x 100 ml) and brine (2 x 50 ml). Anhydrous $MgSO_4$ was used to dry the organic layer, then DCM was removed via rotary evaporator and the product was collected as an oily substance. This product was used for further steps without purification.

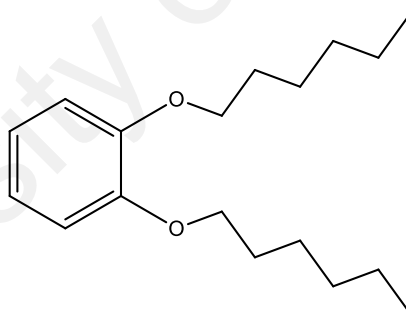


Figure 3.3: Chemical structure of Compound 1

1,2-Dihexyloxybenzene **1**. Brown oily solid. Yield 49.30 g (78 %). $C_{18}H_{30}O_2$ (278.43) 1H NMR (400 MHz, $CDCl_3$) δ (ppm): 0.87 (t, $J = 6.8$ Hz, $6H = 2(-CH_3)$), 1.30–1.33 (m, $8H = 2(-CH_2-)_2$), 1.41–1.47 (m, $4H = 2(-CH_2-)$), 1.75–1.82 (m, $4H = 2(-CH_2-)$), 3.97 (t, $J = 6.8$ Hz, $4H = 2(-CH_2O-)$), 6.86 (s, $4H = ArH$); ^{13}C NMR (400 MHz, $CDCl_3$, δ ppm): 149.29 (Car–O), 121.08, 114.13 (Car), 69.23 ($-CH_2-O$), 31.72 (CH_2), 29.41 ($-CH_2$), 23.83, 22.72 ($-CH_2$), 14.12 ($-CH_3$)

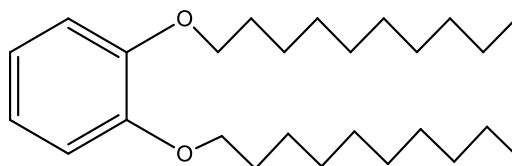


Figure 3.4: Chemical structure of Compound 2

1,2-Didecyloxybenzene **2**. Brown oily solid. Yield 66.50 g (75 %). $C_{26}H_{46}O_2$ (390.64). 1H NMR (400 MHz, $CDCl_3$) δ (ppm): 0.92 (t, $J = 6.8\text{Hz}$, $6H = 2(-CH_3)$), 1.32 (b, $8H = 2(-CH_2-)_2$), 1.51–1.48 (m, $24H = 2(-CH_2-)$), 1.80–1.88 (m, $4H = 2(-CH_2-)$), 4.01 (t, $J = 6.8\text{Hz}$, $4H = 2(-CH_2O-)$), 6.90 (s, $4H = ArH$); ^{13}C NMR (400 MHz, $CDCl_3$, δ ppm): 149.41 (Car–O), 121.11, 114.23 (Car), 69.34 ($-CH_2-O$), 32.09, 29.82, 29.77, 29.62, 29.54, 26.24, 22.84, ($-CH_2$), 14.23 ($-CH_3$)

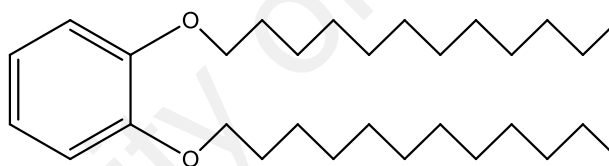


Figure 3.5: Chemical structure of Compound 3

1,2-Didodecyloxybenzene **3**. Brown oily solid. Yield 77.07 g (76 %). $C_{30}H_{54}O_2$ (446.75). 1H NMR (400 MHz, $CDCl_3$) δ (ppm): 0.86 (t, $J = 6.8\text{Hz}$, $6H = 2(-CH_3)$), 1.30–1.33 (m, $32H = 2(-CH_2-)_2$), 1.40–1.48 (m, $4H = 2(-CH_2-)$), 1.75–1.82 (m, $4H = 2(-CH_2-)$), 3.97 (t, $J = 6.6\text{Hz}$, $4H = 2(-CH_2O-)$), 6.86 (s, $4H = ArH$); ^{13}C NMR (400 MHz, $CDCl_3$, δ ppm): 149.27 (Car–O), 121.07, 114.14 (Car), 69.34 ($-CH_2-O$), 32.02, 29.80, 29.73, 29.68, 29.62, 29.54, 29.46, 29.43, 26.14, 22.78, ($-CH_2$), 14.21 ($-CH_3$)

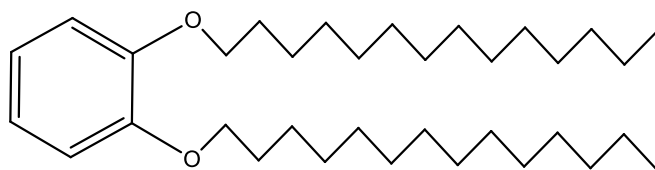


Figure 3.6: Chemical structure of Compound 4

1,2-Ditetradecyloxybenzene **4**. Brown oily solid. Yield 87.90 g (77 %). $C_{34}H_{62}O_2$ (502.85). 1H NMR (400 MHz, $CDCl_3$) δ (ppm): 0.87 (t, $J = 6.8\text{Hz}$, $6H = 2(-CH_3)$), 1.30–1.33 (m, $40H = 2(-CH_2-)_2$), 1.40–1.49 (m, $4H = 2(-CH_2-)$), 1.76–1.83 (m, $4H = 2(-CH_2-)$), 3.97 (t, $J = 6.8\text{Hz}$, $4H = 2(-CH_2O-)$), 6.87 (s, $4H = ArH$); ^{13}C NMR (400 MHz, $CDCl_3$, δ ppm): 149.32 ($Car-O$), 121.07, 114.19 (Car), 69.36 ($-CH_2-O$), 32.03, 29.81, 29.74, 29.55, 29.46, 26.15, 22.79 ($-CH_2$), 14.21 ($-CH_3$)

3.2.3 Nitration of bis(alkyloxy)benzenes to produce intermediate compounds of 1,2-Dinitro-4,5-bis (alkyloxy)benzene

General procedure: A solution of bis(alkyloxy)benzene (9.1 mmol) in dichloromethane (50 ml) was added dropwise to vigorously stirred concentrated nitric acid (20 ml) over a period of 30-40 min in an ice bath. Then concentrated sulfuric acid (10 ml) was added slowly in portions with continuous stirring for 2 h under nitrogen atmosphere at room temperature. The reaction mixture was next poured onto crushed ice and the resultant suspension was extracted with dichloromethane (3 x 50 ml). The organic layer was washed thoroughly with saturated aqueous sodium carbonate, then with water, and finally dried over anhydrous $MgSO_4$. The solvent was evaporated to give a crude product which was crystallized from ethanol.

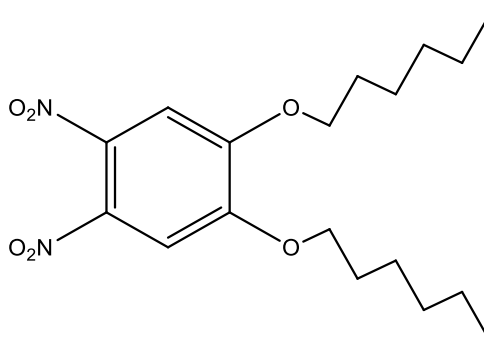


Figure 3.7: Chemical structure of Compound **5**

1,2-Dinitro-4,5-bis(hexyloxy)benzene **5**. Pale-yellow crystals, yield 2.68g (80%).

$C_{18}H_{28}N_2O_6$ (368.42). 1H NMR (400 MHz, $CDCl_3$) δ (ppm): 0.86 (t, $J = 6.8$ Hz, 6H = 2(- CH_3)), 1.25 (s, 8H = 2(- CH_2 -) $_2$), 1.43-1.48 (m, 4H = 2(- CH_2 -)), 1.82-1.87 (m, 4H = 2(- CH_2 -)), 4.08 (t, $J = 6.4$ Hz, 4H = 2(- OCH_2 -)), 7.28 (s, 2H = ArH). ^{13}C NMR (400 MHz, $CDCl_3$) δ (ppm): 151.88, 136.52, 107.92 (Ar), 70.26 (- OCH_2 -), 31.45, 28.73, 25.60, 22.60 (- CH_2 -), 14.04 (- CH_3).

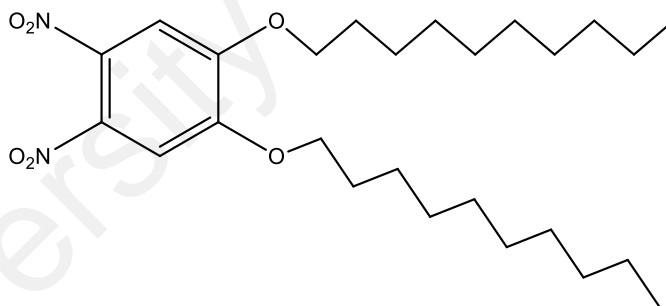


Figure 3.8: Chemical structure of Compound **6**

1,2-Dinitro-4,5-bis(decyloxy)benzene **6**. Pale-yellow crystals, yield 3.46g (79%).

$C_{26}H_{44}N_2O_6$ (480.64). 1H NMR (400 MHz, $CDCl_3$) δ (ppm): 0.86 (t, $J = 6.8$ Hz, 6H = 2(- CH_3)), 1.25 (s, 24H = 2(- CH_2 -) $_6$), 1.43-1.48 (m, 4H = 2(- CH_2 -)), 1.82-1.87 (m, 4H = 2(- CH_2 -)), 4.08 (t, $J = 6.4$ Hz, 4H = 2(- OCH_2 -)), 7.28 (s, 2H = ArH). ^{13}C NMR (400 MHz, $CDCl_3$) δ (ppm): 151.87, 136.53, 107.94 (Ar), 70.27 (- OCH_2 -), 32.15, 31.98, 29.62, 29.41, 29.31, 28.77, 25.89, 25.67, 22.92, 22.76 (- CH_2 -), 14.20 (- CH_3).

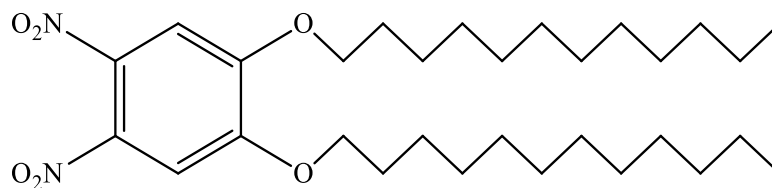


Figure 3.9: Chemical structure of Compound 7

1,2-Dinitro-4,5-bis(dodecyloxy)benzene **7**. Pale-yellow crystals, yield 3.81 g (78%).

$C_{30}H_{52}N_2O_6$ (536.74). 1H NMR (400 MHz, $CDCl_3$) δ (ppm): 0.86 (t, $J = 6.8$ Hz, 6H = 2(- CH_3)), 1.25 (s, 32H = 2(- CH_2 -) $_8$), 1.43-1.48 (m, 4H = 2(- CH_2 -)), 1.82-1.87 (m, 4H = 2(- CH_2 -)), 4.08 (t, $J = 6.4$ Hz, 4H = 2(- OCH_2 -)), 7.28 (s, 2H = ArH). ^{13}C NMR (400 MHz, $CDCl_3$) δ (ppm): 151.86 (-NC=), 136.53(-OC=), 107.93 (Ar), 70.27 (- OCH_2 -), 32.01, 29.76, 29.74, 29.66, 29.64, 29.44, 29.32, 28.77, 25.90, 25.71, 22.78 (- CH_2 -), 14.21 (- CH_3).



Figure 3.10: Chemical structure of Compound 8

1,2-Dinitro-4,5-bis(tetradecyloxy)benzene **8**. Pale-yellow crystals, yield 4.05g (75%).

$C_{34}H_{60}N_2O_6$ (592.85). 1H NMR (400 MHz, $CDCl_3$) δ (ppm): 0.86 (t, $J = 6.8$ Hz, 6H = 2(- CH_3)), 1.25 (s, 40H = 2(- CH_2 -) $_{10}$), 1.43-1.48 (m, 4H = 2(- CH_2 -)), 1.82-1.87 (m, 4H = 2(- CH_2 -)), 4.08 (t, $J = 6.4$ Hz, 4H = 2(- OCH_2 -)), 7.28 (s, 2H = ArH). 151.86 (-NC=), 136.55 (-OC=), 107.93 (Ar), 70.27 (- OCH_2 -), 32.01, 29.79, 29.66, 29.45, 29.32, 28.77, 25.90, 22.78 (- CH_2 -), 14.21 (- CH_3).

3.2.4 Reduction of 1,2-Dinitro-4,5-bis(alkyloxy)benzene to produce 4,5-bis(alkyloxy)benzene-1,2-diamminium chloride compounds.

General procedure: A mixture of 1,2-dinitro-4,5-bis(alkyloxy)benzene (3.37 mmol) and tin(II) chloride dehydrate (26.9 mmol) in ethanol (50 ml) and concentrated hydrochloric acid (20 ml) was heated to 85°C under nitrogen atmosphere, overnight. After cooled to room temperature, the product was poured to 100 ml CH₂Cl₂ and the mixtures were made basic (pH 9-11) with 2M NaOH solution. CH₂Cl₂ layer was collected, then the aqueous layer further extracted with 2 x 50 CH₂Cl₂. Finally, collected CH₂Cl₂ was dried over anhydrous MgSO₄. The solvent was removed using rotary evaporator to give a crude product, used directly (unstable) for the next reaction.

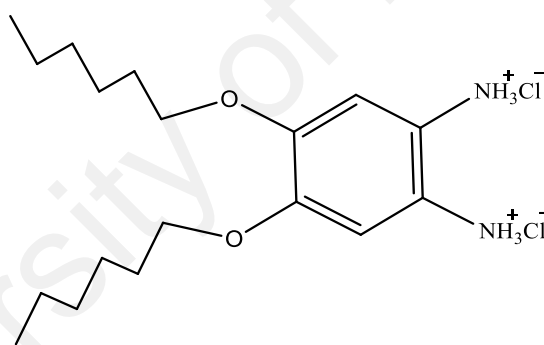


Figure 3.11: Chemical structure of Compound **9**

4,5-bis(hexyloxy)benzene-1,2-diamminium chloride **9**. C₁₈H₃₄Cl₂N₂O₂ (382.38). Yield: 0.97g (75%), greenish solid.

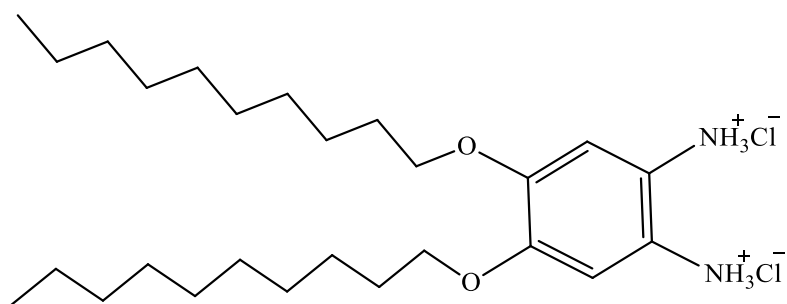


Figure 3.12: Chemical structure of Compound 10

4,5-bis(decyloxy)benzene-1,2-diamminium chloride **10**. $C_{26}H_{50}Cl_2N_2O_2$ (493.59). Yield: 1.21g (73%), greenish solid.

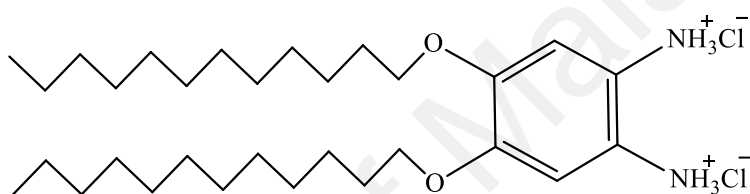


Figure 3.13: Chemical structure of Compound 11

4,5-bis(dodecyloxy)benzene-1,2-diamminium chloride **11**. $C_{30}H_{58}Cl_2N_2O_2$ (549.70). Yield: 1.30g (70%), greenish solid.

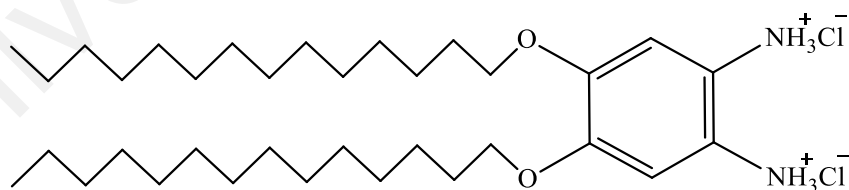


Figure 3.14: Chemical structure of Compound 12

4,5-bis(tetradecyloxy)benzene-1,2-diamminium chloride **12**. $C_{34}H_{66}Cl_2N_2O_2$ (605.81). Yield: 1.33g (65%), greenish solid.

3.3 Synthesis of intermediate compounds of 2-(diformylmethylidene)-5-alkoxy-3,3-dimethylindole

A series of intermediate compounds derived from 2-(diformylmethylidene)-5-alkoxy-3,3-dimethylindole have been synthesized with four different lengths of alkyl chains.

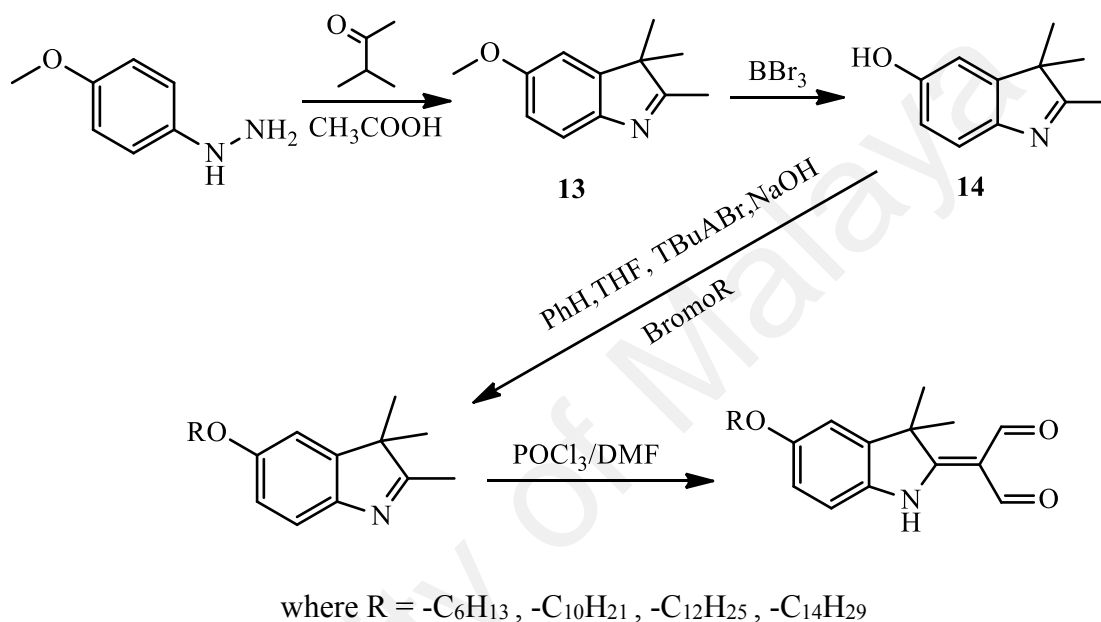


Figure 3.15: Summary of synthesis of new compounds of 5-Alkoxy-2,3,3-trimethylindolenine compounds

3.3.1 Fisher synthesis of 5-methoxy-2, 3, 3-trimethylindoline 13

General procedure: Compound 5-methoxy-2,3,3-trimethylindoline **13** was synthesized using fisher synthesis on 4-methoxy phenylhydrazine hydrochloride and methyl isopropyl ketone in ethanol. Demethylation of compound **13** was done using BBr₃ reagent in cooled methylene chloride to produce 5-hydroxy-2,3,3-trimethylindolenine **14** (Kim et al., 2002; Saikiran et al., 2017).

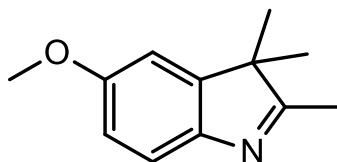


Figure 3.16: Chemical structure of Compound **13**

5-methoxy-2,3,3-trimethylindolenine **13**. A solution of 4-methoxy phenylhydrazine hydrochloride (10 g, 0.057 mol) and methyl isopropyl ketone (6.1 ml, 0.057 mol) and ethanol was refluxed for 4 h. After filtration, the solvent was removed using rotary evaporator to give compound **13**. This product was used directly in the following step without further purification. $C_{12}H_{15}NO$ (189.25). Yield: 8.74g (81%)

3.3.2 Demethylation using BBr_3 to produce intermediate compound of 5-hydroxy-2,3,3-trimethylindolenine **14**

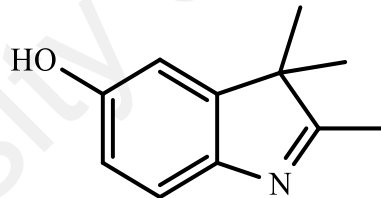


Figure 3.17: Chemical structure of Compound **14**

5-hydroxy-2,3,3-trimethylindolenine **14**; a solution of 5-methoxy-2,3,3-trimethyl indolenine **13** (10 g, 0.057 mol) in 30 ml of methylene chloride was cooled in an ice bath. Cooled reagent of boron tribromide (11 ml, 0.11 mol) in 20 ml DCM was added slowly dropwise while stirring for 15-20 min. The mixture was left at room temperature overnight and neutralized by saturated sodium carbonate solution. Mixture was extracted using DCM (3 x 50 ml) (Bakulina et al., 2017; Saikiran et al., 2017). The organic layer was collected and dried with anhydrous $MgSO_4$. Finally, solvent was evaporated to yield 7.39 g (74%) of brown solid. $C_{11}H_{13}NO$ (175.23); 1H NMR (400 MHz, $CDCl_3$, δ ppm);

1.25 (s, 6H = 2(-CH₃)), 2.24 (s, 3H = -CH₃), 6.76-6.79 (dd, J = 2.3 and 8.5 Hz, 1H = ArH), 6.84-6.85 (d, J = 2.3 Hz, 1H = ArH), 7.29-7.27 (d, J = 8.3 Hz, 1H = ArH), 8.07 (bs, 1H = -OH); ¹³C NMR (400 MHz, CDCl₃, δ ppm); 186.09 (-N=C-), 155.94, 147.23, 144.67, 119.88, 114.36, 109.93 (-ArC-), 53.71 (CH₃CCH₃), 23.21 (CH₃CCH₃), 14.95 (CH₃).

3.3.3 Phase transfer reaction to get series of 5-Alkoxy-2,3,3-trimethylindolenine

5-Alkoxy-2,3,3-trimethylindolenine intermediate compounds were synthesized using phase transfer reaction, a slight modification from the procedure reported by Voloshin et al. (2003) The ethers containing substituents with different length of the carbon chains in the indoline moiety were synthesized.

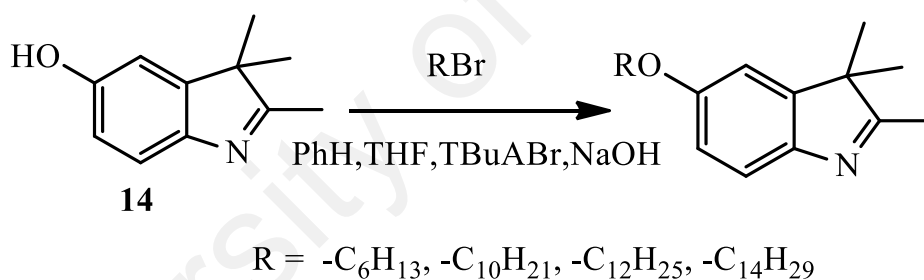


Figure 3.18: Alkylation process by mean of phase transfer reaction using tetrabutylammonium bromide.

General procedure: A mixture of 5-hydroxy-2,3,3-trimethylindolenine **14** (5 mmol) and phase-transfer catalyst, tetrabutylammonium bromide (0.16 g), benzene (20 ml), THF (15 ml), and a 50% NaOH solution (8 ml) was stirred at 20 °C for 15 min and then the respective Alkylbromide (7 mmol) was added. The mixture was stirred at room temperature overnight. Then benzene (35 ml) and water (20 ml) were added. The organic layer was separated and the aqueous layer was extracted further with benzene (2 x 50 ml). The combined extracts were dried with anhydrous MgSO₄ and the solvent was removed

using rotary evaporator. The resulting indolenine was used in the next reaction without purification.

5-Hexyloxy-2,3,3-trimethylindolenine **15**: $C_{17}H_{25}NO$ (259.39). Yield 0.88g (68%). Oily dark-brown liquid.

5-Decyloxy-2,3,3-trimethylindolenine **16**. $C_{21}H_{33}NO$ (315.49) Yield 1.01g (64%). Oily dark-brown liquid.

5-Dodecyloxy-2,3,3-trimethylindolenine **17**. $C_{23}H_{37}NO$ (343.55). Yield 1.12g (65%). Oily dark-brown liquid.

5-Tetradecyloxy-2,3,3-trimethylindolenine **18**. $C_{25}H_{41}NO$ (371.60) Yield 1.17g (63%). Oily dark-brown liquid.

3.3.4 Synthesis of new series compounds of 2-(diformylmethylidene)-5-(alkyloxy)-3,3-dimethylindole.

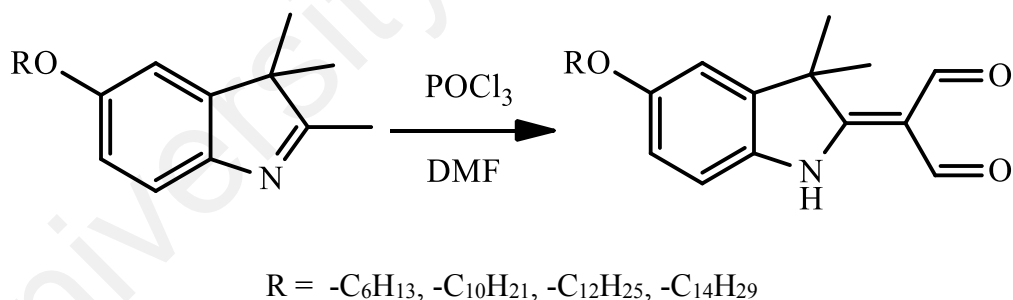


Figure 3.19: Vilsmeier-Haack reaction to get series of 2-(diformylmethylidene)-5-(alkoxy)-3,3-dimethylindole

General procedure: Synthesis of new series of 2-(diformylmethylidene)-5-(alkoxy)-3,3-dimethylindole compounds using Vilsmeier reagent phosphorus oxychloride and N,N-dimethylformamide (Rashidi et al., 2009; Vilsmeier & Haack, 1927). Phosphorus oxychloride was added to cold N,N-dimethylformamide in an ice bath. After the addition, a solution of compounds **15**, **16**, **17** or **18** in DMF was added dropwise over a period of

20 min. The cooling bath was removed and the reaction mixture was refluxed at 85°C for 4-6 h. The resulting solution was added to ice water and made alkaline with 2M NaOH(aq) solution (Helliwell et al., 2006). The mixture was extracted with DCM (3 x 50 ml). The combined organic layer was dried with anhydrous MgSO₄, and then the solvent was removed using rotary evaporator. The resulting dark brown solid substance was collected and dried in air, recrystallized from ethanol, and identified as compounds **19**, **20**, **21** or **22**.

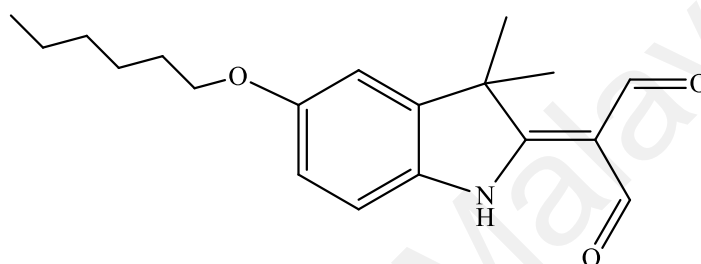


Figure 3.20: Chemical structure of Compound **19**

2-(diformylmethylidene)-5-(hexyloxy)-3,3-dimethylindole **19**. To dimethylformamide (10 ml) in an ice bath (acetone/ice), phosphorus oxychloride (6 ml, 66 mmol) was added dropwise with stirring over a period of 30 min in cooled bath of acetone and ice. After the addition was completed, a solution of compound **15** (12.6 mmol) in dimethylformamide (10 ml) was added slowly. The ice bath was then removed and the reaction mixture was heated at 85°C for 4 h. The resulting solution was added to crushed ice, the pH was adjusted to 8.0 by the addition of aqueous NaOH (2M) and the mixture was extracted with DCM (3 x 30 ml). The combined organic layer was washed with water and dried over anhydrous MgSO₄. Solvent was removed under vacuum, the resulting precipitate was dried in air, and recrystallized from ethanol to produce brown needle shape crystals. Yield 2.5g (64%). C₁₉H₂₅NO₃ (315.41); ¹H NMR (400Hz, CDCl₃, δ ppm); 13.64 (s, 1H = -NH); 9.65, 9.69 (ss, 2H = 2(-CHO)); 7.08 (d, J = 8.4Hz, 1H = ArH); 6.87 (d, J = 2.4Hz, 1H = ArH); 6.81 (dd, J = 8.8, 2.4Hz, 1H = ArH); 3.95 (t, J =

6.6Hz, 2H = $-\underline{CH}_2-$); 1.76-1.80 (m, 2H = $-\underline{CH}_2-$); 1.72 (s, 6H = 2($-\underline{CH}_3$)); 1.46-1.57 (m, 2H = $-\underline{CH}_2-$), 1.32-1.36 (m, 4H = $-\underline{C}_2\underline{H}_4-$); 0.9 (t, J = 7.0Hz, 3H = $-\underline{CH}_3$). ^{13}C NMR (400Hz, CDCl_3 , δ ppm); 190.13 (C=O), 179.09 (=C-NH), 158.33 (C-O), 142.78, 132.38, 113.66, 113.50, 109.53, 109.17 (Ar), 68.83 (Ar-O- CH_2 -), 51.95 (CH_3CCH_3), 31.64, 29.30, 23.09, 22.66 ($-\text{CH}_2-$), 25.78 (CH_3CCH_3), 14.10 ($-\text{CH}_3$). LCMS QTOF, (M^+): 316.1914

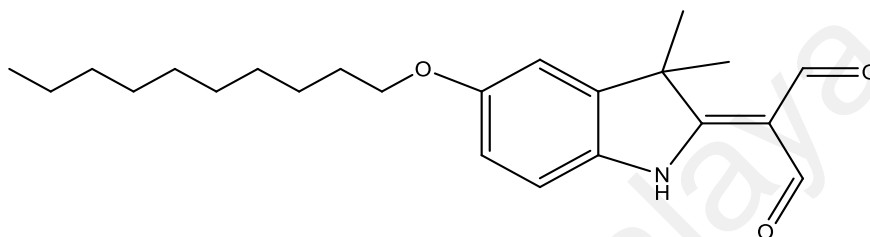


Figure 3.21: Chemical structure of Compound **20**

2-(diformylmethylidene)-5-(decyloxy)-3,3-dimethylindole **20**. Brown needle shape crystal. Yield 2.90g (62%). $\text{C}_{23}\text{H}_{33}\text{NO}_3$ (371.51); ^1H NMR (400Hz, CDCl_3 , δ ppm); 13.64 (s, 1H = $-\underline{NH}$); 9.64,9.68 (ss, 2H = 2($-\underline{CHO}$)); 7.08 (d, J = 8.4Hz, 1H = $\text{Ar}\underline{H}$); 6.87 (d, J = 2.4Hz, 1H = $\text{Ar}\underline{H}$); 6.81 (dd, J = 8.6, 2.2Hz, 1H = $\text{Ar}\underline{H}$); 3.95 (t, J = 6.4Hz, 2H = $-\underline{CH}_2-$); 1.76-1.80 (m, 2H = $-\underline{CH}_2-$); 1.72 (s, 6H = 2($-\underline{CH}_3$)); 1.43-1.45 (m, 2H = $-\underline{CH}_2-$), 1.26-1.34 (m, 8H = $-\underline{C}_4\underline{H}_8-$); 0.87 (t, J = 6.6Hz, 3H = $-\underline{CH}_3$). ^{13}C NMR (400Hz, CDCl_3 , δ ppm); 190.13 (C=O), 179.00 (C-N), 158.22 (C-O), 142.72, 132.46, 113.58, 113.41, 109.53, 109.28 (Ar), 68.81 (Ar-O- CH_2 -), 51.86 (CH_3CCH_3), 31.98, 29.63, 29.46, 29.41, 29.34, 22.77 ($-\text{CH}_2-$), 26.12 (CH_3CCH_3), 14.21 ($-\text{CH}_3$). LCMS QTOF, (M^+): 372.2542

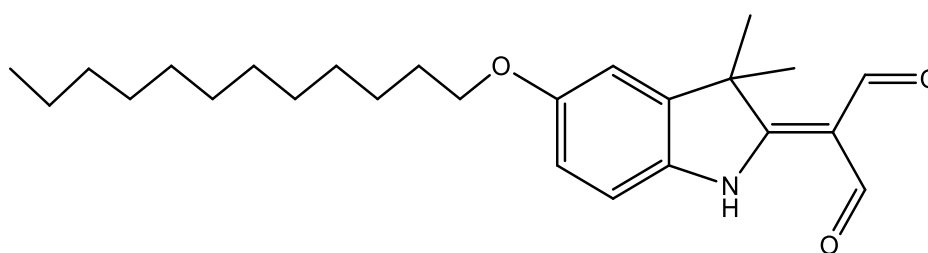


Figure 3.22: Chemical structure of Compound **21**

2-(diformylmethylidene)-5-(dodecyloxy)-3,3-dimethylindole **21**. Brown needle shape crystal. Yield 3.07g (61%). $C_{25}H_{37}NO_3$ (399.57); 1H NMR (400Hz, $CDCl_3$, δ ppm); 13.64 (s, 1H = -NH); 9.64,9.68 (ss, 2H = 2(-CHO)); 7.08 (d, J = 8.4Hz, 1H = ArH); 6.87 (d, J = 2.4Hz, 1H = ArH); 6.81 (dd, J = 8.4, 2.4Hz, 1H = ArH); 3.95 (t, J = 6.6Hz, 2H = -CH₂-); 1.76-1.80 (m, 2H = -CH₂-); 1.72 (s, 6H = 2(-CH₃)); 1.43-1.45 (m, 2H = -CH₂-), 1.26-1.33 (m, 12H = -C₆H₁₂-); 0.87 (t, J = 6.6Hz, 3H = -CH₃). ^{13}C NMR (400Hz, $CDCl_3$, δ ppm); 190.13 (C=O), 179.09 (C-N), 158.33 (C-O), 142.78, 132.38, 113.66, 113.50, 109.53, 109.17 (Ar), 68.83 (Ar-O-CH₂-), 51.95 (CH₃CCH₃), 31.64, 29.30, 23.09, 22.66 (-CH₂-), 25.78 (CH₃CCH₃), 14.10 (-CH₃). LCMS QTOF,(M⁺): 400.2852

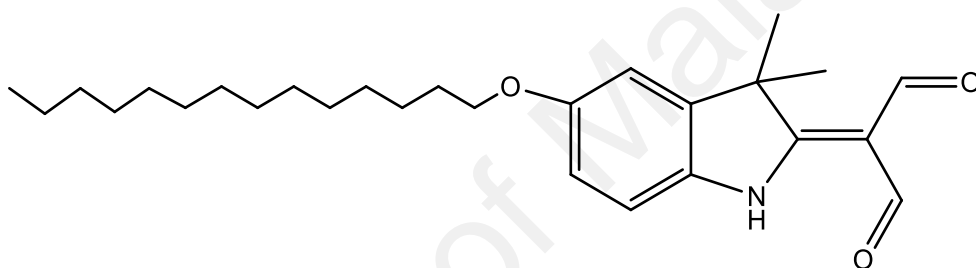


Figure 3.23: Chemical structure of Compound **22**

2-(diformylmethylidene)-5-(tetradecyloxy)-3,3-dimethylindole **22**. Yellow needle crystal. Yield 3.39g (63%). $C_{27}H_{41}NO_3$ (427.62); 1H NMR (400Hz, $CDCl_3$, δ ppm); 13.64 (s, 1H = -NH); 9.64,9.68 (ss, 2H = 2(-CHO)); 7.08 (d, J = 8.4Hz, 1H = ArH); 6.87 (d, J = 2.4Hz, 1H = ArH); 6.81 (dd, J = 8.2, 2.6Hz, 1H = ArH); 3.95 (t, J = 6.6Hz, 2H = -CH₂-); 1.76-1.80 (m, 2H = -CH₂-); 1.72 (s, 6H = 2(-CH₃)); 1.43-1.45 (m, 2H = -CH₂-), 1.26-1.33 (m, 16H = -C₈H₁₆-); 0.87 (t, J = 6.6Hz, 3H = -CH₃). ^{13}C NMR (400Hz, $CDCl_3$, δ ppm); 192.43, 187.94 (C=O), 178.92 (C-N), 158.17 (C-O), 142.68, 132.49, 113.54, 113.40, 109.51, 109.31 (Ar), 68.77 (Ar-O-CH₂-), 51.80 (CH₃CCH₃), 32.00, 29.74, 29.67, 29.46, 29.43, 22.77 (-CH₂-), 26.12 (CH₃CCH₃), 14.21 (-CH₃). LCMS QTOF,(M⁺): 428.3157

3.5 Synthesis series of Macrocylic compounds of DBTAA with six aliphatic chains.

New series of macrocyclic DBTAA compounds were synthesized from respective intermediate compounds of diamines with diformyls. The synthesis of the indolenine substituted dibenzotetraaza[14] annulene was achieved through the 2:2 condensation of 2-(diformylmethylidene)-5-(alkoxy)-3,3-dimethylindole with respective 4,5-bis(alkyloxy)benzene-1,2-diaminium chloride accompanied by migration of the double bond into the pyrrole rings. (Khaledi et al., 2013).

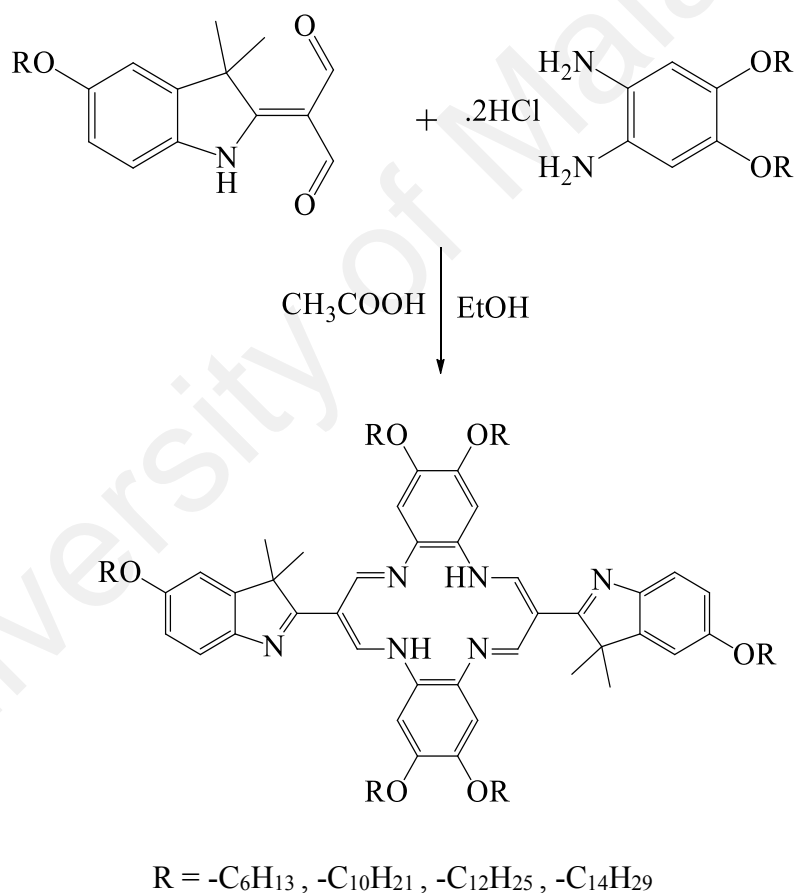


Figure 3.24: Condensation reaction of new series macrocyclic ligands of DBTAA.

General procedure: A solution of 2-(diformylmethylidene)-5-(alkyloxy)-3,3-dimethylindole **19**, **20**, **21** or **22** (2 mmol) and with its respective length of alkyl chain of 4,5-bis(alkyloxy)benzene-1,2-diaminium chloride **9**, **10**, **11** or **12** (2 mmol) in ethanol

(40 ml) with the presence of acetic acid (0.5 ml) was refluxed for 4 hours. Upon cooling the product precipitated as a dark red solid. The solid was filtered off, washed with ethanol and dried over silica-gel.

Dibenzotetraaza[14]annulene 6-hexyloxy **23**. A solution of compound **19** (2 mmol) and a diamine of compound **9** (2 mmol) in ethanol (40 ml) with the presence of acetic acid (0.5 ml) was refluxed for 4 h where the product precipitated as a dark red solid, namely compound **23**. The solid was filtered off, washed with ethanol and dried over silica-gel.

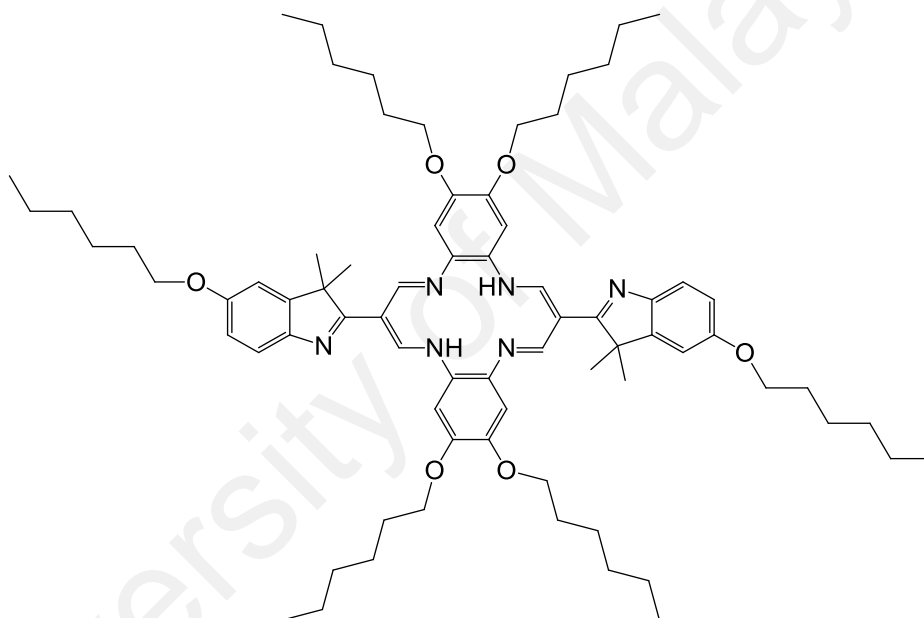


Figure 3.25: Chemical structure of Macrocyclic ligand **23**

Dibenzotetraaza[14]annulene 6-hexyloxy **23**. Dark red solid, yield 0.76g (65%). $C_{74}H_{106}N_6O_6$ (1175.67). Elemental Analysis: Cal; C, 75.60; H, 9.09; N, 7.15; O, 8.17; Found: C, 75.59; H, 9.10; N, 7.14; IR (ATR): ν (cm^{-1}) 3074 w, 2924 s, 2856 s, 1634 s, 1604 m, 1566 m, 1504 s, 1461 s, 1385 m, 1342 m, 1247 s, 1194 s, 1183 s, 1116 m, 1075 m, 1012 m, 903 s, 796 s, 586 s, 540 m. ¹H NMR (400Hz, CDCl₃, δ ppm); 14.86 (t, J = 6.2Hz, 2H = 2(-NH)); 8.64 (d, J = 6.4Hz, 4H = 4(-CHN-)); 7.40 (d, J = 8.4Hz, 2H = Ar-H); 6.80-6.83 (m, 8H = Ar-H); 4.05 (t, J = 6.4Hz, 8H = 4(-OCH₂-)); 3.97 (t, J = 6.6Hz,

4H = 2(-OCH₂-)); 1.74-1.87 (m, 12H = 6(-CH₂-)); 1.55 (s, 12H, 2(-CH₃)₂); 1.27-1.52 (m, 36H, 6(-CH₂-)₃); 0.92 (t, J = 7.0Hz, 12H, 4(-CH₃)); 0.92 (t, J = 6.8Hz, 6H = 2(-CH₃)).
¹³C NMR (400Hz, CDCl₃, δ ppm); 180.80 (-CN=C-), 156.85 (-CN=C-), 148.11, 148.08, 147.00, 147.19, 131.14, 118.94, 112.37, 108.45, 104.18, 101.80 (Ar), 70.09, 68.59 (Ar-O-CH₂-), 52.70 (CH₃CCH₃), 31.65, 29.57, 29.39, 29.33, 25.76, 22.65 (-CH₂-), 26.48 (CH₃CCH₃), 14.12, 14.06 (-CH₃). UV/vis (CHCl₃): λ_{max} = 290, 309, 395 nm

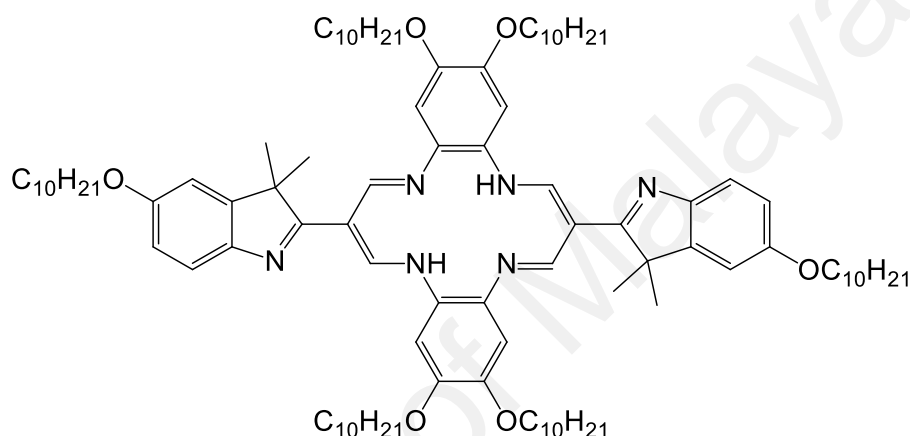


Figure 3.26: Chemical structure of Macrocyclic ligand **24**

Dibenzotetraaza[14]annulene 6-decyloxy **24**. Dark red solid. Yield 0.91g (60%).
 C₉₈H₁₅₄N₆O₆ (1512.31). Elemental Analysis: Cal; C, 77.83; H, 10.26; N, 5.56; O, 6.35;
 Found: C, 77.85; H, 10.28; N, 5.52; IR (ATR): ν (cm⁻¹) 3079 w, 2920 s, 2852 s, 1635 w,
 1604 w, 1567 w, 1504 s, 1462 s, 1390 m, 1342 m, 1312m, 1248 s, 1198 s, 1183 s, 1117
 m, 1076 m, 903 m, 795 s, 767 m, 588 s, 540 m. ¹H NMR (400Hz, CDCl₃, δ ppm); 14.94
 (bs, 2H = 2(-NH)); 8.69 (s, 4H = 4(-CHN-)); 7.44 (d, J = 7.6Hz, 2H = Ar-H); 6.80-6.87
 (m, 8H = Ar-H); 4.07 (t, J = 6.6Hz, 8H = 4(-OCH₂-)); 3.97 (t, J = 6.4Hz, 4H = 2(-OCH₂-
)); 1.77-1.85 (m, 12H = 6(-CH₂-)); 1.56 (s, 12H = 2(-CH₃)₂); 1.53-1.27 (m, 84H = 6(-
 CH₂-)₇); 0.87 (t, J = 6.8Hz, 18H = 6(-CH₃)). ¹³C NMR (400Hz, CDCl₃, δ ppm); 180.21
 (-CN=C-), 156.24 (-CN=C-), 148.88, 148.54, 130.89, 118.33, 113.01, 108.55, 103.30,

101.87 (Ar), 70.19, 68.67 (Ar-O-CH₂-), 52.53 (CH₃CCH₃), 32.04, 29.77, 29.73, 29.63, 29.48, 22.80 (-CH₂-), 26.18 (CH₃CCH₃), 14.23 (-CH₃).

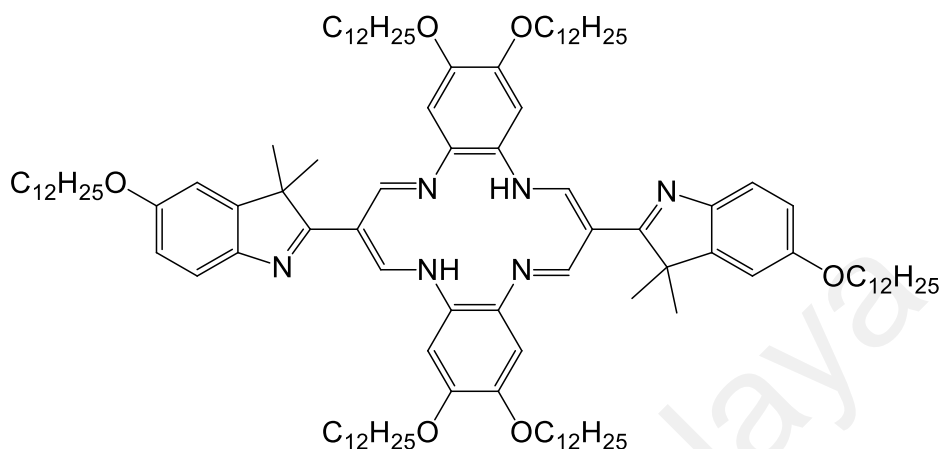


Figure 3.27: Chemical structure of Macrocylic ligand **25**

Dibenzotetraaza[14]annulene 6-dodecyloxy **25**. Dark red solid, yield 1.03g (61%). C₁₁₀H₁₇₈N₆O₆ (1680.63). Elemental Analysis: Cal; C, 78.61; H, 10.68; N, 5.00; O, 5.71; Found: C, 78.62; H, 10.66; N, 4.99; IR (ATR): ν (cm⁻¹) 3022 w, 2918 s, 2851 s, 1635 s, 1604 w, 1567 w, 1504 s, 1463 s, 1390 w, 1342 w, 1248 s, 1199 s, 1183 s, 1077w, 902 w, 796 w, 588 s, 540 m. ¹H NMR (400Hz, CDCl₃, δ ppm); 14.89 (bs, 2H = 2(-NH)); 8.66 (d, J = 6.0Hz, 4H = 4(-CHN-)); 7.42 (d, J = 8.4Hz, 2H = Ar-H); 6.80-6.83 (m, 8H = Ar-H); 4.05 (t, J = 6.4Hz, 8H = 4(-OCH₂-)); 3.97 (t, J = 6.6Hz, 4H = 2(-OCH₂-)); 1.77-1.85 (m, 12H = 6(-CH₂-)); 1.55 (s, 12H = 2(-CH₃)₂); 1.26-1.51 (m, 108H = 6(-CH₂-)₉); 0.86 (t, J = 6.2Hz, 18H = 6(-CH₃)); ¹³C NMR (400Hz, CDCl₃, δ ppm); 180.78 (-CN=C-), 156.97 (-CN=C-), 148.25, 148.10, 147.97, 131.14, 118.90, 112.81, 108.45, 104.10, 101.77 (Ar), 70.43, 68.64 (Ar-O-CH₂-), 52.74 (CH₃CCH₃), 32.03, 29.83, 29.78, 29.74, 29.71, 29.61, 29.55, 29.49, 29.45, 22.79 (-CH₂-), 26.20 (CH₃CCH₃), 14.23 (-CH₃). UV/vis (CHCl₃): λ_{\max} = 237, 310, 395 nm).

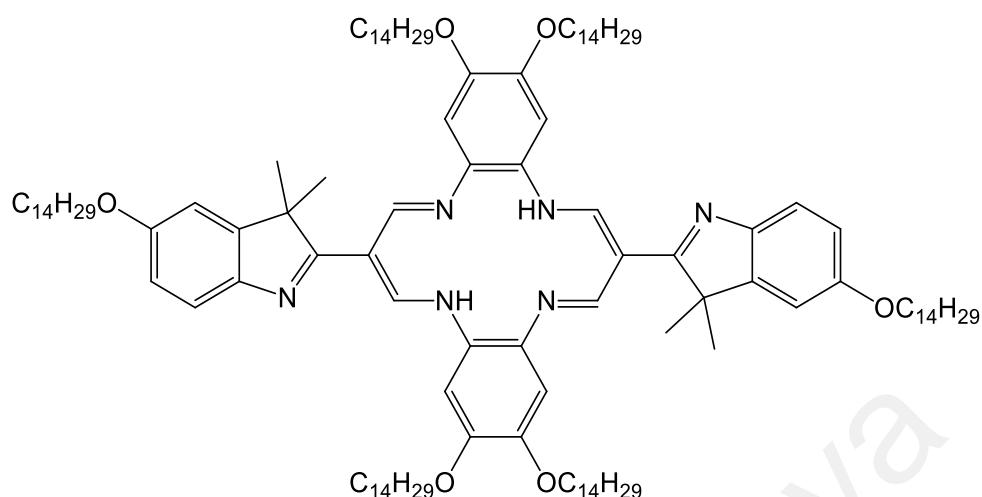


Figure 3.28: Chemical structure of Macrocylic ligand **26**

Dibenzotetraaza[14]annulene 6-tetradecyloxy **26**. Dark red solid, yield 1.09g (59%). $C_{122}H_{202}N_6O_6$ (1848.95). Elemental Analysis: Cal; C, 79.25; H, 11.01; N, 4.55; O, 5.19; Found: C, 79.26; H, 11.00; N, 4.56; IR (ATR): ν (cm^{-1}) 2917 s, 2849 s, 1636 s, 1604 w, 1567 w, 1504 s, 1463 s, 1390 m, 1343 m, 1250 s, 1200 m, 1183 s, 1075 m, 903 m, 797 s, 588 s, 540 m. 1H NMR (400Hz, CD_2Cl_2 , δ ppm); 14.91 (bs, 2H = 2(-NH)); 8.66 (s, 4H = 4(-CHN-)); 7.43 (d, $J = 7.6Hz$, 2H = Ar-H); 6.80-6.85 (m, 8H = Ar-H); 4.06 (t, $J = 6.6Hz$, 8H = 4(-OCH₂-)); 3.97 (t, $J = 6.6Hz$, 4H = 2(-OCH₂-)); 1.79-1.85 (m, 12H = 6(-CH₂-)); 1.55 (s, 12H = 2(-CH₃)₂); 1.25-1.49 (m, 132H = 6(-CH₂-)₁₁); 0.86 (t, $J = 6.2Hz$, 18H = 6(-CH₃)). ^{13}C NMR (400Hz, $CDCl_3$, δ ppm); 178.56 (-CN=C-), 158.41 (-CN=C-), 142.53, 133.79, 147.97, 122.36, 113.70, 112.81, 108.45, 99.67 (Ar), 70.62, 68.83 (Ar-O-CH₂-), 51.77 (CH_3CCH_3), 32.01, 29.84, 29.77, 29.70, 29.64, 29.47, 29.37, 22.79 (-CH₂-), 26.20 (CH_3CCH_3), 14.22 (-CH₃).

3.6 Synthesis of Nickel complex of Macrocylic dibenzotetraaza[14] annulene

6-alkyloxy

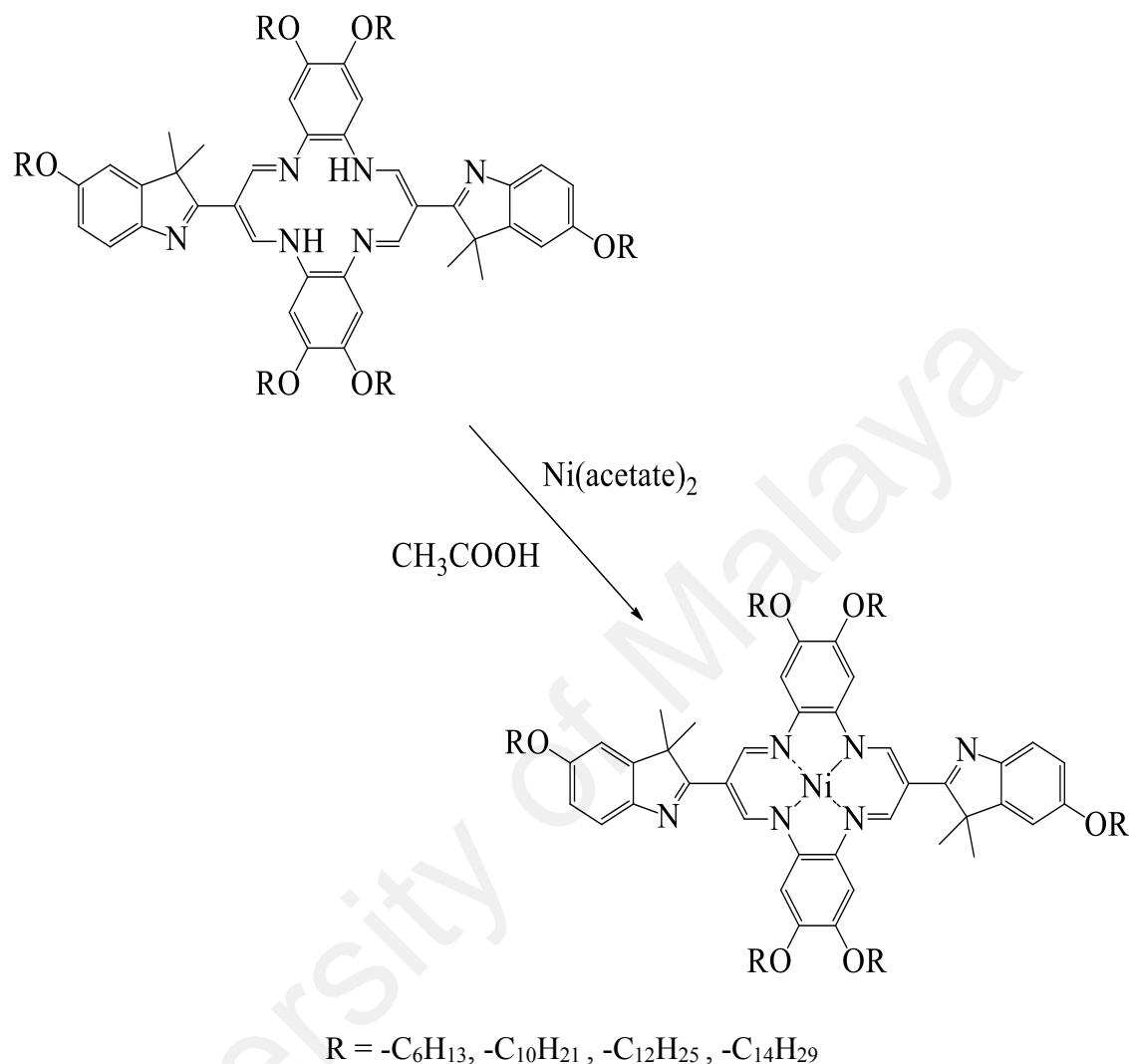


Figure 3.29: Synthesis of nickel complex from Macrocylic DBTAA 6-alkyloxy.

General procedure: Synthesis of this new nickel complex of Macrocylic dibenzotetraaza[14] annulene 6-alkoxy was done by adding nickel(II) acetate tetrahydrate (0.3 mmol, 1.5 eq) to dissolved ligand of macrocyclic ligand **23**, **24**, **25** and **26** (0.2 mmol, 1 eq) in minimum amount of glacial acetic acid then heating for 2-4 hours. Upon cooling, the dark red precipitates were identified as complex **27**, **28** and **29**. The precipitates were collected by filtration, then washed with ethanol and dried in oven 60°C (Khaledi et al., 2014). Macrocylic ligand **26** was unable to dissolve in glacial acetic acid, so nickel complex for this ligand failed to be synthesized.

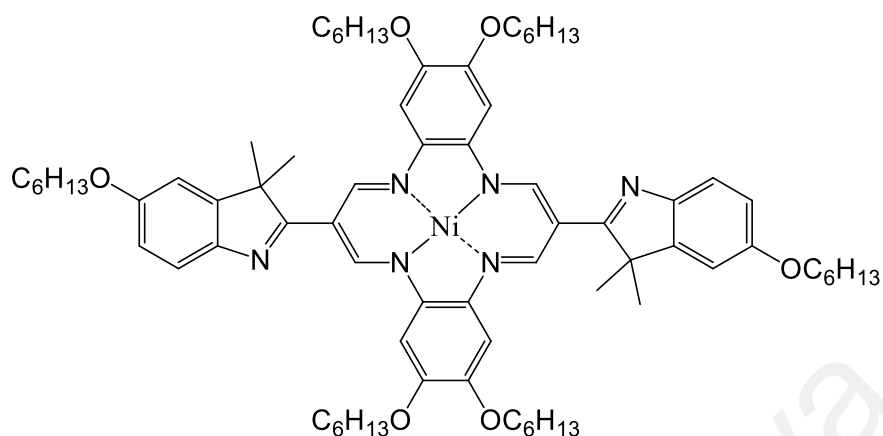


Figure 3.30: Chemical structure of Complex 27

Nickel complex of macrocyclic dibenzotetraaza[14]annulene 6-hexyloxy **27**. Dark red solid, yield 0.17g (71%). $C_{74}H_{104}N_6NiO_6$ (1232.35). Elemental Analysis: Cal; C, 72.12; H, 8.51; N, 6.82; Ni, 4.76; O, 7.79; Found: C, 72.10; H, 8.50; N, 6.83; IR (ATR): ν (cm^{-1}) 2918 s, 2851 s, 1600 w, 1506 s, 1461 s, 1415 w, 1340 s, 1266 s, 1127 m, 1077 m, 1036m, 964 m, 821 s, 797s, 545 s, 531 m. 1H NMR (400Hz, $CDCl_3$, δ ppm); 8.18 (s, 4H = 4(- \underline{CHN} -)); 7.43 (b, 2H = Ar- \underline{H}); 6.80-6.88 (m, 8H = Ar- \underline{H}); 3.92-3.97 (m, 12H = 6(- $\underline{OCH_2}$ -)); 1.77-1.84 (m, 4H = 2(- $\underline{CH_2}$ -)); -); 1.66-1.73 (m, 8H = 4(- $\underline{CH_2}$ -)); 1.50 (s, 12H = 2(- $\underline{CH_3}$)₂); 1.27-1.42 (m, 36H = 6(- $\underline{CH_2}$ -)₃); 0.86-0.93 (m, 18H = 6(- $\underline{CH_3}$)); ^{13}C NMR (400Hz, $CDCl_3$, δ ppm); 178.90 (-CN=C-), 157.66 (-CN=C-), 149.09, 137.70, 133.77, 117.51, 113.36, 108.58, 100.41 (Ar), 70.31, 68.73 (Ar-O- $\underline{CH_2}$ -), 52.35 ($\underline{CH_3CCH_3}$), 31.82, 29.80, 29.66, 29.41, 27.19, 22.78, 22.71 (- $\underline{CH_2}$ -), 25.84 ($\underline{CH_3CCH_3}$), 14.22, 14.19 (- $\underline{CH_3}$). UV/vis ($CHCl_3$): λ_{max} = 290, 394, 451, 504 nm.

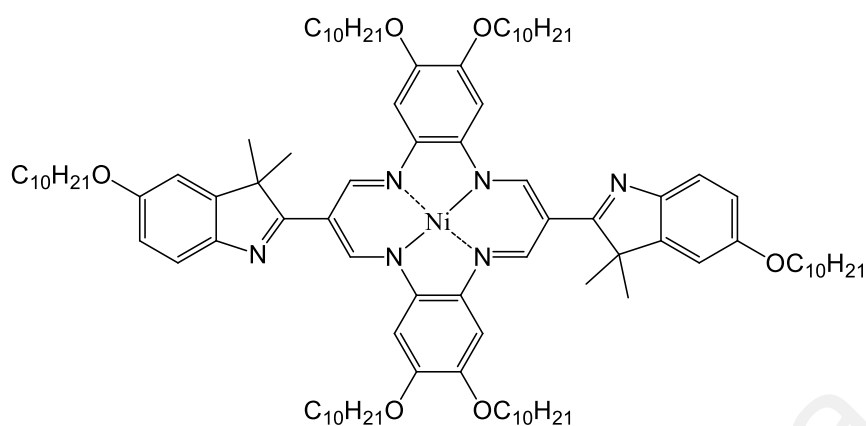


Figure 3.31: Chemical structure of Complex **28**

Nickel complex of macrocyclic dibenzotetraaza[14] annulene 6-decyloxy **28**: Dark red solid, yield 0.22g (69%). $C_{98}H_{152}N_6NiO_6$ (1568.99). Elemental Analysis: Cal; C, 75.02; H, 9.76; N, 5.36; Ni, 3.74; O, 6.12; Found: C, 75.05; H, 9.77; N, 5.35; IR (ATR): ν (cm^{-1}) 3022 w, 2920 s, 2852 s, 1604 w, 1595 w, 1505 s, 1461 s, 1339 s, 1265 s, 1192 s, 1127 m, 1074 m, 1023 m, 821 m, 797 s, 545 s. 1H NMR (500Hz, $CDCl_3$, δ ppm); 8.25 (s, 4H = 4(- \underline{CHN} -)); 7.43 (d, $J = 8.0Hz$, 2H = Ar- \underline{H}); 6.90 (s, 4H = Ar- \underline{H}); 6.81-6.84 (m, 4H = Ar- \underline{H}); 3.94-3.99 (m, 12H = 4(- $\underline{OCH_2}$ -)); 1.73-1.80 (m, 12H = 6(- $\underline{CH_2}$ -)); 1.52 (s, 12H = 2(- $\underline{CH_3}$)₂); 1.28-1.48 (m, 84H = 6(- $\underline{CH_2}$ -)₇); 0.88 (t, $J = 6.7Hz$, 18H = 6(- $\underline{CH_3}$)). LCMS QTOF, M^+ : 1568.9855

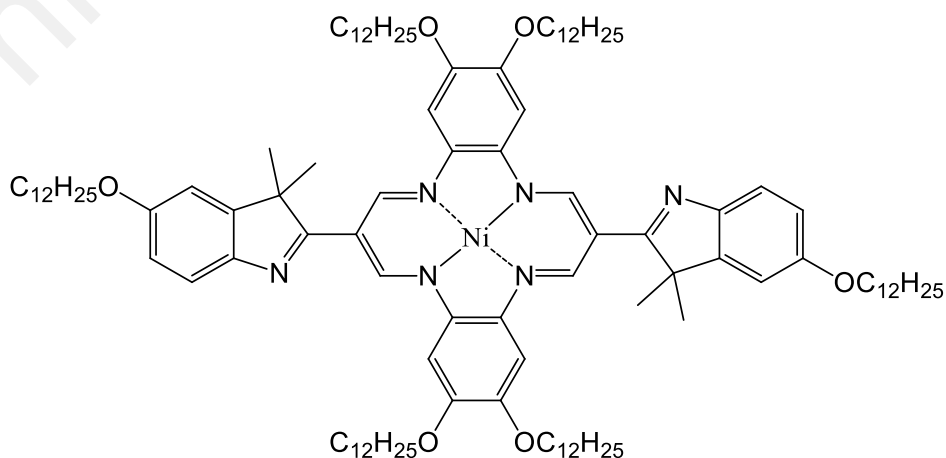


Figure 3.32: Chemical structure of Complex **29**

Nickel complex of macrocyclic dibenzotetraaza[14] annulene 6-dodecyloxy **29**: Dark red solid, yield 0.24g (68%). $C_{110}H_{176}N_6NiO_6$ (1737.30). Elemental Analysis: Cal; C, 76.05; H, 10.21; N, 4.84; Ni, 3.38; O, 5.53; Found: C, 76.06; H, 10.20; N, 4.83; IR (ATR): ν (cm^{-1}) 2919 s, 2851 s, 1595 w, 1605 s, 1595 s, 1506 s, 1461 s, 1377 m, 1340 s, 1266 s, 1193 s, 1076 m, 1037 m, 821 m, 797s, 545 s, 1H NMR (500Hz, $CDCl_3$, δ ppm); 8.33 (s, 4H = 4(- \underline{CHN} -)); 7.48 (d, J = 8.0Hz, 2H = Ar- \underline{H}); 6.99 (s, 4H = Ar- \underline{H}); 6.87 (s, 4H = Ar- \underline{H}); 4.01 (b, 12H = 4(- $\underline{OCH_2}$ -)); 1.78-1.84 (m, 12H = 6(- $\underline{CH_2}$ -) $_2$); 1.52 (s, 12H = 2(- $\underline{CH_3}$) $_2$); 1.31-1.46 (m, 108H = 6(- $\underline{CH_2}$ -) $_9$); 0.90-0.91 (m, 18H = 6(- $\underline{CH_3}$) $_3$); ^{13}C NMR (400Hz, $CDCl_3$, δ ppm); 178.75 (-CN=C-), 157.71 (-CN=C-), 149.21, 145.67, 137.59, 117.34, 113.40, 108.55, 105.63, 100.42 (Ar), 70.32, 68.73 (Ar-O- $\underline{CH_2}$ -), 52.32 ($\underline{CH_3CCH_3}$), 32.05, 32.02, 29.85, 29.83, 29.78, 29.74, 29.57, 29.51, 27.29, 22.80 (- $\underline{CH_2}$ -), 26.22 ($\underline{CH_3CCH_3}$), 14.23 (- $\underline{CH_3}$). UV/vis ($CHCl_3$): λ_{max} = 238, 290, 394, 451, 505 nm.

3.7 Synthesis of macrocyclic ligand from *o*-phenylenediamine and 2-(diformylmethylidene)-5-(hexyloxy)-3,3-dimethylindole **19**

For X-ray crystallographic studies, the basic compounds have been synthesized. This basic macrocyclic ligand and complex need to be synthesized as all the compounds that attached with six alkyloxy chains were unable to obtain suitable single crystals that could be scanned and provides good data to solve.

A solution of compound **19** (2 mmol) and *o*-phenylenediamine (2 mmol) in ethanol (40 ml) with the presence of acetic acid (0.5 ml) was refluxed for 4 h. The product precipitated out as a dark red solid, namely compound **30**. The solid was filtered, washed with ethanol and dried over silica-gel. $C_{50}H_{58}N_6O_2$ (775.03). Yield 1.09g (70%). Red solid. Synthesis of this new nickel complex of macrocyclic dibenzotetraaza[14] annulene 2-hexyloxy **31** was done by adding nickel(II) acetate tetrahydrate (0.45 mmol, 1.5eq) to

macrocyclic ligands **30** (0.3 mmol, 1eq) in a minimum amount of glacial acetic acid, and then heating for 2-4 hours. The dark red solution was left over the weekend so as to afford a suitable single crystal for x-ray crystallography studies. $C_{50}H_{56}N_6NiO_2$ (831.71). Yield 0.19g (75%). Dark red crystal.

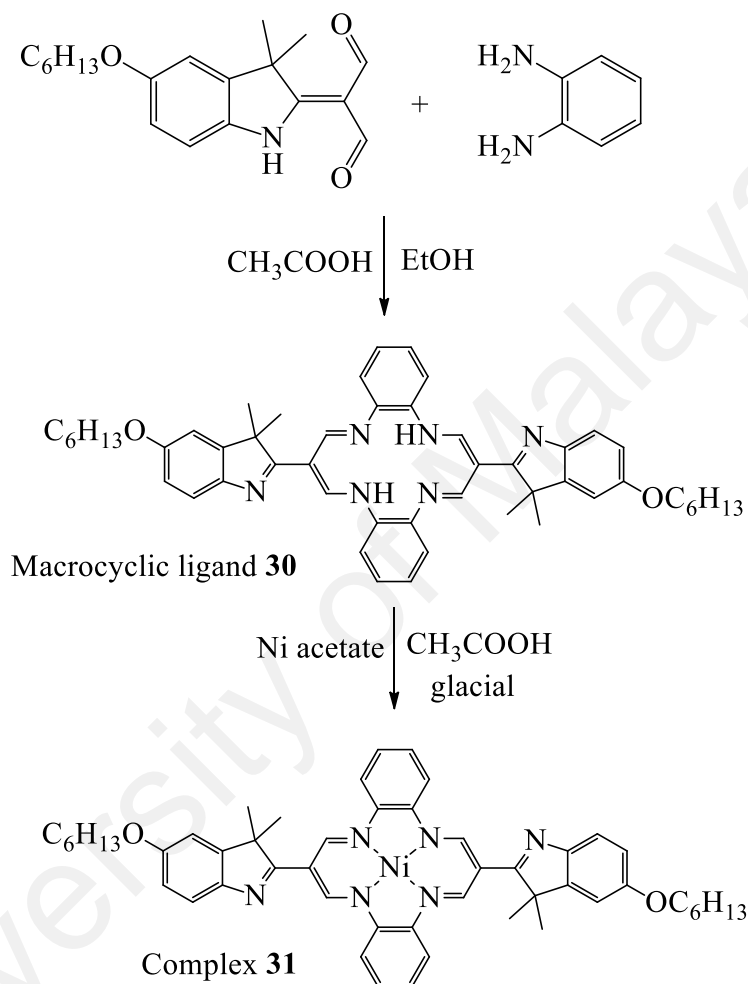


Figure 3.33: Synthesis of macrocyclic ligand and its nickel complex from *o*-phenylenediamine and 2-(diformylmethylidene)-5-(hexyloxy)-3,3-dimethylindole **19**

CHAPTER 4 : RESULT AND DISCUSSION

4.1 Suggested Reaction Mechanisms

4.1.1 Reaction Mechanism for Fischer indole synthesis.

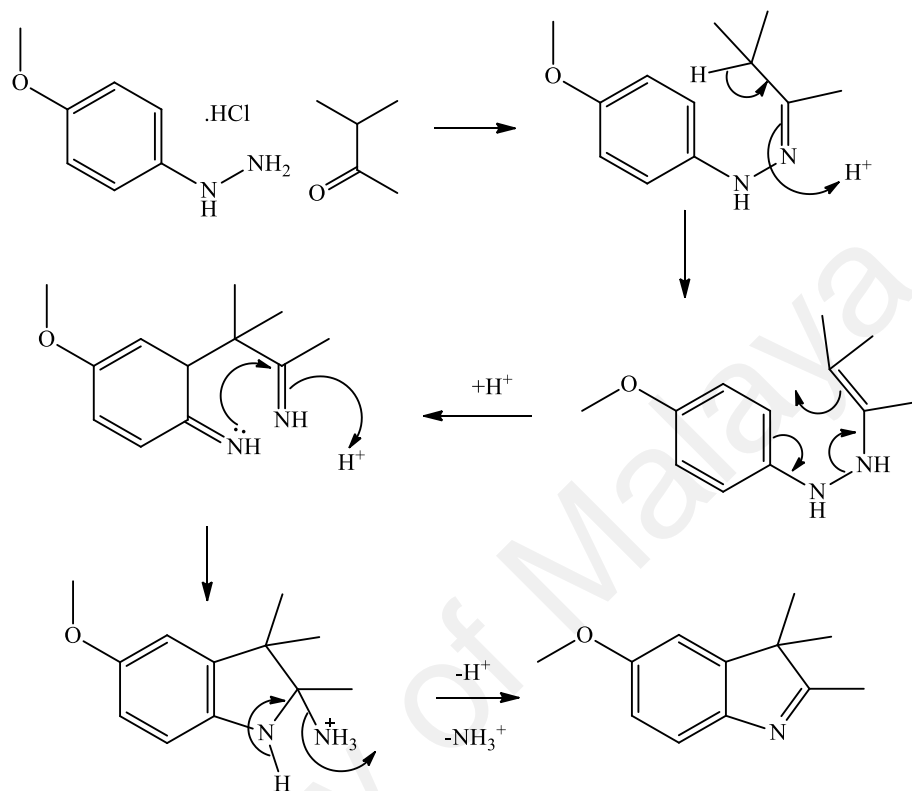


Figure 4.1: Reaction Mechanism for Fischer indole synthesis. (Clayden et al., 2012)

4.1.2 Reaction Mechanism for Vilsmeier-Haack reaction on 5-Alkoxy-2,3,3-trimethylindolenine

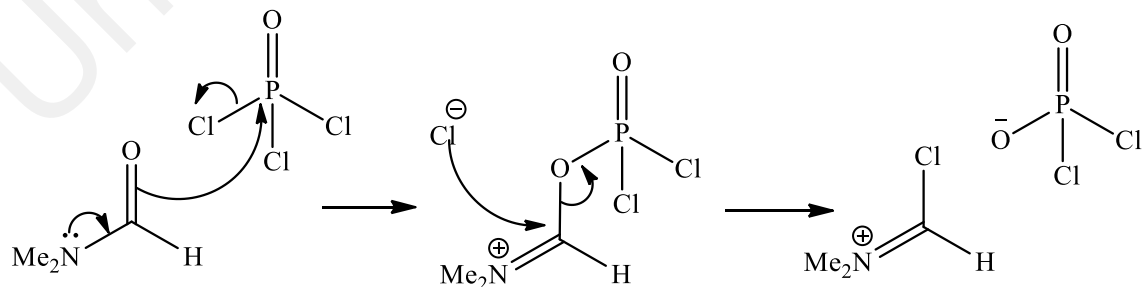


Figure 4.2: Activation of DMF molecule by POCl₃

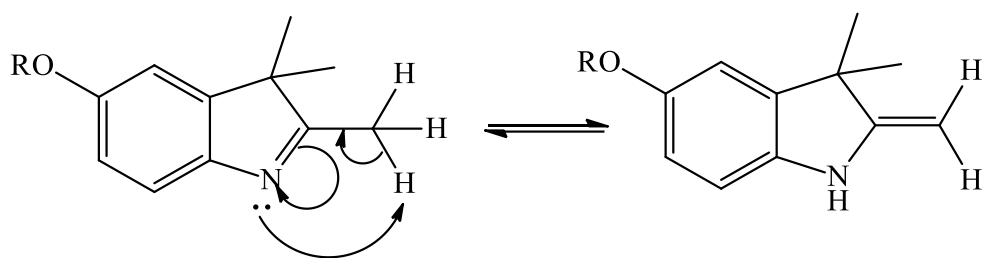


Figure 4.3: Rearrangement of 5-Alkoxy-2,3,3-trimethylindolenine

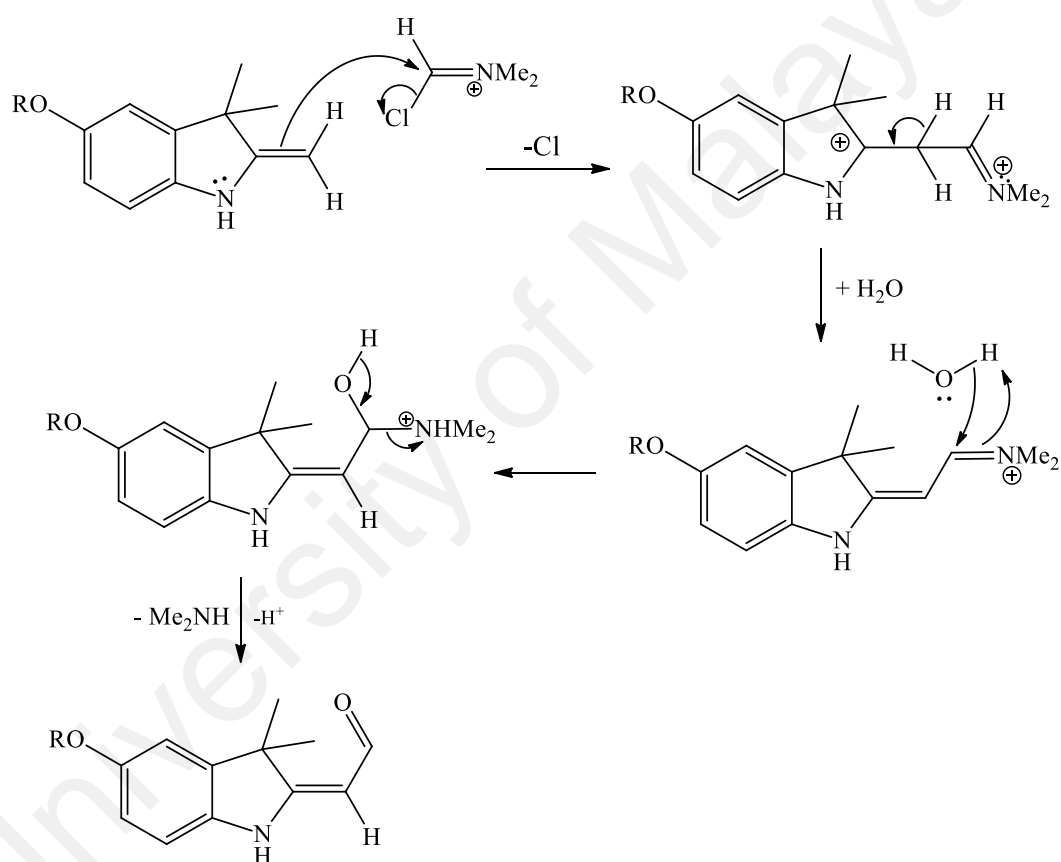


Figure 4.4: Reaction mechanism of the first attack from activated molecule of DMF on 5-alkoxy-2,3,3-trimethylindolenine

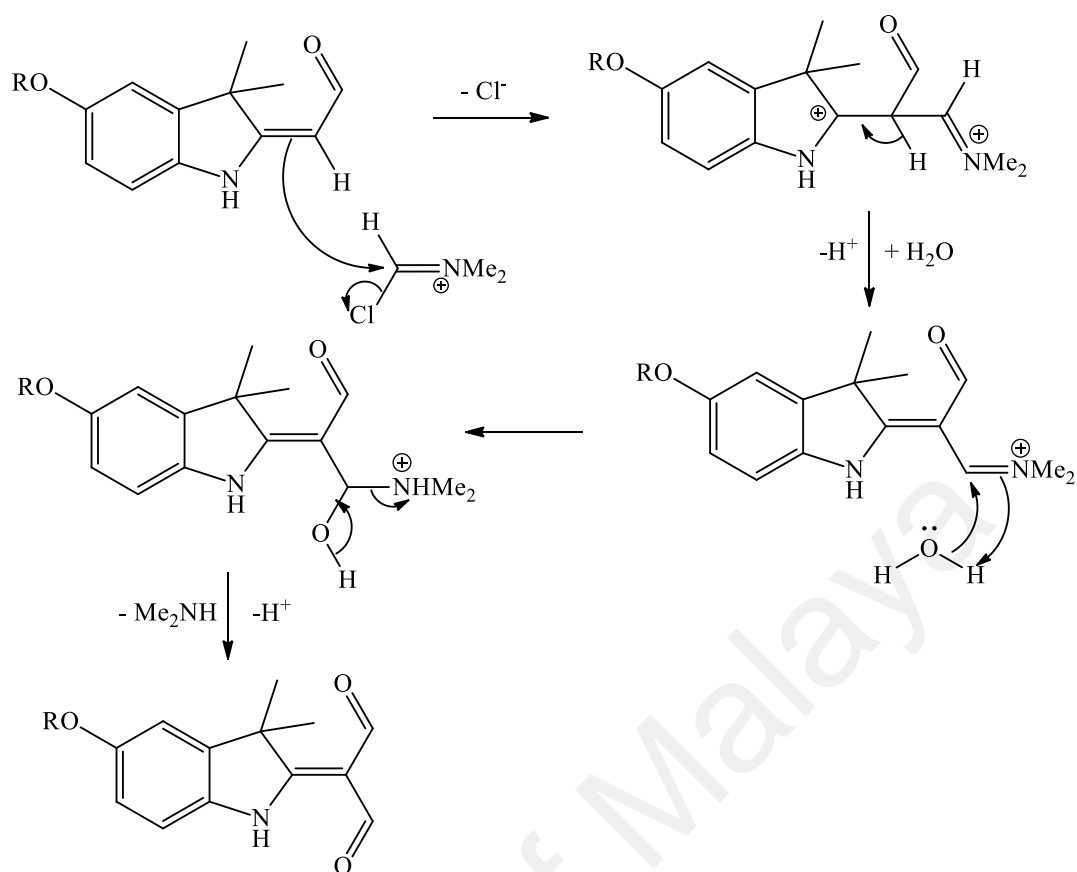


Figure 4.5: Reaction mechanism of the Second attack from activated molecule of DMF on 5-alkoxy-2,3,3-trimethylindolenine

4.2 Physical properties of macrocyclic ligands and complexes.

The series of macrocyclic dibenzo tetraaza[14]annulene ligands were synthesized using condensation reaction in a 1:1 molar ratio of the 2-(diformylmethyldene)-5-(alkyloxy)-3,3-dimethylindole with 4,5-bis(alkyloxy)benzene-1,2-diamine as shown in Scheme 3-5. Interaction of nickel(II) salt with the macrocyclic ligands in 1:1 (L:M) molar ratio in ethanolic solution produced a series of metal complexes **27–29** in an appreciable yield. The synthesized compounds were characterized by the elemental analysis and spectroscopic techniques chemical analysis and some physical properties of the macrocyclic ligands and nickel(II) complexes are listed in Table 4.1.

Table 4.1: Physical properties of macrocyclic ligands and complexes.

Compounds/Complex	Color	Very Soluble	Melting Point(°C)
Macrocyclic ligand 23	Dark red powder	CH ₂ Cl ₂ , CHCl ₃	182-184
Macrocyclic ligand 24	Dark red powder	CH ₂ Cl ₂ , CHCl ₃	181-183
Macrocyclic ligand 25	Dark red paste	CH ₂ Cl ₂ , CHCl ₃	176-177
Macrocyclic ligand 26	Dark red paste	CH ₂ Cl ₂ , CHCl ₃	153-154
Complex 27	Dark red powder	CH ₂ Cl ₂ , CHCl ₃	208-209
Complex 28	Dark red paste	CH ₂ Cl ₂ , CHCl ₃	183-184
Complex 29	Dark red paste	CH ₂ Cl ₂ , CHCl ₃	178-179

The analytical results demonstrate that all the complexes have (1:1) metal ligand stoichiometry (Honeybourne, 1973). The compounds are dark red in colour and they are stable as solid or in solution under atmospheric conditions. Both the macrocyclic ligands and nickel(II) complexes are soluble in chloroform and dichloromethane but completely insoluble in water and other organic solvents. Decomposition of these compounds and their complexes took place above 300°C. The IR spectra and NMR spectra showed the confirmation structure for the targeted compounds of the macrocyclic ligands and complexes. Geometrical configuration of the complexes was found to be square planar, where 4 nitrogen atoms coordinated to the nickel ion which showed a weak d-d transition in UV-Vis spectra. Observation through OPM and confirmed by DSC showed that macrocyclic compound **23**, **24** and the Nickel complex **27** did not have liquid crystal

properties, whereas compound **25**, **26**, nickel complex **28** and **29** appeared as discotic columnar liquid crystals.

4.3 Elemental Analysis Studies (CHN) and Mass Spectra (LCMS data)

Elemental analysis (CHN) of macrocyclic ligands and their nickel complexes showed that the found percentage value of carbon, hydrogen and nitrogen were in good agreement with the predicted structure, as the CHN data agree well with the theoretical values. The elemental analysis data for each macrocyclic ligand and their nickel complexes are given in table 4.2.

Table 4.2: Summary CHN data on new synthesized compounds.

Compounds	Calculated (%)			Found (%)		
	C	H	N	C	H	N
Macrocyclic ligand 23	75.60	9.09	7.15	75.59	9.10	7.14
Macrocyclic ligand 24	77.83	10.26	5.56	77.85	10.28	5.52
Macrocyclic ligand 25	78.61	10.68	5.00	78.62	10.66	4.99
Macrocyclic ligand 26	79.25	11.01	4.55	79.26	11.00	4.56
Complex 27	72.12	8.51	6.82	72.10	8.50	6.83
Complex 28	75.02	9.76	5.36	75.05	9.77	5.35
Complex 29	76.05	10.21	4.84	76.06	10.20	4.83

Table 4.3 shows the summary of mass spectrum that confirmed the formula of new synthesized compounds. Macrocyclic ligand **26** and complex **29**, their mass spectra cannot be determined as too many fragments were found and the total mass of the compounds were out of instrument range.

Table 4.3: Summary of LCMS of new synthesized compounds.

Compounds	Formula	Exact Mass	Measured Ion Mass m/z
Intermediate compound 19	C ₁₉ H ₂₅ NO ₃	315.4067	316.1915
Intermediate compound 20	C ₂₃ H ₃₃ NO ₃	371.5130	372.2542
Intermediate compound 21	C ₂₅ H ₃₇ NO ₃	399.5662	400.2849
Intermediate compound 22	C ₂₇ H ₄₁ NO ₃	427.6193	428.3162

4.4 Infrared Spectroscopy Study

Important vibration bands of the free macrocyclic ligands and their nickel(II) complexes along with their assignments, which are useful for determining the mode of coordination of the ligands, are given in Table 4.4.

Table 4.4: Summary of IR spectra (refer to Appendix B)

	CH₂	NH	C=O	C=N	C-N	C=C	C-O	-Ar-
Compound 19	2922,2853	3145	1654	-	1371	1523	1078,1020	815
Macrocyclic Ligand 23	2924,2857	-	-	1634	1390	1504,1463	1075,1013	797
Complex 27	2919,2851	-	-	1595	1377	1506,1462	1078,1036	797
Compound 20	2932,2854	3190	1654	-	1371	1521	1079,1026	803
Macrocyclic Ligand 24	2920,2852	-	-	1635	1390	1504,1462	1076,1013	795
Complex 28	2920,2850	-	-	1604	1377	1505	1074,1023	795
Compound 21	2919,2851	3189	1653	-	1372	1520	1077,1018	808
Macrocyclic Ligand 25	2919,2851	-	-	1635	1390	1504,1462	1077,1035	796
Complex 29	2919,2851	-	-	1595	1377	1506,1462	1077,1037	797
Compound 22	2920,2850	3188	1654	-	1371	1527	1077,1019	807
Macrocyclic Ligand 26	2917,2849	-	-	1636	1390	1504,1463	1075,1014	797

Sharp absorption band range 2851 - 2924 cm^{-1} is attributed to aliphatic $\nu^{\text{s}}_{\text{CH}}$ and $\nu^{\text{as}}_{\text{CH}}$ bands. This supports the existence of long alkyl chains in the structure of macrocyclic ligands and complexes. The intermediate compounds exhibit medium bands in the region 1653-1654 cm^{-1} assigned to the C=O, stretching of aldehyde group (El-Motaleb et al., 2005; Kunda et al., 2013).

This band disappears upon condensation to form macrocyclic ligand, and the appearance of strong bands at 1634-1635 cm^{-1} indicating the formation of azomethine group C=N (Bernhard et al., 2018; Clougherty et al., 1957; Wang et al., 2016). A significant change, with respect to the spectra of the macrocyclic ligands, is observed in the spectra of the corresponding nickel complexes as shown in Figure 4.6. In the

complexes, the azomethine band (C=N) of the Schiff-base linkage undergoes a remarkable shift toward lower wave numbers compared with its position in the spectra of the free ligands, because of coordination of the nitrogen atom to the metal (Rosa et al., 1992; Sakata et al. (2002))

Coordination of the azomethine group to the nickel ion is expected to reduce the electron density on the Schiff-base linkage (C=N), causing a reduction in its vibrational frequency (Kim & Lee, 2013). The $\nu(\text{C-N})$ stretching frequency is also shifted to lower wave numbers in all the complexes. This behaviour is compatible with the participation of both amide nitrogen atoms in the coordination to the metal centres (Maroney & Rose, 1984). Other absorption bands in the range $\sim 1462\text{-}1520\text{ cm}^{-1}$ may be attributed to $\nu(\text{C=C})$ aromatic stretching vibrations of the aromatic moiety (Sakata et al., 2002; Salavati-Niasari & Bazarganipour, 2006).

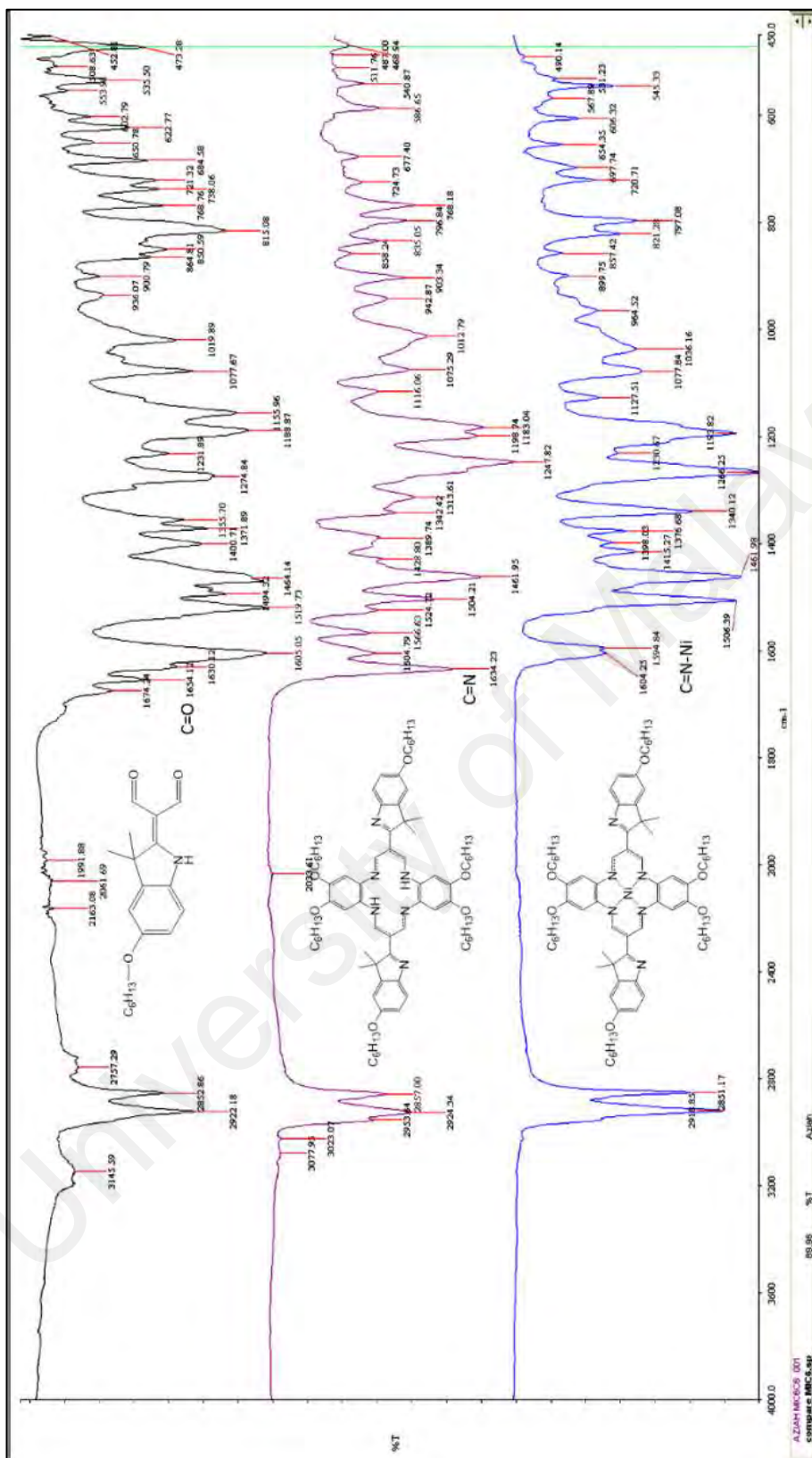


Figure 4.6: Comparison between IR spectrum intermediate compound of diformyl, macrocyclic ligand and its nickel complex

4.5 NMR Spectra of intermediate compounds.

4.5.1 ^1H NMR and ^{13}C NMR spectroscopy for intermediate compounds of

4,5-bis(alkoxy) benzene-1,2-diaminium chloride

The preparation of 4,5-bis(alkoxy)benzene-1,2-diaminium chloride was done through three steps synthesis which began with the alkylation of pyrocatechol using alkyl bromide following the slight modification of a literature procedure (Howard et al., 2008; Kanth Siram et al., 2012; Schlamp et al., 2012). The next step was nitration of alkylated benzene using concentrated nitric and sulphuric acid (Grolik et al., 2006; Yun et al., 2013). Lastly, followed by reduction process of dinitro derivatives to diaminium diether intermediate compounds using tin(II) chloride and concentrated hydrochloric acid (Ding et al., 2012; Song et al., 2013). This compound is known to be a very unstable compound and was used directly in the next procedure for macrocyclic ligands synthesis.

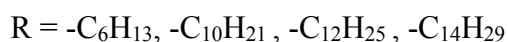
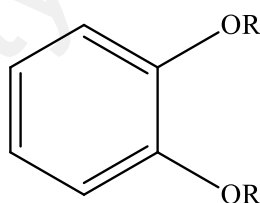


Figure 4.7: Chemical structure for 1,2-Dialkyloxybenzene

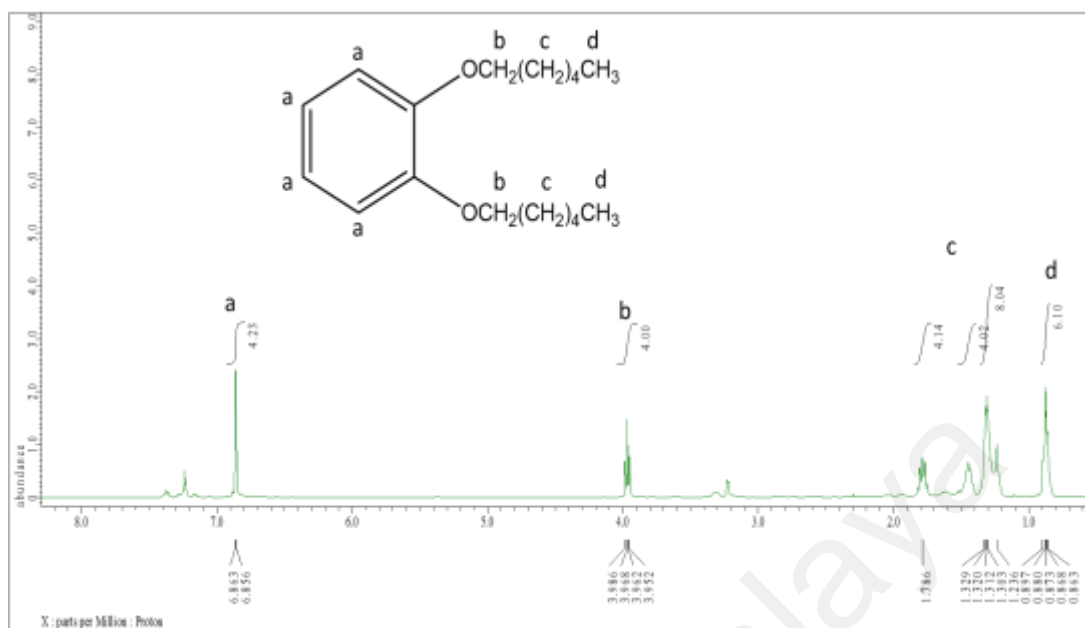


Figure 4.8: ^1H NMR spectra of compound **1**

^1H NMR characterization was done on the crude product. NMR data shows the main product give 70-75% in the crude mixture. The appearance of significant peak such as a singlet at 6.86 ppm with was integrated as 4 protons assigned as an aromatic proton. A triplet peak at 3.97 ppm belonged to the proton of an ether group ($-\text{OCH}_2-$) and also a triplet at 0.88 ppm was attributed to proton at the end of the alkyl chains ($-\text{CH}_3$) which was integrated as 4 protons and 6 protons. The rest of the protons that belong to the aliphatic proton ($-\text{CH}_2-$) on alkyl chain were observed as multiple peaks between 1.24-1.79 ppm (Appendix B). The results were significantly consistent with what has been found and reported elsewhere (Chen et al., 2013; Howard et al., 2008; Schlamp et al., 2012).

^{13}C NMR spectroscopy of these intermediate series also found to be in agreement with the data published before.

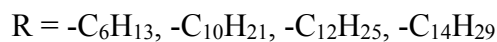
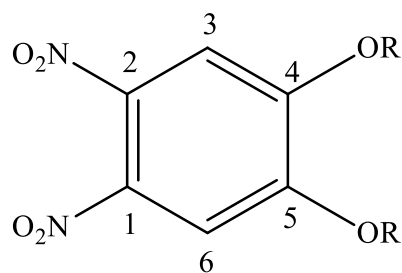


Figure 4.9: Chemical structure of 1,2-Dinitro-4,5-bis(alkyloxy)benzene

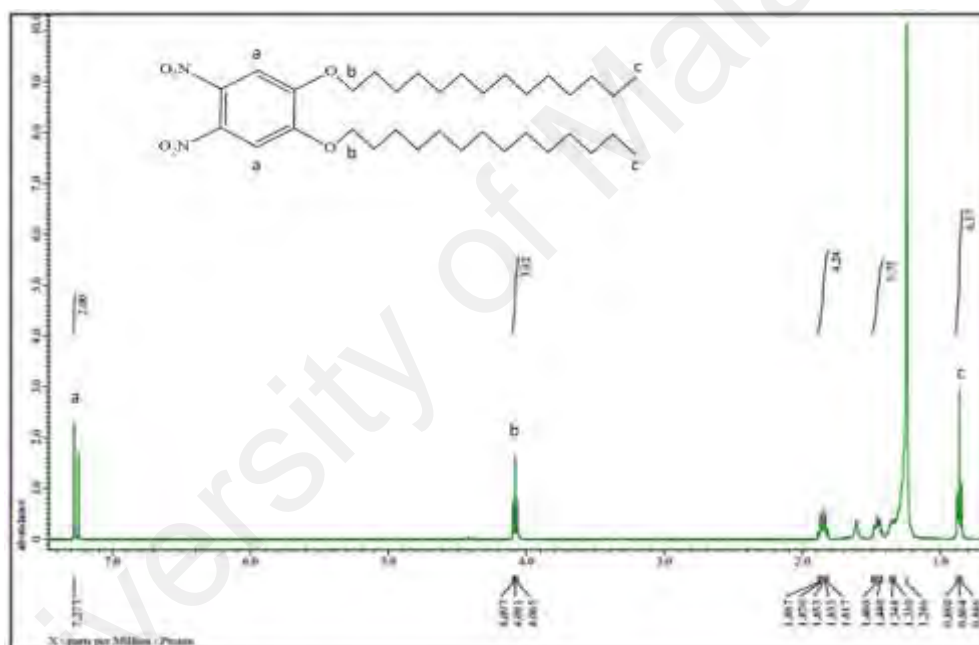


Figure 4.10: ¹H NMR spectra of compound 8

¹H NMR chemical shift observed at 7.28 as a singlet peak integrated as 2 protons had proven the disappearance of another 2 aromatic protons as it was replaced by 2 nitro group. The appearance of chemical shift as a singlet showed that the aromatic protons were attached at C3 and C6 on the aromatic ring, showing that no neighbouring proton was detected (Ding et al., 2012; Song et al., 2013).

^{13}C NMR spectra support the confirmation of chemical structure of 1,2-Dinitro-4,5-bis(alkyloxy)benzene of compound **5**, **6**, **7** and **8**. (Refer Appendix D). All ^{13}C NMR shifting was found to be the significantly agree with the published data by Gautrot and Hodge (2007), Lim et al. (2013), Yun et al. (2013) and Zhang et al. (2013).

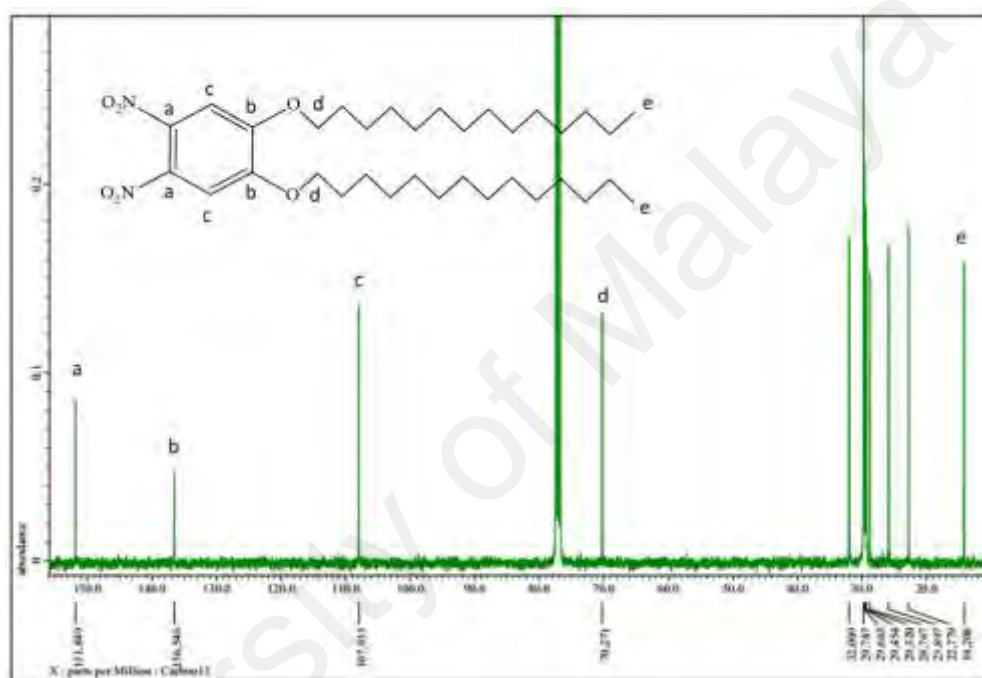
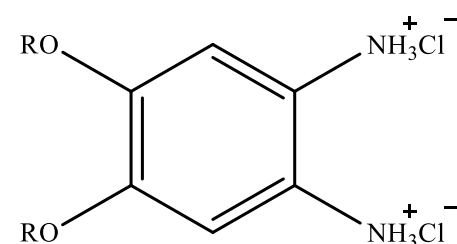


Figure 4.11: ^{13}C NMR spectra of compound **8**



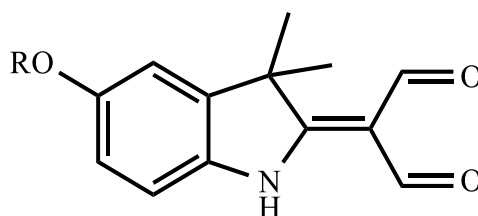
$\text{R} = -\text{C}_6\text{H}_{13}, -\text{C}_{10}\text{H}_{21}, -\text{C}_{12}\text{H}_{25}, -\text{C}_{14}\text{H}_{29}$

Figure 4.12: Chemical structure of 4,5-bis(alkyloxy)benzene-1,2-diaminium chloride

The synthesis procedure for above diamine derivatives was carried out by combining and a slight modification in the procedures reported elsewhere. (Grolík et al., 2006; Howard et al., 2008). The products are known to be very reactive and easily decomposed when exposed to air. The reaction must be done under a nitrogen atmosphere. The compounds were used directly in the next step with respective diformyl for condensation reaction of macrocyclic ligands. Therefore, no ^1H NMR data were collected for this intermediate compounds.

4.5.2 ^1H and ^{13}C NMR for intermediate compounds of 2-(diformyl methylidene)-5-(alkoxy)-3,3-dimethyl-indole

^1H NMR and ^{13}C NMR spectral data for intermediate compound **14** were significantly matched with the data published by Bakulina et al. (2017) and Saikiran et al. (2017). Intermediate compounds of **15**, **16**, **17** and **18** have not been characterized as a confirmation of the structure can be elucidated in the next product. Furthermore as the reagent of BBR_3 was very limited so all the compounds were directly used in the next steps. Those compounds also have been synthesized and published by Baradarani et al. (2006) and Voloshin et al. (2003).



R = $-\text{C}_6\text{H}_{13}$, $-\text{C}_{10}\text{H}_{21}$, $-\text{C}_{12}\text{H}_{25}$, $-\text{C}_{14}\text{H}_{29}$

Figure 4.13: Chemical structure for 2-(diformylmethylidene)-5-(alkoxy)-3,3-dimethyl-indole

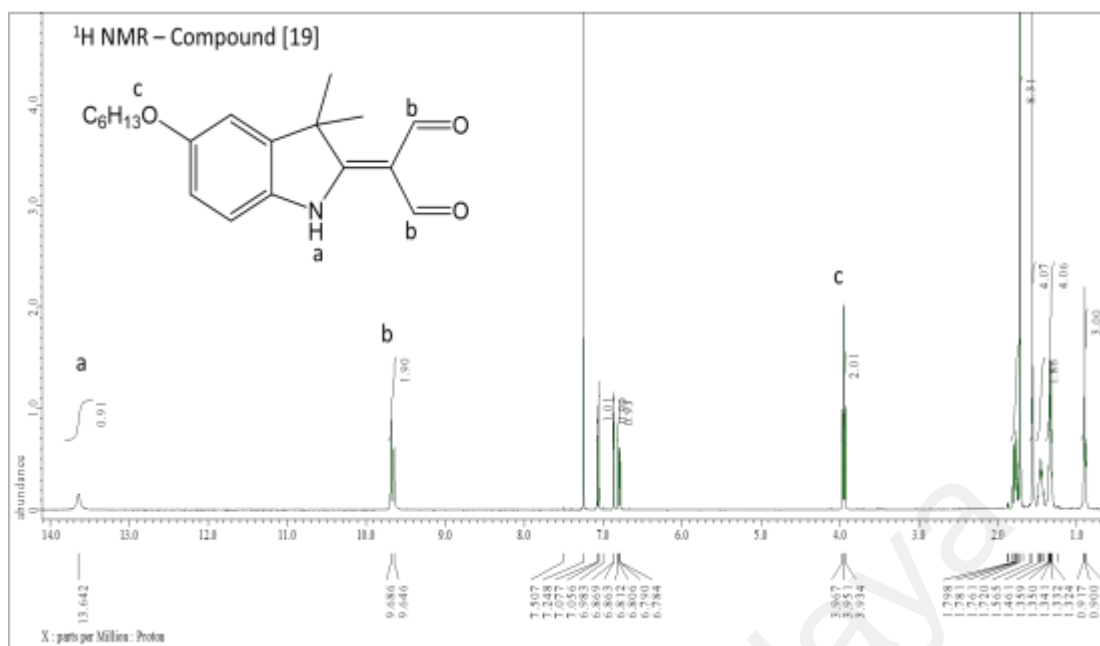


Figure 4.14: ^1H NMR spectra of compound **19**

^1H NMR spectra results of the synthesized intermediate compounds were in good agreement with the formation of diformyl group in these new indolenine compounds **19**, **20**, **21** and **22**. A broad singlet peak at 13.64 ppm was attributed to a proton atom belonging to an amine group (-NH) (Baradarani et al., 2006).

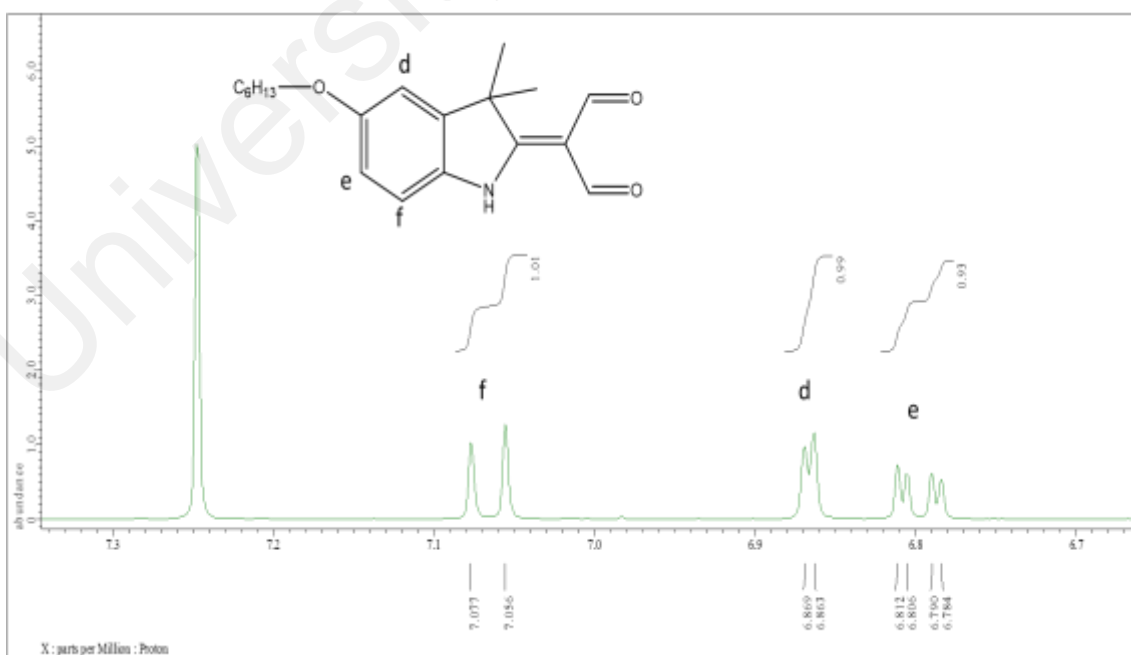


Figure 4.15: ^1H NMR spectra 6.7-7.3ppm for compound **19**

At 9.65 and 9.69 ppm, (refer to Appendix C) two singlet peaks can be observed, these two peaks were assigned as two proton atoms from each aldehyde group (-CHO) (Alyari et al., 2014; Rashidi et al., 2009). Proton atoms that belong to the aromatic ring (H_d, H_e, H_f) can be identified at NMR chemical shift 6.81 ppm as doublet-doublet peaks, 6.87 and 7.08 ppm as doublet peaks where their J coupling value is calculated as 8.8, 2.4, 2.4 and 8.4 Hz, respectively (Voloshin et al., 2003).

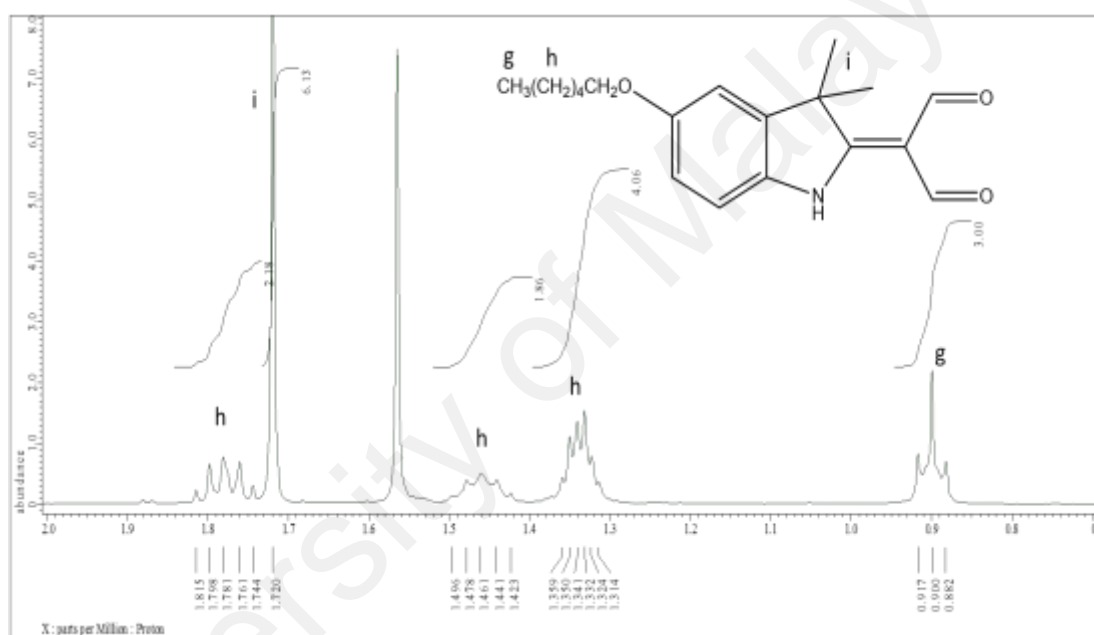


Figure 4.16: ¹H NMR spectra 0.8-1.9ppm of compound **19**

The ¹H NMR spectra above show that aliphatic alkyl chain protons can be observed between 1.31-1.81 ppm as multiplet peaks (refer to Appendix C). Meanwhile, chemical shift at 1.72 ppm appeared as singlet peak attributed to indolenine germinal dimethyl group which give integration of 6 protons (Helliwell et al., 2006). Lastly, a triplet peak at 0.90 ppm with J coupling value of 7.0 Hz can be assigned to three protons allocated at the end of the alkyl chain (Pyta et al., 2016; Voloshin et al., 2003). ¹³C NMR spectra in Figure 4.17 supports the confirmation of chemical structure for

2-(diformylmethylidene)-5-(alkoxy)-3,3-dimethyl-indole as compound **19**, **20**, **21** and **22** (refer Appendix D).

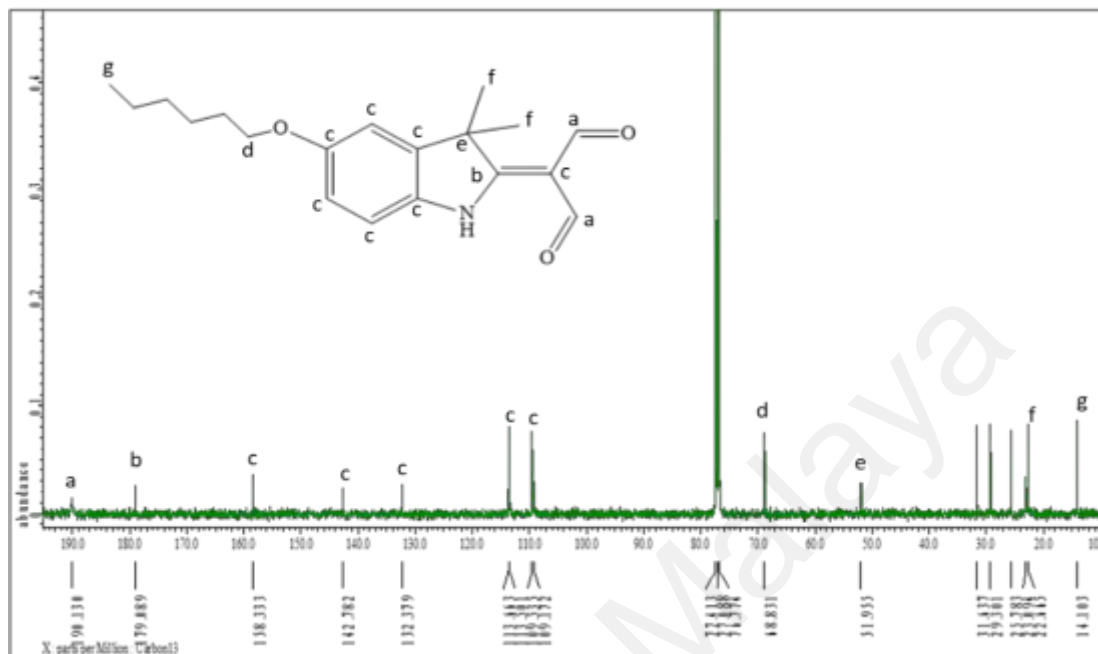


Figure 4.17: ^{13}C NMR spectra of compound **19**

4.6 ^1H and ^{13}C NMR for Macrocyclic compounds of dibenzotetraaza[14]annulene 6-alkyloxy.

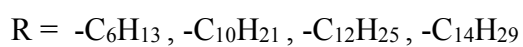
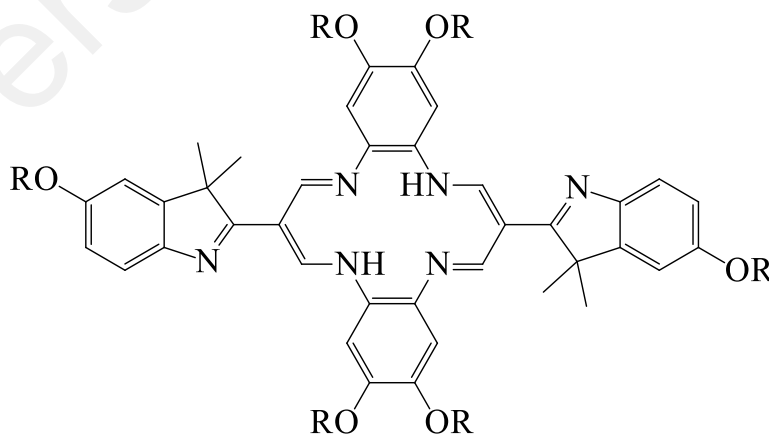


Figure 4.18: Chemical structure for Macrocyclic compounds of dibenzotetraaza[14]annulene 6-alkyloxy

^1H NMR spectral data have confirmed the molecular structure of this new macrocyclic ligand of dibenzotetraaza[14]annulene derivatives, where proton N-H is the most important signature for DBTTA, that it can be found at the downfield chemical shift of 14.86 ppm and appears as a triplet with J coupling value of 6.2 Hz (Grolík et al., 2011; Khaledi et al., 2013).

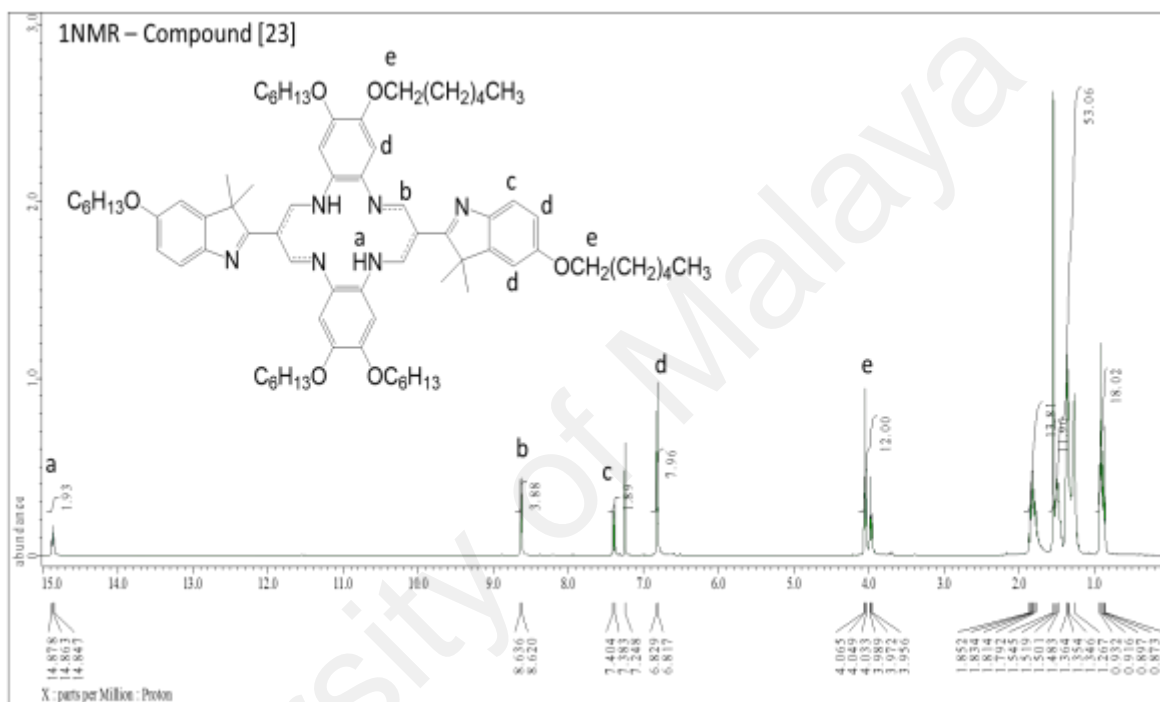


Figure 4.19: ^1H NMR spectra of compound **23**

As reported by Honeybourne (1974), the triplet peak implies a bridging position between two nitrogen atoms and undergoing a trans-coupling to two equivalent $-\text{NCH}$ protons or is explained as a rapid imine-enamine tautomerism by Dudek et al. (2011) and Azuma et al. (1995). This appeared very far downfield (14.86-14.93 ppm) because of the diamagnetic anisotropic and deshielding effect caused by two neighbouring aromatic rings of dibenzo and two extra π electrons imposed by the bridging (Honeybourne, 1973; Stojković et al., 2010). The electron donating group of ether ($-\text{OR}$) on dibenzo moiety increases the activity of π resonance. Hence, this increases diamagnetic anisotropic and

deshielding effect (Grolík et al., 2012; Grolík et al., 2006; Kleinpeter et al., 2011) that make the chemical shifts of N-H protons further downfield compare to macrocyclic DBTAA compounds (14.13-14.58 ppm) synthesized by Khaledi et al. (2013) and Grolík et al. (2011). Chemical shift for a proton -CHN group appeared as a doublet at 8.63 ppm ($J = 6.4$ Hz), supporting the explanation of the trans-coupling (Ricciardi et al., 1995; Sigg et al., 1982).

For the aromatic proton, H_c and H_d appeared at chemical shift between 6.80 ppm and 7.40 ppm with total integration of 12 hydrogen atoms (Khaledi et al., 2013), whereas, two triplet peaks that appeared at 4.05 ppm and 3.97 ppm with J coupling value of 6.4 Hz and 6.6 Hz are attributed to protons of ether groups (-OCH₂-) (Grolík et al., 2006).

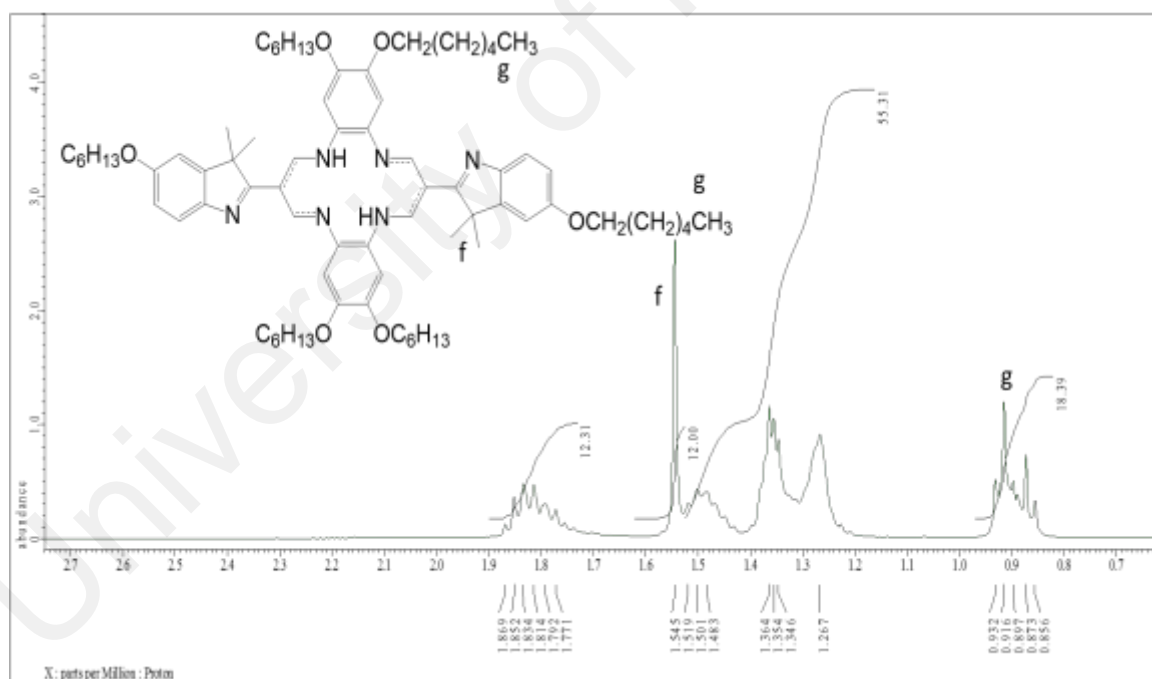


Figure 4.20: ¹H NMR spectra 0.7-2.7ppm for compound **23**

Multiplet peaks appearing at chemical shift between 1.27 ppm to 1.87 ppm can be assigned as aliphatic protons along the alkyl chains (Pyta et al., 2016). Meanwhile, the germinal methyl group appears as a singlet at 1.55 ppm, and two triplet peaks appear

farther upfield of this ^1H NMR spectra at 0.87 ppm and 0.92 ppm attributed to three protons at the end of alkyl chains with total integrations of 18 protons which are supporting the existence of six alkyl chains surrounding the macrocyclic compounds (Hoshino & Imamura, 1990).

^{13}C NMR spectra in Figure 4.21 shows primary carbons and quaternary carbons labeled as C1 and C4, whereas the rest are secondary carbons. Signals at 180.78 ppm and 156.97 ppm were attributed to quaternary carbons of $-\text{N}=\underline{\text{C}}_a-$ and $\underline{\text{C}}_b-\text{N}=\text{}$ groups. The signals shifted further downfield as the carbon bonded to more electronegative nitrogen atoms (Neiss, 2000). The peaks appearing in a range between 101.77-148.26 ppm were assigned to carbon atoms of aromatic rings. As for aliphatic carbon signals, these can be observed at range 14.23-70.12 ppm. All the assigned peaks were confirmed by HMBC, HSQC and ^{13}C Dept (refer to Appendix C).

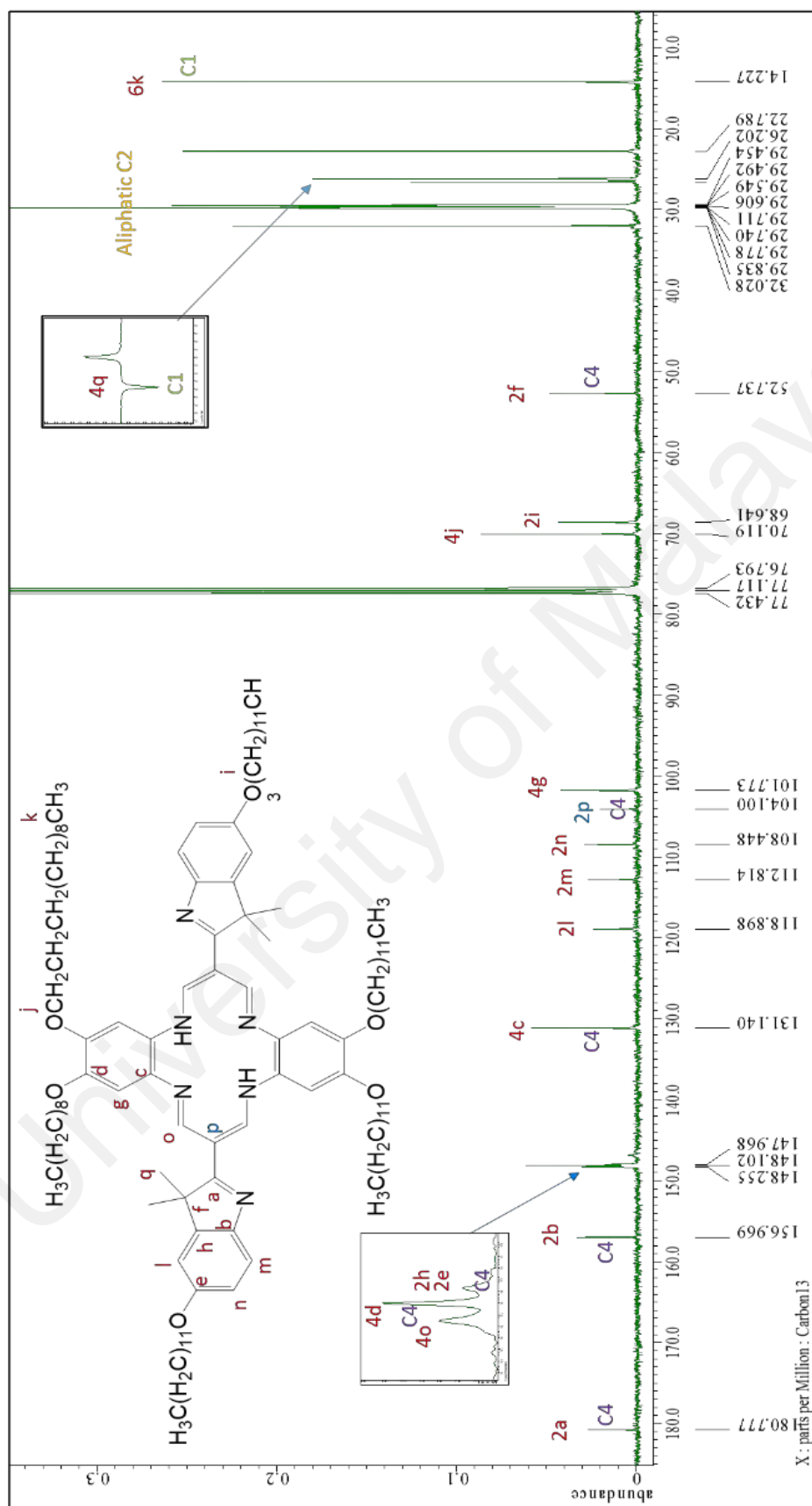


Figure 4.21: ^{13}C NMR spectrum of macrocyclic ligand 25

4.7 ^1H and ^{13}C NMR for Nickel Complexes of Macrocyclic compounds of dibenzotetraaza [14]annulene 6-alkyloxy.

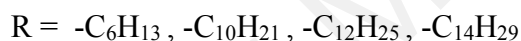
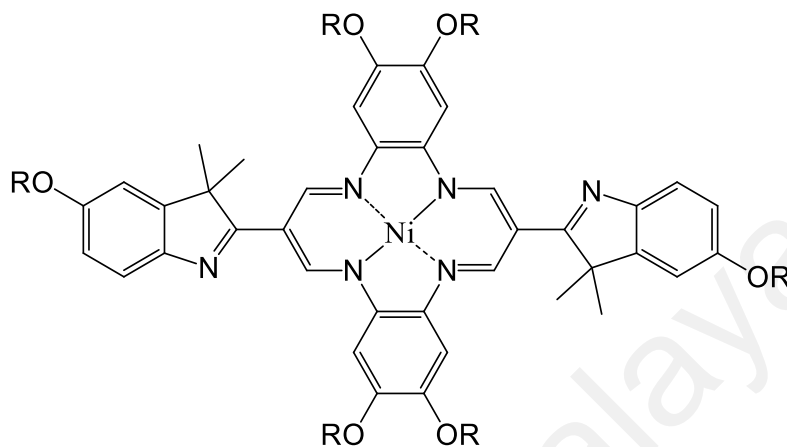


Figure 4.22: Chemical structure for Nickel Complexes of Macrocyclic compounds of dibenzotetraaza[14]annulene 6-alkyloxy

In the ^1H NMR spectrum of the nickel complexes, the NH chemical shift of the ligand no longer exists. This showed the deprotonation of amine proton inside the macrocyclic ligands followed by coordination with the Ni^{2+} ion (Eilmes et al., 1999; Khaledi et al., 2013; Klose et al., 1999,). The four CHN protons of the diiminato moieties appear as a singlet around $\delta = 8.09$ to 8.33 ppm (Khaledi et al., 2013; Khaledi et al., 2014) as shown in Figure 4.23, supporting that there is no more trans-coupling as in the macrocyclic ligands.

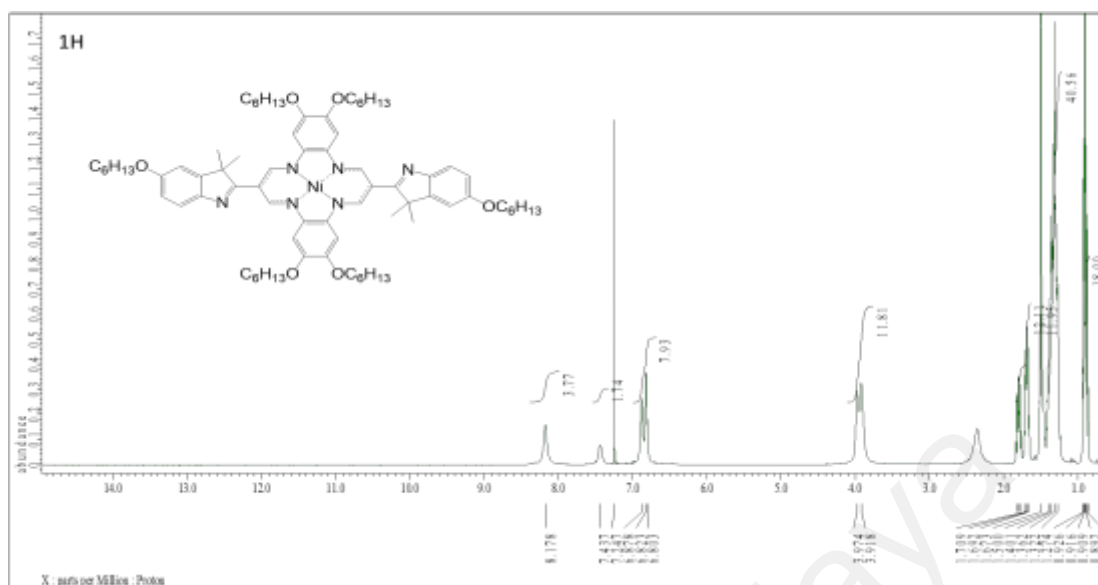


Figure 4.23: ^1H NMR spectrum of complex **27**

In Figure 4.24, ^{13}C NMR spectrum of complex **27** the chemical shift of carbon (C-N-Ni) appeared shifted to 178.90 ppm compare from 180.88 ppm in its macrocyclic ligand **23**. This shows the confirmation of the nickel has coordinated to atom nitrogen in the centre of macrocyclic ligands (Neiss, 2000; Orzeł et al., 2010; Paquette et al., 2015).

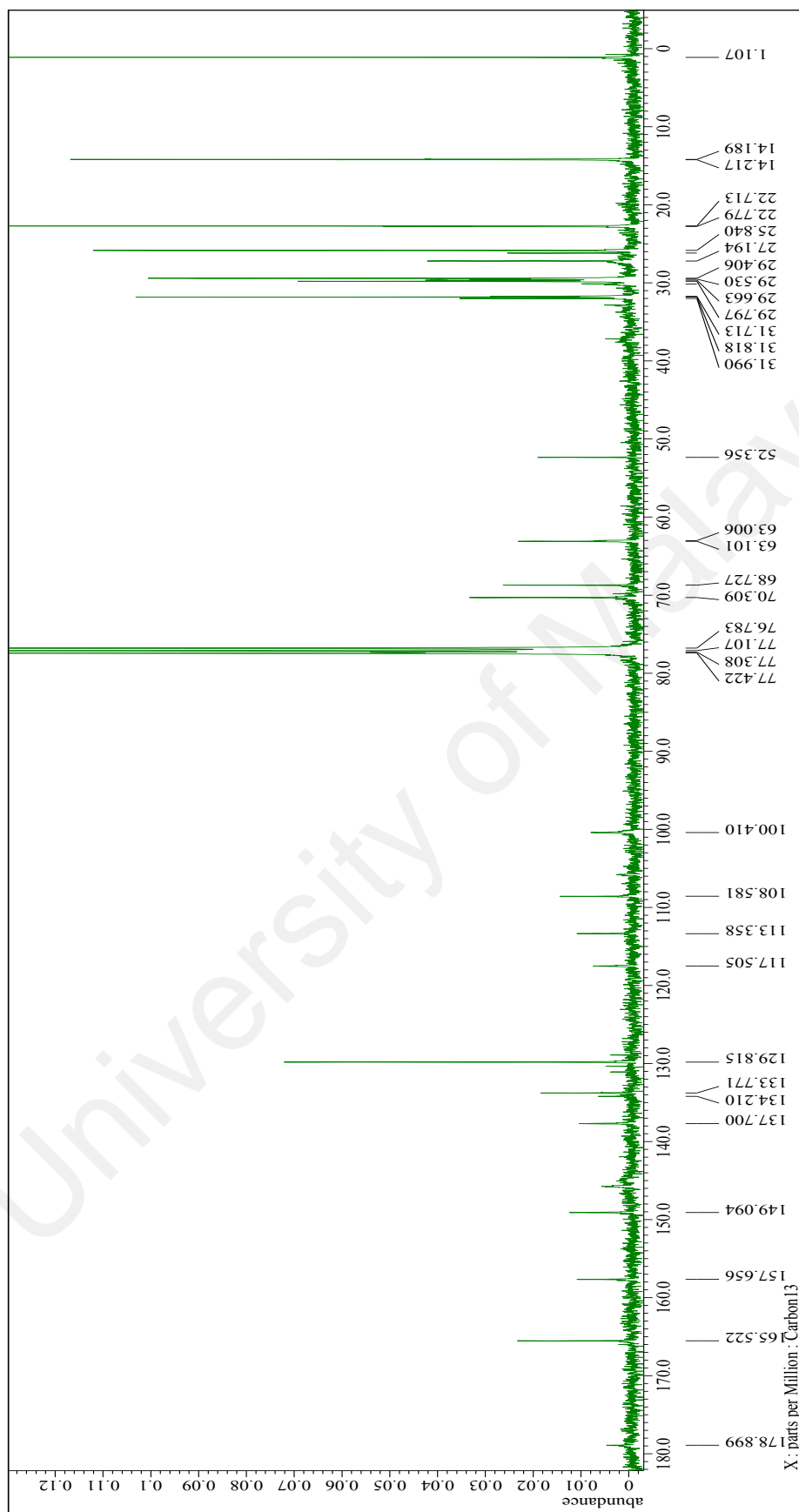


Figure 4.24: ^{13}C NMR spectrum (400 MHz, CDCl_3) of Complex 27

4.8 Thermogravimetric Analysis (TGA)

Thermogravimetric analysis (TGA) studies of the macrocyclic ligands **23**, **24**, **25** and **26** and its nickel complexes **27**, **28**, **29**, and **30** were carried out in a nitrogen atmosphere at 10°C per minute from 50°C up to 900°C. TGA results of the macrocyclic ligands showed that the compounds were stable up to range 270-280°C and decomposition was completed without any residue. Instead, the thermal decomposition of their nickel complexes occurred in the ratio of residue range 4.31-5.94% which represented the formation of nickel(II) oxide (NiO) as a final product. This supports the complexation of macrocyclic ligands with nickel ion (Appendix E).

Table 4.5: Summary of TGA analysis on synthesized compounds.

Compounds	Decomposition	Calculated % of residue ratio	Found % of residue ratio (NiO)
Macrocyclic 23	100	0	0
Macrocyclic 24	100	0	0
Macrocyclic 25	100	0	0
Macrocyclic 26	100	0	0
Complex 27	94.06	6.06	5.94
Complex 28	95.29	4.76	4.71
Complex 29	95.69	4.30	4.31

4.9 UV-Visible Spectra Studies

The absorption bands appearing around ~ 300 and ~ 395 nm are attributed to $\pi \leftrightarrow \pi^*$ transitions within macrocyclic ligand molecules (Każmierska et al., 2015; Pawlica et al., 2006; Reichardt & Scheibelein, 1978; Rosa et al., 1992). The absorption bands around ~ 451 nm that appeared sharp can be attributed to charge transfer (CT) transition from metal to the macrocyclic ligand (Hashemnia et al., 2014; Reichardt & Scheibelein, 1978; Sakata et al., 1985; Salavati-Niasari & Bazarganipour, 2006). The absorption bands around the 504-505 nm range can be attributed to ligand-field transitions (d-d transition), that appeared as a weak absorption and were compatible with square-planar nickel(II) complexes which coordinated to four nitrogen donors (see Appendix F) (Bailey et al., 1984; Mames et al., 2015; Rodakiewicz-Nowak et al., 2005; Streeky et al., 1980).

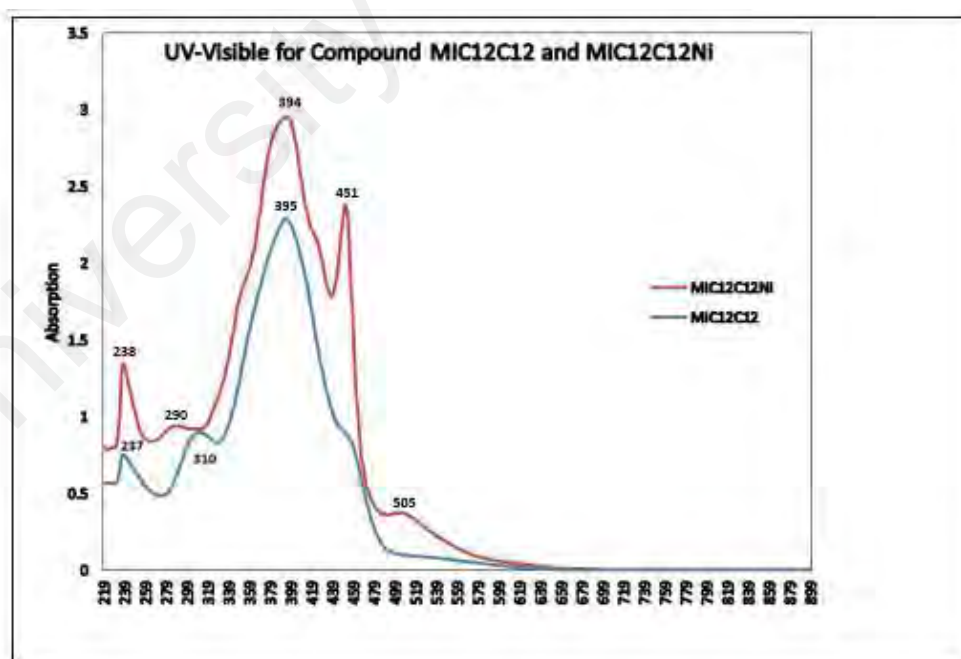


Figure 4.25: UV-Vis spectra of macrocyclic ligand **25** and its complex **29**

4.10 X-Ray Crystallography Studies

These basic nickel complexes of DBTAA have been synthesized to study the structure of the compound using X-Ray Crystallography Studies. Diffraction data for these complexes were measured using a Bruker SMART Apex II CCD area-detector diffractometer. The structures were solved by my former research colleague, Dr. Hamid Khaledi, currently at the University of Washington.

Most of the liquid crystals especially columnar liquid crystalline compounds were very hard to get a suitable single crystal for X-ray scanning purposes. The disc-like structures tend to stack on each other to form needle or hair type crystals (Pisula et al., 2010).

According to crystal data and refinement, the empirical formula for complex **32** was $C_{50}H_{56}N_6NiO_2$ and formula weight 831.71 g/mol. The crystal system is monoclinic with a space group of $C2/m$. Cell length was measured (\AA) as $a=22.1256(10)$, $b=6.8194(4)$ and $c=13.8693(7)$ with cell angle $\alpha=90^\circ$, $\beta=95.308^\circ(50)$ and $\gamma=90^\circ$. Cell volume is 2083.67\AA^3 , where $Z = 2$, $Z'=0$, with R-Factor being 3.42%.

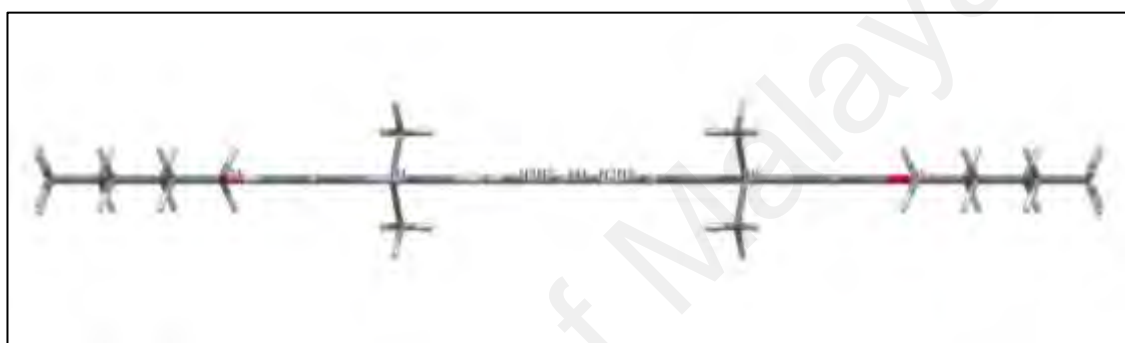


Figure 4.27: Default view on c^* axis.

Figure 4.27 above shows the view from c^* axis, where the structure is geometrically planar, and except for the dimethyl group lies on either side of the plane (Gompper et al., 1992; Khaledi et al., 2013; Weiss et al., 1977; Whyte et al., 2012), together with all hydrogen atoms along the aliphatic alkyl chains. This packing diagram (Figure 4.28) reveals that this nickel complex is stacked peripherally with the aliphatic alkyl chains pointing in the same direction. There is no interaction between nickel-nickel atoms in the packing. The existence of 2 aliphatic chains in the structure is not enough to allow the structure to be stacked in a columnar manner.

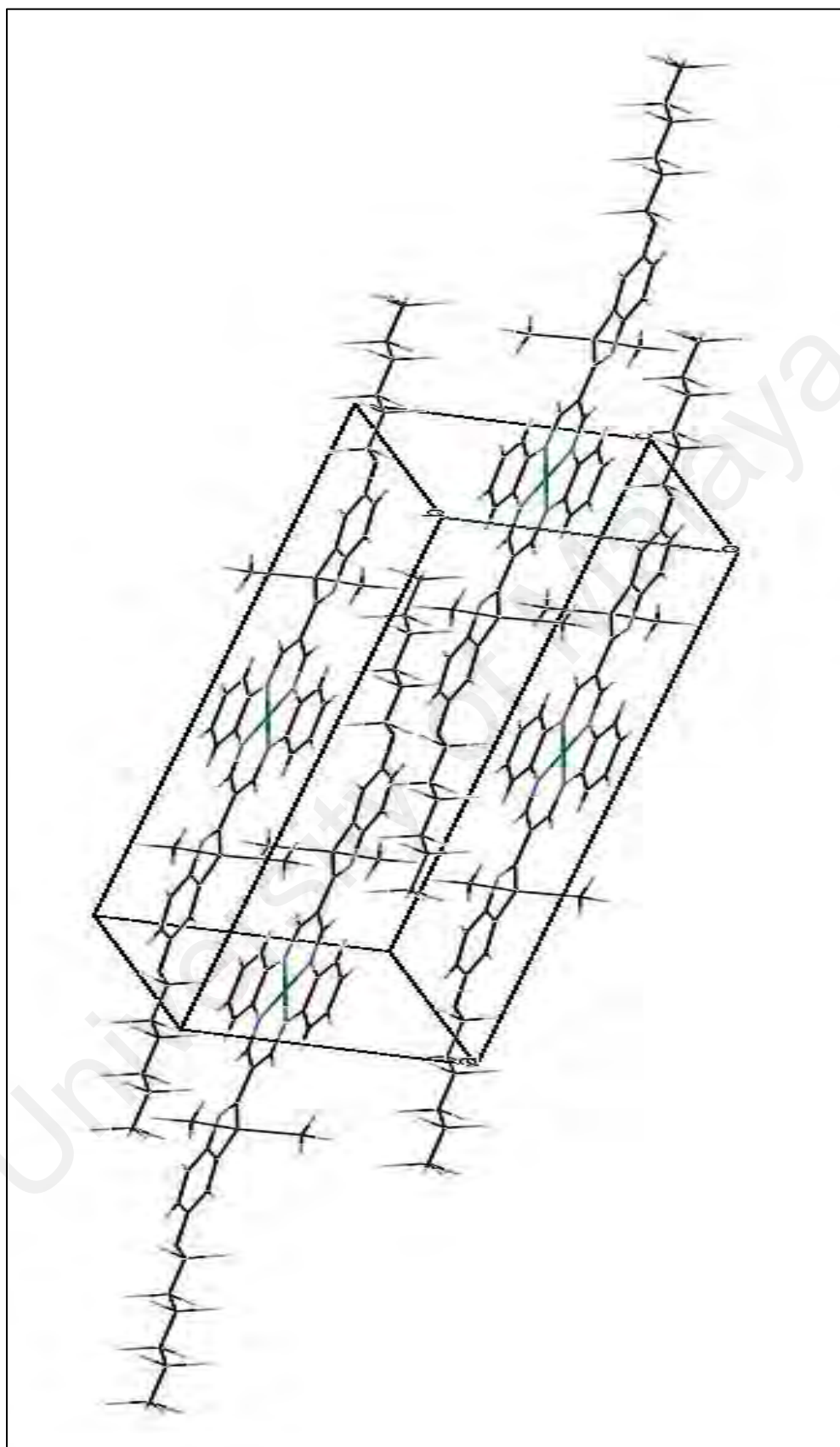


Figure 4.28: Packing diagram of nickel complex 32

Table 4.6: Selected bond lengths (Å) and bond angles (°) for this nickel complex.

Bond lengths (Å)		Bond angles (°)	
Ni1-N2	1.864	N2-Ni1-N3	94.31
Ni1-N3	1.852	N2-Ni1-N2	180.00
O1-C4	1.371	N2-Ni1-N3	85.69
O1-C19	1.428	C4-O1-C19	118.5
N1-C1	1.408	C1-N1-C9	107.7
N1-C9	1.300	Ni1-N2-C11	126.4
N2-C11	1.333	Ni1-N2-C12	113.7
N2-C12	1.407	C11-N2-C12	119.9
N3-C18	1.311	Ni1-N3-C18	126.9
N3-C17	1.415	Ni1-N3-C17	113.7
C10-C11	1.392	C18-N3-C17	119.5
C10-C18	1.406	N1-C1-C2	126.7

CHAPTER 5 : LIQUID CRYSTAL STUDIES

The synthesized compounds were designed with six aliphatic alkyl chains so they could have a mesomorphic discotic columnar behaviour. According to Grolik et al. (2006), this behaviour is mostly influenced by the shape structure, a number of flexible pendant chains and its length surrounding the discotic units. Their mesomorphic behaviour is governed more by the behaviour of the chains than by the ordering of the core inside the columns (Jakli & Saupe, 2006). Disc-like substances which are formed of a flat shaped aromatic core and surrounded by several peripheral aliphatic chains can easily exhibit liquid crystalline behaviour, especially discotic columnar, and can be identified by the typical optical textures of fan-shaped birefringent defects which can be observed through OPM (Chandrasekhar et al., 1977).

5.1 Optical Polarized Microscopy Studies (OPM)

Macrocyclic ligands and its nickel complexes were studied under OPM by exposing them to heating and cooling on the rate range from 1-5°C per minute. This was done until the compound shows its liquid crystals behaviour. Figure 5.1 to Figure 5.7 where the images captured under OPM at the stated temperature.

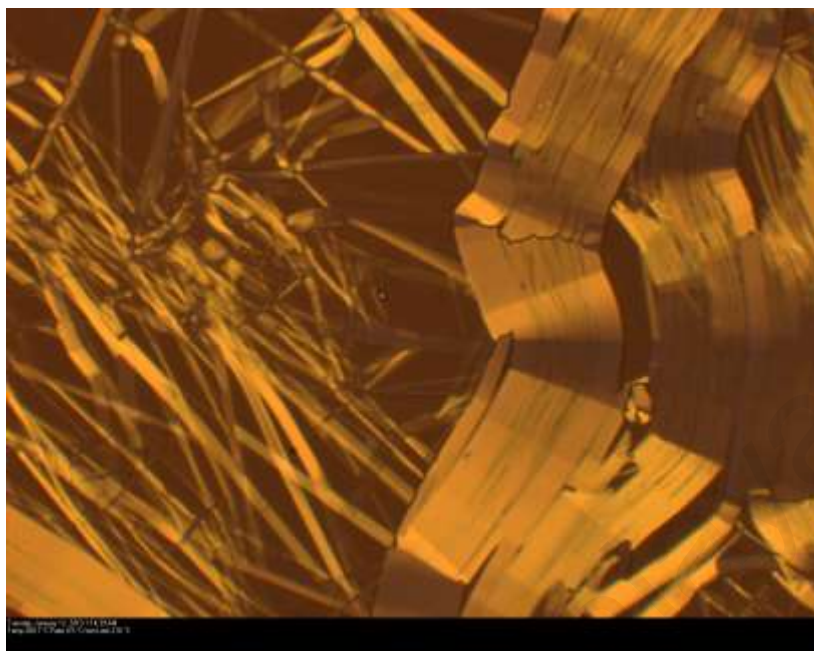


Figure 5.3: Image from OPM for Complex **27** at 209.7°C

Observation under optical polarized microscopy (OPM) showed that macrocyclic ligands of compound **23** and **24**, and also complex **27** do not show liquid crystalline phases. They melted directly into the isotropic liquid at temperature 182.2°C, 179.1°C and 209.7°C, respectively, and on cooling the samples crystallized. This shows there is a high mesophase stability, because of the existence of strong interdisc core-core π interactions (Giroto et al., 2014). As the length of flexible peripherals affected the mesogenic behaviour (Hirose et al., 2014), this result shows that the synthesized macrocyclic compounds required longer carbon chains.

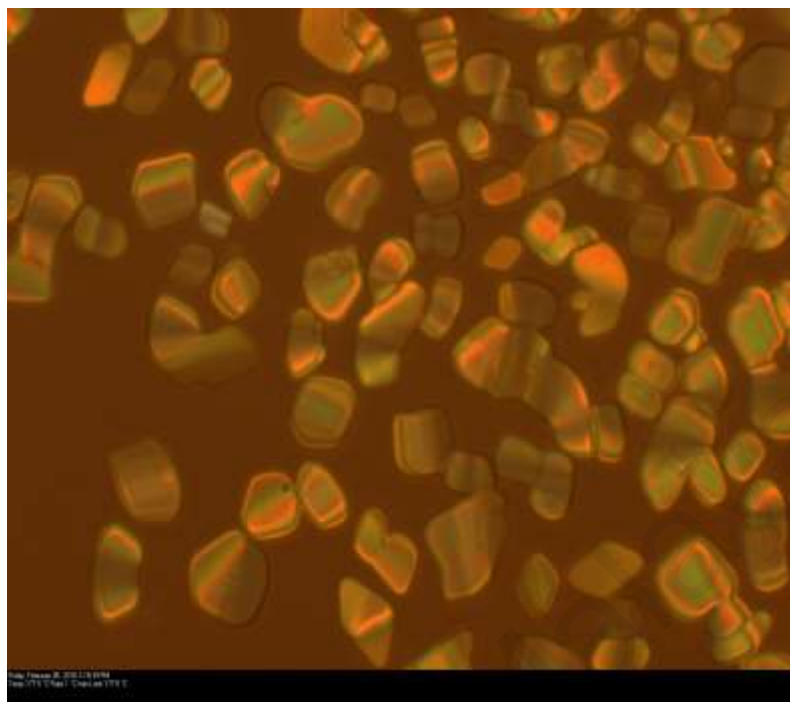


Figure 5.4: Image from OPM for Complex **25** at 177.5°C

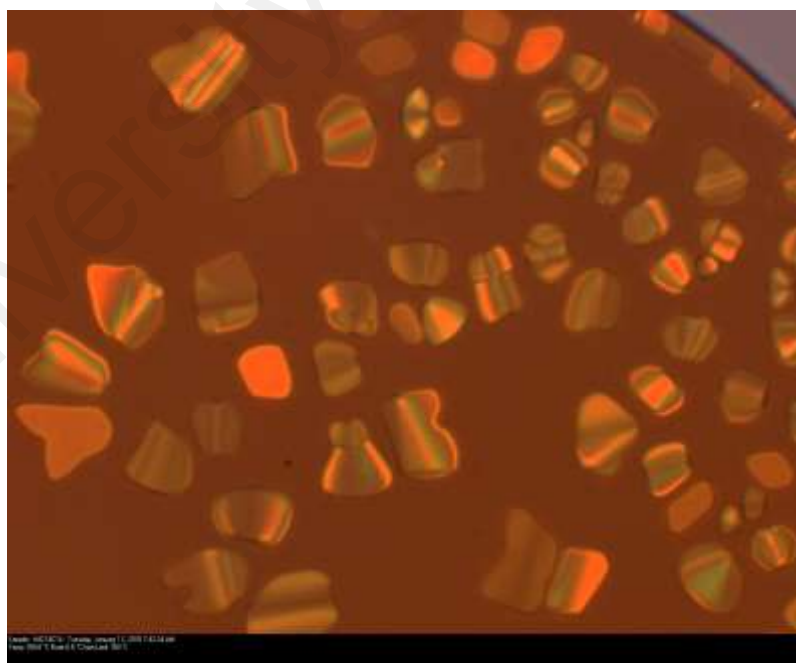


Figure 5.5: Image from OPM for Macrocylic ligand **26** at 159.8°C

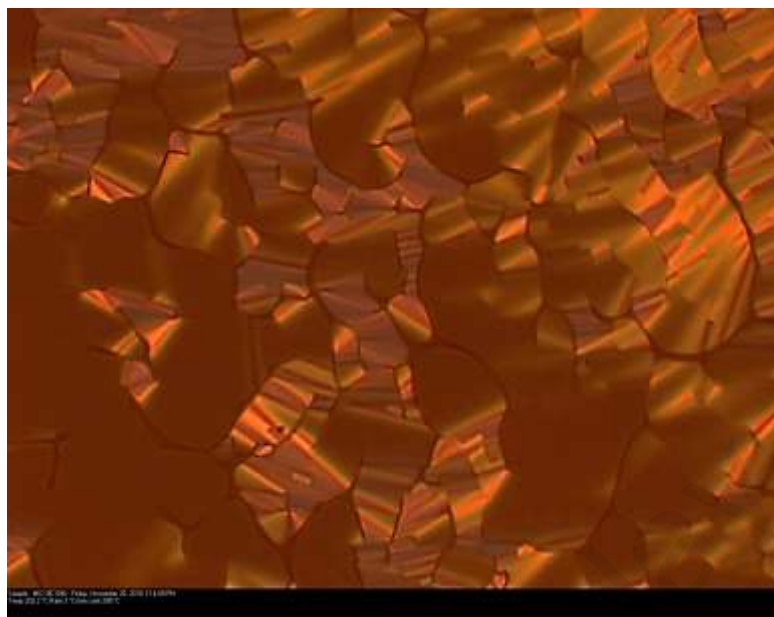


Figure 5.6: Image from OPM for Complex **28** at 202.2 °C

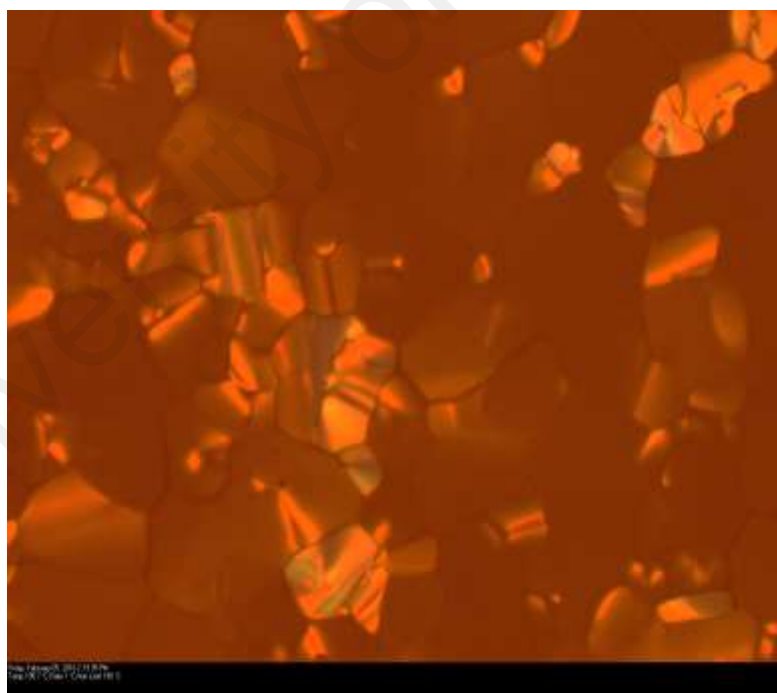


Figure 5.7: Image from OPM for Complex **29** at 195.7°C

Macrocyclic compounds **25** and **26**, nickel complexes **28** and **29** have shown fan-shaped texture under OPM at temperatures of 177.5°C, 159.8°C, 202.2 °C, and 195.7°C, respectively. From the appearance of this fan-shaped texture, indicates that compounds and complexes possess discotic columnar liquid crystals phase at respective temperature (Collings, 1990; Tanaka et al., 2012).

Comparing macrocyclic compound **24** and its complex **28**, both structures have the same length of 10 carbon chains but only the complex **28** showed liquid crystalline properties. This can be explained in terms of interaction between Ni-Ni atom having increased the molecular anisotropy and facilitated the formation of liquid crystals phase of the compound (Giroud-Godquin & Maitlis, 1991).

5.2 Differential Scanning Calorimetry (DSC) studies

The thermal behaviour of the compounds was further studied using DSC, with a scanning rate of 10°C/min on heating and cooling. During the heating, DSC traced sharp endothermic peaks which were attributed to the melting transition from crystal into a liquid phase and from crystal to columnar phase (Table 5.1). On cooling, the transition temperatures were slightly shifted down compare to heating, by 2.5-7.5°C (Grolík et al., 2012).

Table 5.1: DSC measurement of the macrocyclic ligands and complexes

Compounds	Heating(°C)	Cooling(°C)
Macrocyclic ligand 23	Cr 181.3 Liq	Liq 177.0 Cr
Macrocyclic ligand 24	Cr 180.0 Liq	Liq 175.0 Cr
Macrocyclic ligand 25	Cr 175.0 Col	Col 170.0 Cr
Macrocyclic ligand 26	Cr 152.5 Col	Col 145.0 Cr
Complex 27	Cr 207.5 Liq	Liq 200.0 Cr
Complex 28	Cr 202.5 Col	Col 200.0 Cr
Complex 29	Cr 197 Col	Col 194 Cr

Cr – Crystal; Col – discotic columnar; Liq – Liquid

The behaviours on heating and cooling are fully reversible (Appendix G). From the results of DSC, we can conclude that the increases in length of aliphatic chains will decrease the melting transition between phases (Collings, 1990).

Enthalpy change (ΔH) can be determined by the formula $\Delta H = KA$, where K is machine constant and A is the area under the curve. Here enthalpy of fusion (ΔH_f) was chosen for the comparison. For compounds **23**, **24** and complex **27** the ΔH_f is 8.92, 6.78 and 10.92 kJ/mol, respectively. As for macrocyclic ligands **25** and **26**, and complexes **28** and **29**, the ΔH_f is 2.10, 2.82, 3.24 and 3.32 kJ/mol, respectively (Acree & Chickos, 2006). The results show that more energy was released to form bonding of crystal lattice and also proves that lesser energy was released to form liquid crystalline phases.

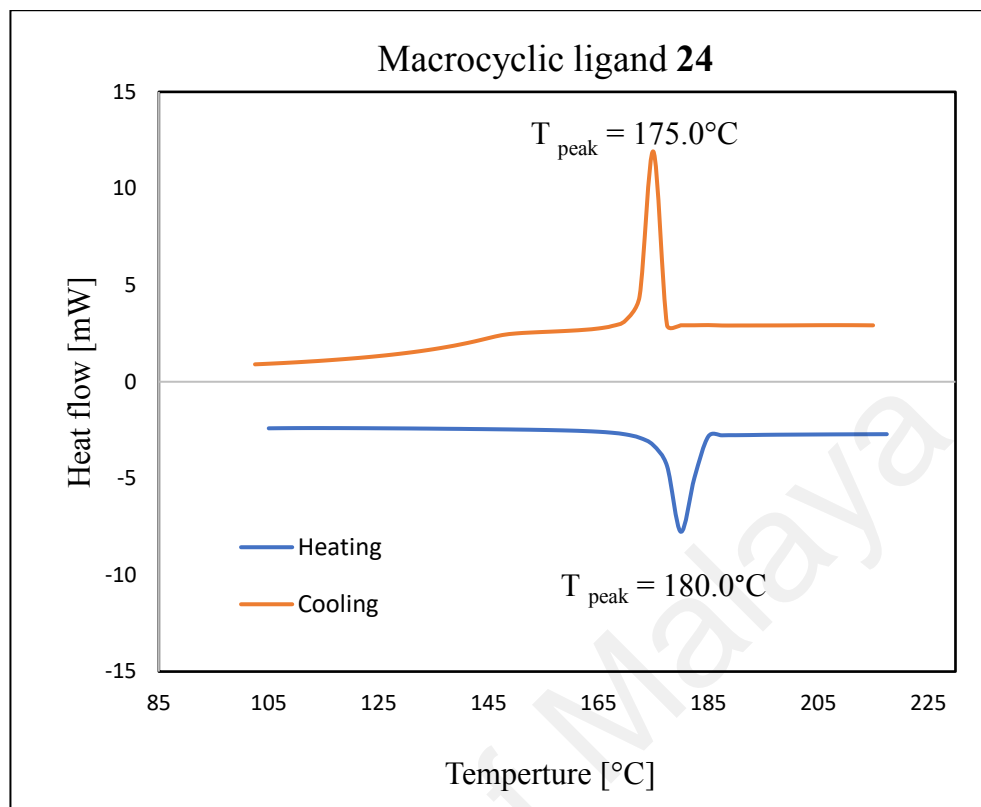


Figure 5.8: DSC measurement of macrocyclic ligand **24** on scanning rate 10°C/min.

CHAPTER 6 : CONCLUSION

New series of macrocyclic DBTAA ligands **23**, **24**, **25** and **26** have been successfully synthesized through a condensation reaction of 2 ratio 2 of new synthesized series of 2-(diformylmethylidene)-5-(alkoxy)-3,3-dimethylindole compounds and 4,5-bis(alkyloxy)benzene-1,2-diaminium chloride compounds. Each macrocyclic ligand was surrounded by six symmetrical aliphatic alkyl chains. (6, 10, 12 and 14 carbon chains). All the chemical structures of the new compounds have been successfully characterized by physico-chemical techniques of elemental analysis (CHNS), Fourier transforms infrared spectroscopy (ATR-FTIR), nuclear magnetic resonance spectroscopy (^1H and ^{13}C NMR), ultraviolet-visible spectroscopy (UV-Vis), thermal gravimetric analysis (TGA), and single crystal X-ray crystallography.

They were designed in such a way as to create a disc-like molecule, so the molecule will behave as discotic columnar in the mesophases. Nickel complexes from macrocyclic ligand **23**, **24**, and **25** have been synthesized successfully, except for macrocyclic ligand **26**, as the compound had solubility problem. The x-ray crystallographic studies on the basic structure of nickel complex **32** revealed the planarity of the core structure. Upon complexation with nickel salt, the metal atom could be easily inserted into the central cavity of the macrocyclic and coordinated to four nitrogen atoms in the centre.

Observation under OPM shows that only macrocyclic ligands **25** and **26**, and complexes **28** and **29** were having behaviour of discotic columnar, which can be seen as a fan-like texture in their mesophases form. This result was confirmed by DSC studies, as the transition peak appeared around the same temperature observed under OPM. The rest of the compounds **23**, **24** and complex **27** only showed changes from liquid to crystal, and thus it can be concluded that the compounds and complex do not have liquid crystal

properties. The enthalpy change of fusion (ΔH_f) for the transition also shows the double value for compounds **23**, **24** and complex **27**, as more energy was released in order to form a crystal lattice. The compounds **23**, **24** and complex **27** give ΔH_f with values of 2.10, 2.82 and 3.32 kJ/mol, respectively, the values showing significantly lower energy for formation of columnar liquid crystal phases.

This research can be widened up in the future. The synthesized compounds which are having columnar liquid crystal properties were promising to be active as organic semiconducting materials and optical storage. This required more work to be carried out in order to find the suitable application of these compounds. I would like to suggest a modification of the type of peripheral chains surrounding the DBTAA. By applying longer flexible chains can ensure a more promising result in producing liquid crystalline compounds. Introducing longer flexible peripheral carbon chains could decrease the melting point and temperature of mesogenic phases. With a lower melting point, a variety of applications can be introduced by the compounds such as dye sensitized solar cell, organic or inorganic light-emitting diode, biosensor and optical storage.

LIST OF REFERENCES

- Acree, W. E., & Chickos, J. S. (2006). Phase change enthalpies and entropies of liquid crystals. *Journal of Physical and Chemical Reference Data*, 35(3), 1051-1330.
- Allen, F. H. (2002). The Cambridge Structural Database: a quarter of a million crystal structures and rising. *Acta Crystallographica Section B*, B58, 380-388.
- Alyari, M., Baradarani, M. M., Afghan, A., & Joule, J. A. (2014). The synthesis of new heterocycles using 2-(4-Chloro-1,3-dihydro-3,3,7-trimethyl-2H-indol-2-ylidene) propanedial. *Journal of Heterocyclic Chemistry*, 51(3), 854-859.
- Azuma, N., Tani, H., Ozawa, T., Niida, H., Tajima, K., & Sakata, K. (1995). A crystal modification of Dibenzo[b,i][1,4,8,1]tetraaza[14]annulene: x-ray molecular structure and proton tautomerism of the highly x-conjugated form. *Journal of the Chemical Society, Perkin Transactions 2*, 343-348.
- Bailey, C. L., Bereman, R. D., Rillema, D. P., & Nowak, R. (1984). Redox and spectral properties of nickel(II) macrocycles containing dianionic, tetraazaannulene ligands. *Inorganic Chemistry*, 23(24), 3956-3960.
- Bakulina, O., Ivanov, A., Suslonov, V., Dar'in, D., & Krasavin, M. (2017). A speedy route to sterically encumbered, benzene-fused derivatives of privileged, naturally occurring hexahydropyrrolo[1,2-b]isoquinoline. *Beilstein Journal of Organic Chemistry*, 13, 1413-1424.
- Baradarani, M. M., Afghan, A., Zebarjadi, F., Hasanzadeh, K., & Joule, J. A. (2006). The synthesis of 3,3-dimethyl-2-(1-aryl-1h-pyrazol-4-yl)-3h-indoles. *Journal of Heterocyclic Chemistry*, 43, 1591-1595.
- Basiuk, V. A., Henao-Holguín, L. V., Álvarez-Zauco, E., Bassioui, M., & Basiuk, E. V. (2013). Gas-phase noncovalent functionalization of carbon nanotubes with a Ni(II) tetraaza[14]annulene complex. *Applied Surface Science*, 270, 634-647.
- Bernhard, Y., Lioret, V., & Decreau, R. A. (2018). Subphthalocyanine basicity: reversible protonation at the azomethine bridge. *New Journal of Chemistry*, 1144-0546.
- Bhattacharjee, C. R., Datta, C., Das, G., Chakrabarty, R., & Mondal, P. (2012). Induction of photoluminescence and columnar mesomorphism in hemi-disc salphen type Schiff bases via nickel(II) coordination. *Polyhedron*, 33(1), 417-424.

- Bin, Y., Zhang, F., & Yi, J. (2010). Patent No. CN101157660 (B). Dibenz tetraaza [14] annulene compound and preparation method and application thereof. China: European Patent Office.
- Chandrasekhar, S., Sadashiva, B. K., & Suresh, K. A. (1977). Liquid crystals of disc-like molecules. *Pramana*, 9(5), 471-480.
- Chen, L., Li, X., Ying, W., Zhang, X., Guo, F., Li, J., & Hua, J. (2013). 5,6-Bis(octyloxy)benzo[c][1,2,5]thiadiazole-bridged dyes for dye-sensitized solar cells with high open-circuit voltage performance. *European Journal of Organic Chemistry*, 2013(9), 1770-1780.
- Clougherty, L., Sousa, J., & Wyman, G. (1957). Notes - C=N stretching frequency in infrared spectra of aromatic azomethines. *The Journal of Organic Chemistry*, 22(4), 462-462.
- Collings, P. J. (1990). *Liquid Crystals : Nature's Delicate Phase of Matter*. . Bristol, England: Adam Hilger. 45-47.
- Cotton, F. A., & Czuchajowska, J. (1990). Recent developments in the chemistry of mono- and dinuclear complexes of the macrocyclic dianion, 5,7,12,14-tetramethyldibenzo[b,i][1,4,8,11] tetraazac. *Polyhedron*, 9(21), 2553-2566.
- de Sousa Sousa, N., de Lima, R. B., Silva, A. L. P., Tanaka, A. A., da Silva, A. B. F., & de Jesus Gomes Varela, J. (2015). Theoretical study of dibenzotetraaza[14]annulene complexes with first row transition metals. *Computational and Theoretical Chemistry*, 1054, 93-99.
- Ding, P., Chu, C.-C., Zou, Y., Xiao, D., Pan, C., & Hsu, C.-S. (2012). New low bandgap conjugated polymer derived from 2, 7-carbazole and 5, 6-bis(octyloxy)-4, 7-di(thiophen-2-yl) benzothiadiazole: Synthesis and photovoltaic properties. *Journal of Applied Polymer Science*, 123(1), 99-107.
- Donnio, B. (2014). Liquid-crystalline metallodendrimers. *Inorganica Chimica Acta*, 409, 53-67.
- Dudek, Ł., Grolík, J., Kaźmierska, A., Szneler, E., Eilmes, A., Stadnicka, K., & Eilmes, J. (2011). F⁻ and OH⁻ induced monodeprotonation of a lacunar cationic dibenzotetraaza[14]annulene: experimental evidence of tautomerism in a monoanionic macrocycle. *Tetrahedron Letters*, 52(28), 3597-3601.
- Eilmes, J., Basato, M., & Valle, G. (1999). Nickel complexes of tetradentate asymmetric ligands. *Inorganica Chimica Acta*, 290(1), 14-20.

- El-Motaleb, A., Ramadan, M., & Issa, R. M. (2005). Synthesis, characterization and ascorbic acid oxidase mimetic catalytic activity of copper(II) picolyl hydrazone complexes. *Transition Metal Chemistry*, 30(4), 471-480.
- Feng, X., Pisula, W., & Müllen, K. (2009). Large polycyclic aromatic hydrocarbons: Synthesis and discotic organization *Pure and Applied Chemistry* (Vol. 81, pp. 2203).
- Flores-Jarillo, M., Alvarez-Hernandez, A., Vazquez-García, R. Á., Arias, E., Moggio, I., & Torres, J. R. (2016). Synthesis and photophysical properties of highly fluorescent 2-aryl-6-(aryleneethynylene)-1H-indoles. *Dyes and Pigments*, 133, 41-50.
- Forget, S., & Kitzerow, H. S. (1997). Preliminary communication optical storage effect in a discotic columnar liquid crystal. *Liquid Crystals*, 23(6), 919-922.
- Forget, S., & Veber, M. (1997a). Dibenzotetraaza[14]annulene complexes. Part 2: Mesomorphic properties of four chain substituted compounds. *Molecular Crystals and Liquid Crystals Science and Technology. Section A. Molecular Crystals and Liquid Crystals*, 300(1), 229-243.
- Forget, S., & Veber, M. (1997b). Dibenzotetraaza[14]annulene complexes. Part. 3: Mesomorphic properties of six and eight chain substituted compounds. *Molecular Crystals and Liquid Crystals Science and Technology. Section A. Molecular Crystals and Liquid Crystals*, 308(1), 27-42.
- Gaspard, S., Maillardet, P., & Billard, J. (1985). Influence du nombre de chaînes latérales sur les propriétés mésogènes de dérivés porphyriniques. *Molecular Crystals and Liquid Crystals*, 123(1), 369-375.
- Gautrot, J. E., & Hodge, P. (2007). Poly(dibenzo[a,c]phenazine-2,7-diyl)s – Synthesis and characterisation of a new family of electron-accepting conjugated polymers. *Polymer*, 48(24), 7065-7077.
- Gawinkowski, S., Eilmes, J., & Waluk, J. (2010). Structure, vibrations, and hydrogen bond parameters of dibenzotetraaza[14]annulene. *Journal of Molecular Structure*, 976(1-3), 215-225.
- Giroto, E., Eccher, J., Vieira, A. A., Bechtold, I. H., & Gallardo, H. (2014). Luminescent columnar liquid crystals based on 1,3,4-oxadiazole. *Tetrahedron*, 70(20), 3355-3360.
- Giroud-Godquin, A.-M., & Maitlis, P. M. (1991). Metallomesogens: Metal complexes in organized fluid phases. *Angewandte Chemie International Edition*, 30(4), 375-402.

- Gompper, R., Illek, C., & Polborn, K. (1992). An access to unsymmetrically substituted dibenzo[14]annulenes. *Tetrahedron Letters*, 33(28), 3989-3992.
- Gregg, B. A., Fox, M. A., & Bard, A. J. (1989). 2,3,7,8,12,13,17,18-Octakis(.beta.-hydroxyethyl)porphyrin (octaethanolporphyrin) and its liquid crystalline derivatives: synthesis and characterization. *Journal of American Chemical Society*, 111(8), 3024-3029.
- Grolik, J., Dudek, Ł., Eilmes, J., Eilmes, A., Górecki, M., Frelek, J., . . . Donnio, B. (2012). New chiral discotics with helical organization of the mesophase—liquid crystalline derivatives of dibenzotetraaza[14]annulene. *Tetrahedron*, 68(20), 3875-3884.
- Grolik, J., Sieroń, L., & Eilmes, J. (2006). A new liquid crystalline derivative of dibenzotetraaza[14]annulene: synthesis, characterization and the preliminary evaluation of mesomorphic properties. *Tetrahedron Letters*, 47(47), 8209-8213.
- Grolik, J., Zwoliński, K., Sieroń, L., & Eilmes, J. (2011). Lacunar derivatives of dibenzotetraaza[14]annulene: synthesis and crystal structure of new receptors produced via bis-alkylation of the macrocyclic precursor. *Tetrahedron*, 67(14), 2623-2632.
- Hashemnia, S., Mehranpour, A. M., Rezvani, S., & Ameri Rad, J. (2014). Synthesis, electronic spectroscopy, electrochemistry and catalytic activity of a new Co (II) complex of 1,4,8,11-tetraaza[14]annulene derivative. *Synthetic Metals*, 187, 68-74.
- Helliwell, M., Afgan, A., Baradarani, M. M., & Joule, J. A. (2006). Formylation of an indolenine: 2-(diformylmethylidene)-3,3-dimethyl-2,3-dihydro-1H-indole. *Acta Crystallographica Section E Structure Reports Online*, 62(2), o737-o738.
- Hiller, H., Dimroth, P., & Pfitzner, H. (1968). 14-Dihydro-dibenzo[b .i] [5.9.14.18] tetraaza[14] annulen, ein makrocyclischer Chelat-Bildner. *Justus Liebigs Annalen der Chemie*, 717, 137-147.
- Hirose, T., Takai, H., Watabe, M., Minamikawa, H., Tachikawa, T., Kodama, K., & Yasutake, M. (2014). Effect of alkoxy terminal chain length on mesomorphism of 1,6-disubstituted pyrene-based hexacatenar liquid crystals: columnar phase control. *Tetrahedron*, 70(34), 5100-5108.
- Honeybourne, C. L. (1973). A study of porphin analogues—II: Reactivity indices and spin distribution in some conjugated polyaza macrocycles and their radical ions. *Tetrahedron*, 29(11), 1549-1557.

- Honeybourne, C. L. (1974). Evidence for paramagnetic exaltation in a $4n-\pi$ electron, $(4n-2)$ -atom, conjugated macrocycle. *Tetrahedron Letters*, 15(35), 3075-3078.
- Hoshino, T., & Imamura, Y. (1990). The dependence on alkyl chain length of ^1H NMR spectra of surfactant micelles with aromatic solubilize. *Bulletin of the Chemical Society of Japan*, 63(2), 502-506.
- Howard, M. J., Heirtzler, F. R., & Dias, S. I. G. (2008). Synthesis and stereochemistry of long-chain quinoxaline metallocyclophanes. *The Journal of Organic Chemistry*, 73(7), 2548-2553.
- Hunziker, M. (1985). Basel, Switzerland Patent No. EP0162804 B1. E. P. Register.
- Jager, E.-G. (1969). Aminomethylen- β -dicarbonylverbindungen als komplexliganden. v. neue konjugiert-ungesättigte neutralkomplexe mit vierzehngliedrigen, makrozyklischen liganden. *Zeitschrift für Anorganische und Allgemeine Chemie*, 364(3-4), 177-191.
- Jakli, A., & Saupe, A. (2006). *One- and Two-Dimensional Fluids : Properties of Smectic, Lamellar and Columnar Liquid Crystals*. New York, USA: Taylor & Francis Group. 89-95.
- Kanth Siram, R. B., Smith, J., Anthopoulos, T. D., & Patil, S. (2012). Acenaphtho[1,2-b]quinoxaline based low band gap copolymers for organic thin film transistor applications. *Journal of Materials Chemistry*, 22(10), 4450-4458.
- Kaźmierska, A., Gryl, M., Stadnicka, K., & Eilmes, J. (2013). New tetraaza[14]annulene receptors derived from 2,3-diaminonaphthalene: synthesis and crystal structures. *Supramolecular Chemistry*, 25(5), 276-285.
- Kaźmierska, A., Gryl, M., Stadnicka, K., Sieroń, L., Eilmes, A., Nowak, J., . . . Eilmes, J. (2015). Dicationic derivatives of dinaphthotetraaza[14]annulene: synthesis, crystal structures and the preliminary evaluation of their DNA binding properties. *Tetrahedron*, 71(24), 4163-4173.
- Khaledi, H., Olmstead, M. M., Ali, H. M., & Thomas, N. F. (2013). Indolenine meso-substituted dibenzotetraaza[14]annulene and its coordination chemistry toward the transition metal ions Mn(III), Fe(III), Co(II), Ni(II), Cu(II), and Pd(II). *Inorganic Chemistry*, 52(4), 1926-1941.
- Khaledi, H., Olmstead, M. M., Fukuda, T., & Ali, H. M. (2014). Heterometallic Pd(II)-Ni(II) complexes with meso-substituted dibenzotetraaza[14]annulene: double C-H bond activation and formation of a rectangular tetradibenzotetraaza[14]annulene. *Inorganic Chemistry*, 53(21), 11348-11350.

- Kim, E., & Lee, H. (2013). Template synthesis and x-ray crystal structures of 15-membered unsymmetric monobenzotetraazaannulene nickel(II) complexes. *Inorganica Chimica Acta*, 399, 62-66.
- Kim, S.-H., Choi, S.-W., Suh, H.-J., Jin, S.-H., Gal, Y.-S., & Koh, K. (2002). Surface plasmon resonance spectroscopy on the interaction of a self-assembled monolayer with linear hydrocarbon such as pentane, hexane, heptane and octane. *Dyes and Pigments*, 55, 17.
- Kleinpeter, E., Lammermann, A., & Kuhn, H. (2011). The anisotropic effect of functional groups in ¹H NMR spectra is the molecular response property of spatial nucleus independent chemical shifts (NICS)--conformational equilibria of exo/endo tetrahydrodicyclopentadiene derivatives. *Organic & Biomolecular Chemistry*, 9(4), 1098-1111.
- Klose, A., Solari, E., Heschbrouck, J., & Floriani, C. (1999). Ruthenium-carbene functionality bonded to dibenzotetramethyltetraaza[14]annulene: Metal-to-macrocyclic ligand-induced carbene migration. *Organometallics*, 18, 360-372.
- Kunda, P. K., Rao, J. V., Mukkanti, K., Induri, M., & Reddy, G. D. (2013). Synthesis, anticonvulsant activity and in silico studies of schiff bases of 2-aminothiophenes via guanidine-catalyzed Gewald reaction. *Tropical Journal of Pharmaceutical Research*, 12(4), 566-576.
- Lagerwall, J. P. F., & Scalia, G. (2012). A new era for liquid crystal research: Applications of liquid crystals in soft matter nano-, bio- and microtechnology. *Current Applied Physics*, 12(6), 1387-1412.
- Lee, J. H., Jang, I., Hwang, S. H., Lee, S. J., Yoo, S. H., & Jho, J. Y. (2012). Self-assembled discotic nematic liquid crystals formed by simple hydrogen bonding between phenol and pyridine moieties. *Liquid Crystals*, 39(8), 973-981.
- Li, H., Pang, M., Wu, B., & Meng, J. (2015). Synthesis, crystal structure and photochromism of a novel spiro[indoline-naphthalene]oxazine derivative. *Journal of Molecular Structure*, 1087, 73-79.
- Lim, S. Z. H., Neo, W. T., Cho, C. M., Wang, X., Tan, A. Y. X., Chan, H. S. O., & Xu, J. (2013). Electrochromic π -conjugated copolymers derived from azulene, fluorene, and dialkyloxybenzothiadiazole. *Australian Journal of Chemistry*, 66(9), 1048.
- Mames, I., Rodger, A., & Kowalski, J. (2015). Tetraaza[14]macrocyclic transition metal complexes as DNA intercalators. *European Journal of Inorganic Chemistry*, 2015(4), 630-639.

- Markovitsi, D., Andre, J.-J., Mathis, A., Simon, J., Spegt, P., Weill, G., & Ziliox, M. (1984). Three-stage melting of an annelide-type copper complex. A new type of organized phase: Tegma crystals. *Chemical Physics Letters*, 104(1), 46-49.
- Maroney, M. J., & Rose, N. J. (1984). Coordination chemistry of copper macrocyclic complexes: synthesis and characterization of copper complexes of TIM. *Inorganic Chemistry*, 23(15), 2252-2261.
- Meth-Cohn, O., & Tarnowski, B. (1982). *Advances in Heterocyclic Chemistry* (A. R. Katritzky Ed. Vol. 31). London, UK: Academic Press. p207.
- Mewis, R. E., & Archibald, S. J. (2010). Biomedical applications of macrocyclic ligand complexes. *Coordination Chemistry Reviews*, 254(15), 1686-1712.
- Miljanić, S., Dijanošić, A., Kalac, M., Radić Stojković, M., Piantanida, I., Pawlica, D., & Eilmes, J. (2012). Surface-enhanced raman scattering study of the binding modes of a dibenzotetraaza[14]annulene derivative with DNA/RNA polynucleotides. *Croatica Chemica Acta*, 85(4), 577-584.
- Mountford, P. (1998). Dibenzotetraaza[14]annulenes: versatile ligands for transition and main group metal chemistry. *Chemical Society Reviews*, 27, 105-116.
- Muena, J. P., Villagrán, M., Costamagna, J., & Aguirre, M. J. (2008). Dinaphthotetraaza[14]annulene copper(II) complexes in the electrocatalytic reduction of carbon dioxide and bisulfite anion. *Journal of Coordination Chemistry*, 61(4), 479-489.
- Neiss, T. G. (2000). Carbon-13 Nuclear Magnetic Resonance Spectroscopy. In R. A. Meyers (Ed.), *Encyclopedia of Analytical Chemistry: Applications, Theory and Instrumentation* (Vol. 13). New Jersey, US: John Wiley & Sons Inc. p11991-12017.
- Orzeł, Ł., Kania, A., Rutkowska-Żbik, D., Susz, A., Stochel, G., & Fiedor, L. (2010). Structural and electronic effects in the metalation of porphyrinoids. Theory and experiment. *Inorganic Chemistry*, 49(16), 7362-7371.
- Paquette, J. A., Sauv e, E. R., & Gilroy, J. B. (2015). Polymers Containing Nickel(II) Complexes of Goedken's Macrocyclic: Optimized synthesis and electrochemical characterization. *Macromolecular Rapid Communications*, 36(7), 621-626.
- Pathak, S. K., Pradhan, B., Gupta, R. K., Gupta, M., Pal, S. K., & Achalkumar, A. S. (2016). Aromatic [small pi]-[small pi] driven supergelation, aggregation induced emission and columnar self-assembly of star-shaped 1,2,4-oxadiazole derivatives. *Journal of Materials Chemistry C*, 4(27), 6546-6561.

- Pawlica, D., Radić Stojković, M., Sieroń, L., Piantanida, I., & Eilmes, J. (2006). Synthesis, crystal structures and the preliminary evaluation of the new dibenzotetraaza[14]annulene-based DNA/RNA binding agents. *Tetrahedron*, 62(39), 9156-9165.
- Pisula, W., Feng, X., & Mullen, K. (2010). Tuning the columnar organization of discotic polycyclic aromatic hydrocarbons. *Advanced Materials*, 22(33), 3634-3649.
- Pyta, K., Blecha, M., Janas, A., Klich, K., Pecyna, P., Gajecka, M., & Przybylski, P. (2016). Synthesis, structure and antimicrobial evaluation of a new gossypol triazole conjugates functionalized with aliphatic chains and benzyloxy groups. *Bioorganic & Medicinal Chemistry Letters*, 26(17), 4322-4326.
- Qian, X., Yan, R., Hang, Y., Lv, Y., Zheng, L., Xu, C., & Hou, L. (2017). Indeno[1,2-b]indole-based organic dyes with different acceptor groups for dye-sensitized solar cells. *Dyes and Pigments*, 139, 274-282.
- Rabaa, H., Khaledi, H., Olmstead, M. M., & Sundholm, D. (2015). Computational studies of a paramagnetic planar dibenzotetraaza[14]annulene Ni(II) complex. *Journal of Physical Chemistry A*, 119(21), 5189-5196.
- Rashidi, A., Afghan, A., Baradarani, M. M., & Joule, J. A. (2009). The synthesis of 4-(3,3-dimethyl-3H-pyrrolo[2,3-f]quinolin-2-yl)pyrazoles and 4-(3,3-dimethyl-3H-pyrrolo[3,2-h]quinolin-2-yl)pyrazoles. *Journal of Heterocyclic Chemistry*, 46(3), 428-431.
- Reddy, G. S. M., Jayaramudu, J., Varaprasad, K., Sadiku, R., Jailani, S. A., & Aderibigbe, B. A. (2014). Nanostructured liquid crystals. *Nanostructured Polymer Blends*. Elsevier. 299-324.
- Reddy, P. M., Rohini, R., Krishna, E. R., Hu, A., & Ravinder, V. (2012). Synthesis, spectral and antibacterial studies of copper(II) tetraaza macrocyclic complexes. *International Journal of Molecular Sciences*, 13(4), 4982-4992.
- Reichardt, C., & Scheibelein, W. (1978). Syntheses with aliphatic dialdehydes, XXVII [1] A non-template synthesis for the preparation of metal-free 1,4,8,11-tetraaza[14]annulene derivatives. *Zeitschrift für Naturforschung*, 33b, 1012-1015.
- Ricciardi, G., Bavoso, A., Rosa, A., Lelj, F., & Cizov, Y. (1995). Porphyrin-like macrocyclic complexes: molecular and electronic structure of (5,14-dihydro 6,8,15,17-tetramethyldibenzo[b,i][1,4,8,11] tetraazacyclotetradecinato) copper(II). *Journal of the Chemical Society, Dalton Transactions*(14), 2385-2389.

- Rodakiewicz-Nowak, J., Nowak, P., Rutkowska-Żbik, D., Ptaszek, M., Michalski, O., Mynarczuk, G., & Eilmes, J. (2005). Spectral and electrochemical characterization of dibenzotetraaza[14]annulenes. *Supramolecular Chemistry*, 17(8), 643-647.
- Rosa, A., Ricciardi, G., & Lelj, F. (1992). Porphyrin-like macrocyclic complexes: a spectroscopic and theoretical study of dibenzo [b,i] [1,4,8,11] tetraaza [14] annulenenickel (II). *Chemical Physics Letters*, 161(1-2), 127-140.
- Rosen, B. M., Wilson, C. J., Wilson, D. A., Peterca, M., Imam, M. R., & Percec, V. (2009). Dendron-mediated self-Assembly, disassembly, and self-organization of complex systems. *Chemical Reviews*, 109(11), 6275-6540.
- Saikiran, M., Sato, D., Pandey, S. S., Ohta, T., Hayase, S., & Kato, T. (2017). Photophysical characterization and BSA interaction of the direct ring carboxy functionalized unsymmetrical NIR cyanine dyes. *Dyes and Pigments*, 140, 6-13.
- Sakata, K., Hashimoto, M., & Naganawa, T. (1985). Preparation and spectral properties of nickel(II) and chloroiron(III) complexes with a macrocyclic N4-ligand: 5,14-dihydro-7,16-diethyldibenzo [b,i] [1,4,8,11]tetraazacyclotetradecine. *Inorganica Chimica Acta*, 98(1), L11-L14.
- Sakata, K., Shibata, H., Hashimoto, M., & Tsuge, A. (2002). Synthesis and reaction of novel tetraaza[14]annulene(nickel(II) complexes with amino groups in their side chains. *Journal of Coordination Chemistry*, 55(2), 225-239.
- Salavati-Niasari, M., & Bazarganipour, M. (2006). Host (nanodimensional pores of zeolite Y)-guest (tetraaza[14]annulene nickel(II) complexes, [Ni(Me4R2Bzo[14]tetraeneN4)]) nanocomposite materials: Ship-in-a-bottle synthesis, characterization and liquid phase oxidation of phenol with hydrogen peroxide. *Catalysis Communications*, 7(6), 336-343.
- Schlamp, S., Thoma, P., & Weber, B. (2012). New octahedral, head-tail iron(II) complexes with spin crossover properties. *European Journal of Inorganic Chemistry*, 2012(16), 2759-2768.
- Senthilkumar, N., Raghavan, A., Narasimhaswamy, T., & Kim, I.-J. (2013). Novel macro metallomesogens derived from simple dihydroxy benzenes. *Inorganica Chimica Acta*, 397, 129-139.
- Setia, S., Sidiq, S., De, J., Pani, I., & Pal, S. K. (2016). Applications of liquid crystals in biosensing and organic light-emitting devices: future aspects. *Liquid Crystals*, 43(13-15), 2009-2050.

- Shen, X., Sun, L., Jiang, B.-K., Wang, X., Nakashima, A., Miyamoto, N., . . . Zhu, D.-R. (2011). A macrocyclic ligand 5,14-dihydro-6,15-dimethyl-8,17-diphenyldibenzo-[b,i][1,4,8,11]tetraazacyclotetradecine and its nickel(II) complex: Syntheses, reaction mechanism and structures. *Inorganic Chemistry Communications*, 14(10), 1555-1560.
- Sigg, I., Georges, H., & Tammo, W. (1982). The Reaction of 3-formylchromone with ortho-substituted anilines. Preparation of a tetraaza[14]annulene *Helvetica Chimica Acta*, 65, 275-279.
- Simoneau, C. A., & Ganem, B. (2005). Multiple component Fischer indole reactions. *Tetrahedron*, 61(48), 11374-11379.
- Śliwiński, J., Eilmes, J., Oleksyn, B. J., & Stadnicka, K. (2004). Conformational polymorphism and aromaticity in crystalline dibenzotetraaza[14]annulene derivatives. *Journal of Molecular Structure*, 694(1-3), 1-19.
- Song, H. J., Lee, E. J., Kim, D. H., Lee, S. M., Lee, J. Y., & Moon, D. K. (2013). Enhancement of external quantum efficiency through steric hindrance of phenazine derivative for white polymer light-emitting diode materials. *Synthetic Metals*, 181, 98-103.
- Stojković, M. R., Marjanović, M., Pawlica, D., Dudek, L., Eilmes, J., Kralj, M., & Piantanida, I. (2010). Cationic side-chains control DNA/RNA binding properties and antiproliferative activity of dicationic dibenzotetraaza[14]annulene derivatives. *New Journal of Chemistry*, 34(3), 500-507.
- Streeky, J. A., Pillsbury, D. G., & Busch, D. H. (1980). Substituent effects in the control of the oxidation-reduction properties of metal ions in complexes with macrocyclic ligands. *Inorganic Chemistry*, 19(10), 3148-3159.
- Tanaka, D., Ishiguro, H., Shimizu, Y., & Uchida, K. (2012). Thermal and photoinduced liquid crystalline phase transitions with a rod-disc alternative change in the molecular shape. *Journal of Materials Chemistry*, 22(48), 25065.
- Tschierske, C. (2013). Development of structural complexity by liquid-crystal self-assembly. *Angewandte Chemie International Edition*, 52(34), 8828-8878.
- Vilsmeier, A., & Haack, A. (1927). Über die einwirkung von halogenphosphor auf alkylformanilide. Eine neue methode zur darstellung sekundärer und tertiärer p-alkylamino-benzaldehyde. *Berichte der deutschen chemischen Gesellschaft (A and B Series)*, 60(1), 119-122.
- Vinay Kumar, B., Bhojya Naik, H. S., Girija, D., Sharath, N., Pradeepa, S. M., Joy Hoskeri, H., & Prabhakara, M. C. (2012). Synthesis, DNA-binding, DNA-

photonuclease profiling and antimicrobial activity of novel tetra-aza macrocyclic Ni(II), Co(II) and Cu(II) complexes constrained by thiadiazole. *Spectrochimica Acta Part A: Molecular and Biomolecular Spectroscopy*, 94, 192-199.

- Voloshin, N. A., Metelitsa, A. V., Micheau, J.-C., Voloshina, E. N., Besugliy, S. O., Vdovenko, A. V., . . . Minkina, V. I. (2003). Spiropyrans and spirooxazines 1. Synthesis and photochromic properties of 9'-hydroxy- and 9'-alkoxy-substituted spironaphthooxazines. *Russian Chemical Bulletin, International Edition*, 52(5), 1172-1181.
- Wang, W., Daran, J.-C., Poli, R., & Agustin, D. (2016). OH-substituted tridentate ONO Schiff base ligands and related molybdenum(VI) complexes for solvent-free (ep)oxidation catalysis with TBHP as oxidant. *Journal of Molecular Catalysis A: Chemical*, 416, 117-126.
- Wang, X., Shen, X., Zhang, Y.-J., Su, F., Liu, G., Xu, Y., & Zhu, D.-R. (2013). Two one-dimensional germanium(IV) coordination polymers based on macrocyclic tetraaza[14]annulene with notable semiconducting property. *Inorganic Chemistry Communications*, 35, 45-49.
- Weiss, M. C., Gordon, G., & Goedken, V. L. (1977). Crystal and molecular structure of the macrocyclic nickel(II) complex Ni(C₁₈H₁₄N₄): Dibenzo[b,i][1,4,8,11]tetraaza[14]annulenenickel(II). *Inorganic Chemistry*, 16(2), 305-310.
- Whyte, A. M., Shuku, Y., Nichol, G. S., Matsushita, M. M., Awaga, K., & Robertson, N. (2012). Planar Ni(ii), Cu(ii) and Co(ii) tetraaza[14]annulenes: structural, electronic and magnetic properties and application to field effect transistors. *Journal of Materials Chemistry*, 22(34), 17967.
- Wöhrle, T., Wurzbach, I., Kirres, J., Kostidou, A., Kapernaum, N., Litterscheidt, J., . . . Laschat, S. (2016). Discotic liquid crystals. *Chemical Reviews*, 116(3), 1139-1241.
- Yu, J., Zhao, B., Nie, X., Zhou, B., Li, Y., Hai, J., . . . Tang, W. (2015). Correlation of structure and photovoltaic performance of benzo[1,2-b:4,5-b']dithiophene copolymers alternating with different acceptors. *New Journal of Chemistry*, 39(3), 2248-2255.
- Yun, D.-H., Yoo, H.-S., Heo, S.-W., Song, H.-J., Moon, D.-K., Woo, J.-W., & Park, Y.-S. (2013). Synthesis and photovoltaic characterization of D/A structure compound based on N-substituted phenothiazine and benzothiadiazole. *Journal of Industrial and Engineering Chemistry*, 19(2), 421-426.

- Yusoff, L. M., Yusoff, S. F. M., Ismail, W., & Yamin, B. M. (2014). Synthesis and characterization of Ni(II) complex with 5,5,7,12,12,14-hexamethyl-1,4,8,11-tetraazacyclotetradeca-7,14-dienium bromide. *AIP Conference Proceedings*. AIP Publishing LLC (AIP). 358-361.
- Zalevsky, Z., & Abdulhalim, I. (2014). *Liquid Crystals Nanophotonics. Integrated Nanophotonic Devices* (Second ed.). Oxford, UK: William Andrew, Elsevier Inc. pp273-311.
- Zhang, Z., Peng, Q., Yang, D., Chen, Y., Huang, Y., Pu, X., . . . Liu, Y. (2013). Novel conjugated polymers with planar backbone bearing acenaphtho[1,2-b]quinoxaline acceptor subunit for polymer solar cells. *Synthetic Metals*, 175(Supplement C), 21-29.
- Zhao, P., Zhong, C., Hunag, L., Niu, L., & Zhang, F. (2008). Corrosion inhibition of dibenzo [1,4,8,11] tetraaza [14] annulene nickel on steel in 1M HCl. *Corrosion Science*, 50(8), 2166-2171.
- Zheng, W., Hu, Y. T., Chiang, C. Y., & Ong, C. W. (2010). Orientational packing of a confined discotic mesogen in the columnar phase. *International Journal of Molecular Sciences.*, 11(3), 943-955.
- Zwolińska, K. M., & Eilmes, J. (2016). New developments in porphyrin-like macrocyclic chemistry: a novel family of dibenzotetraaza[14]annulene-based cofacial dimers. *Chemical Communications*(21), 1-3.